Phosphaalkene Ligands - A New Perspective on Wittig-Type Transformations

Cumulative Dissertation

in partial fulfillment for the degree of

***doctor rerum naturalium* (Dr. rer. nat.)**

at the University of Rostock

Faculty for Mathematics and Natural Sciences

submitted by

M.Sc. Kushik

Born 02. 09. 2000, India.

Leibniz Institute for Catalysis

2025

https://doi.org/10.18453/rosdok_id00005664

Selbstständigkeitserklärung

Ich versichere hiermit an Eides statt, dass ich die vorliegende Arbeit selbständig angefertigt und ohne fremde Hilfe verfasst habe, keine außer die von mir angegebenen Hilfsmittel und Quellen dazu verwendet habe und die den benutzten Werken inhaltlich und wörtlich entnommenen Stellen als solche kenntlich gemacht habe.

Rostock, den 06.11.2025

.....

Name

Gutachter:

Prof. Dr. Torsten Beweries, Leibniz-Institut für Katalyse

Dr. habil. Christian Hering-Jughans, Leibniz-Institut für Katalyse

Prof. Dr. Gabriele Hierlmeier, Julius-Maximilians-Universität Würzburg

Jahr der Einreichung: July 2025

Jahr der Verteidigung: Nov 2025

Acknowledgements

First and foremost, I am extremely grateful to my supervisors, Prof. Dr. Torsten Beweries and Dr. Christian Hering-Junghans for providing me this wonderful opportunity to carry out my doctoral studies under their guidance. Their immense knowledge and plentiful experience have encouraged me in all the time of my academic research and daily life. I deeply value their work ethics and supervision skills. It is their constant motivation and support that have made my student life in Germany a wonderful time. I am extremely thankful for believing in me and allowing me to grab all the opportunities coming my way. Undoubtedly, I could not have a better Ph.D. experience.

I would like to offer my special thanks to Dr. Fabian Reiß for his assistance in experimental work and valuable suggestion during group meetings and Dr. Hans-Joachim Drexler and Dr. Anke Spannenberg for patiently performing SC-XRD experiments on my crystals.

I would like to extend my thanks to Studienstiftung des deutschen Volkes for providing financial support that allowed me to conduct the research for this thesis and LIKAT to provide with facilities and scientific environment. Also, my appreciation goes out to Dr. Wolfgang Baumann, Mr. Andreas Koch, Mrs. Astrid Lehmann, Dr. Marcus Klahn, Mrs. Susann Buchholz, and the other colleagues of the analytic department for their precise analysis and generous support.

I am indebted to wonderful members of my group, Dr. Henrik Beer, Dr. Edger Zander, Dr. Andrey Petrov, Ayu Afiqah Nasrullah, Dr. Alexander Linke, Dr. Jan-Erik Siewert, Benjamin Andres, Dr. Laura Tadiello, Dr. Sihan Li, Dr. Tobias Täufer, Dr. Thea Mayer, Mirko Rippke, Marie-Sophie Lenz, Shubham Goel, Simon Walkenhorst, Maximilian Greiner, Dr. Peter Fritz, Max Neubauer, Niels Hildebrandt, and Luisa Zach for being so accommodating and providing a pleasant working atmosphere. It was so easy working with all of you and I will always cherish the time that we spent together.

I would also like to sincerely thank all my friends and colleagues in Germany, Katharina Konieczny, Dr. Phong Dam, Kaushik Soni, Florian Voss, for all the good time that we had together.

A big share of my gratitude goes to all the teachers whose positive influence have shaped my life. My special thanks go to Mr. Balbir Kajla (Maths teacher), Dr. Anil Boora (Chemistry teacher), Prof. Raja Angamuthu (M.Sc. Thesis supervisor) because they were the one who pushed me during the hard time and due to their effort, I got big push in my life.

I am endlessly thankful to universe for bringing love in my life, my moonlight-Gopika Narayanan Nair. I would like to extend my thanks to my dearest friends, Lakshay Jora, Shubham Singh, Virjesh Singhmar, Saksham Narada, Cyrus Taneja, Pooran Kumar, Mandeep Punia, Pankaj Rathee, Sahil Bakher, Neha Singh, Kaushal Singh Tomar, for being my moral support and celebrating every small victory of mine.

Acknowledgements

Finally, I would like to thank the most important people in my life, my family, Mr. Parikshit Olla, Mrs. Chanderpati Olla, Mr. Sukarnu Olla, Mrs. Sunita Olla, Mr. Devvart Olla, Mrs. Kavita Olla, Mr. Mandav Olla, Ms. Sushila Olla. I am grateful to God for giving me such supportive and loving family. I could not have done this without them.

My gratitude to all the mentioned people knows no boundaries. Thank you!

Abstract

This thesis is structured into four main sections. The first explores the attempted synthesis of phosphaalumenes using phospha-Wittig reagents and various Al(I) sources. Although direct isolation was unsuccessful, spectroscopic and crystallographic data provided evidence for their transient formation and subsequent deactivation via dimerization or intramolecular C–H activation. In the second part, a novel azide-Wittig reaction is introduced, representing a new route to triazabutadienes (TBDs) from azides and aldehydes in the presence of phosphines. This transformation proceeds under mild conditions, displays a broad substrate scope, and enables the synthesis of structurally diverse TBDs with high selectivity. The third section focuses on the synthesis of bis-phosphaalkene-based P,N,P-type ligands derived from carbazole frameworks, followed by their deprotonation to give alkali metal amido ligand precursors. These ligands exhibit strong donor properties and enable unusual binding motifs in transition metal coordination. In the final section, coordination of these ligands to Rh(I) afforded dinuclear complexes that feature distinct phosphaalkene coordination modes and intramolecular C–H activation. The results highlight new reactivity patterns in phosphorus–main group and phosphorus–transition metal chemistry, expanding the scope of phospha-Wittig reagents in small molecule activation and organophosphorus ligand design.

Diese Arbeit gliedert sich in vier Hauptabschnitte. Im ersten wird die versuchte Synthese von Phosphaalumenen mit Phospha-Wittig-Reagenzien und verschiedenen Al(I)-Quellen untersucht. Obwohl die direkte Isolierung nicht erfolgreich war, lieferten spektroskopische und kristallografische Daten Hinweise auf ihre vorübergehende Bildung und anschließende Deaktivierung durch Dimerisierung oder intramolekulare C-H-Aktivierung. Im zweiten Teil wird eine neuartige Azid-Wittig-Reaktion vorgestellt, die einen neuen Weg zu Triazabutadienen (TBDs) aus Aziden und Aldehyden in Gegenwart von Phosphinen darstellt. Diese Umwandlung läuft unter milden Bedingungen ab, weist ein breites Substratspektrum auf und ermöglicht die Synthese von strukturell vielfältigen TBDs mit hoher Selektivität. Der dritte Abschnitt konzentriert sich auf die Synthese von P,N,P-Liganden auf Bis-Phosphaalken-Basis, die von Carbazolgerüsten abgeleitet sind, gefolgt von ihrer Umwandlung in Alkalimetallsalze. Diese Liganden weisen starke Donoreigenschaften auf und ermöglichen ungewöhnliche Bindungsmotive in der Übergangsmetallkoordination. Im letzten Abschnitt wurden durch die Koordination dieser Liganden an Rh(I) zweikernige Komplexe mit unterschiedlichen Phosphaalken-Koordinationsmodi und intramolekularer C-H-Aktivierung erhalten. Die Ergebnisse zeigen neue

Abstract

Reaktivitätsmuster in der Chemie von Phosphor-Hauptgruppen und Phosphor-Übergangsmetallen auf und erweitern den Anwendungsbereich von Phospha-Wittig-Reagenzien bei der Aktivierung kleiner Moleküle und beim Design von Organophosphor-Liganden.

Table of Contents

List of Abbreviations

e.g.	for example	Mes*	2,4,6-*t*Bu$_3$C$_6$H$_2$
Mes	2,4,6-Me$_3$-C$_6$H$_2$	DBU	1,8-diazabicyclo[5,4,0]undec-7-ene
PAs	phosphaalkenes	KOH	potassium hydroxide
Ph	phenyl	rt	room temperature
LP	lone pair	THF	tetrahydrofuran
HOMO	highest occupied molecular orbital	cat.	catalytic
		^{Mes}Ter	2,6-(2,4,6-Me$_3$C$_6$H$_2$)-C$_6$H$_3$
LUMO	lowest unoccupied molecular orbital	Ar	aryl
		et al.	and others
DFT	density functional Theory	*i.e.*	that is
g	gram	PPEP	2-(phospholanylmethyl)-6-(2-phosphaethenyl)pyridine
Et	ethyl		
Me	methyl	quin	quinoline
h	hours	ppm	parts per million
Hz	hertz	[M], M	metal
EIND	1,1,3,3,5,5,7,7-octaethyl-1,2,3,5,6,7-hexahydro-*s*-indacen-4-yl	°C	degree celsius
		Dipp	2,6-*i*Pr$_2$-C$_6$H$_3$
		*i*Pr	isopropyl
Bu	butyl	Cp*	pentamethylcyclopentadienyl
t	tertiary	Tmp	2,2,6,6-tetramethylpiperidyl
IR	infrared spectroscopy	DCM	dichloromethane
NMR	nuclear magnetic resonance	min.	minutes
SC-XRD	single crystal X-ray diffraction	Tol	toluene
UV-Vis	ultraviolet-visible	TFA	trifluoracetic acid
o	ortho	NBO	natural bond order
m	meta	*hv*	light energy
p	para	DMF	dimethylformamide
NHC	*N*-heterocyclic carbene	Ad	adamantane
e	electron	^{Dipp}NacNac	HC[C(Me)NDipp]$_2$
TMS	trimethylsilane	TBDs	triazabutadiene

cod	cyclooctadiene	coe	cyclooctene
nbd	norbornadiene	TD-DFT	time dependent DFT
NLMO	natural localized molecular orbitals	IBO	intrinsic bond orbital
		ELF	electron localization function
nm	nanometer	MLCT	metal to ligand charge transfer

1 Introduction

1.1 Phosphaalkenes

Ligand design has been significantly influenced by the incorporation of phosphorus, as it can mimic various elements (e.g. carbon, silicon, nitrogen) depending on its coordination number, a reasoning that was first recognized by Mathey and co-workers.[1-2] Additionally, it was generally accepted that heavier elements of the p-block would not form stable (np–mp)π (n≥3, m≥2) bonds due to insufficient hybridization and therefore poor orbital overlap at heavier main group elements. Achieving an sp^2 ($\lambda^3\sigma^2$) trivalent phosphorus atom with the coordination number 2 or sp ($\lambda^3\sigma^1$) hybridization is rather unusual, compared to the most common $\lambda^3\sigma^3$ and $\lambda^5\sigma^4$ binding modes (Figure 1). This so-called "double bond rule" was challenged by the discovery of low coordinate phosphorus compounds featuring multiple bonding between phosphorus and other elements such as carbon and nitrogen.

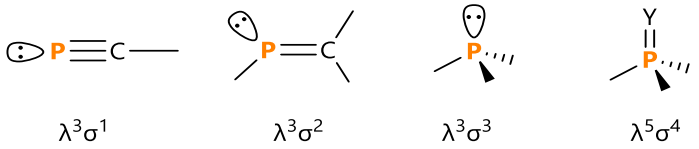

Figure 1. Coordination states of phosphorus.

In 1961, Gier and co-workers reported the characterization of the parent phosphaacetylene H−C≡P in the gas phase.[3] Phosphamethine cyanine cation (**1**), and phosphinines (**2, 3**) were the first isolable species with phosphorus-carbon multiple bonding, stabilized by the delocalization of (3p–2p)π electrons over multiple centers (Figure 2).[4-6]

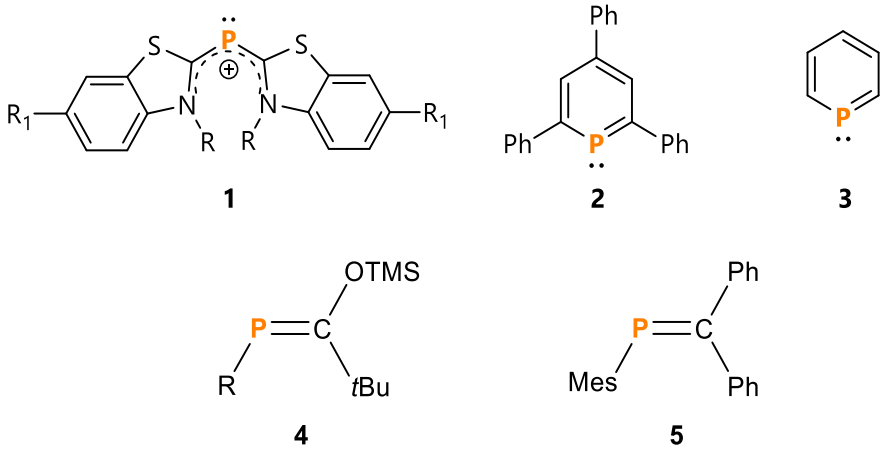

Figure 2. First isolable compounds with P−C multiple bonds: Phosphamethine cyanines (**1**) and phosphinines (**2**, **3**), along with the first isolable phosphaalkenes (**4**, **5**).

The first isolable compounds with localized P=C bonds[4], phosphaalkenes, were prepared in 1976 by Becker and co-workers, where between −30 °C and −10 °C, substituted bis(trimethylsilyl)phosphines react with pivaloyl chloride to form acylated products and these compounds rearrange near room temperature to their stable enol forms featuring an unusual P=C double bond (**4**; Figure 2).[7] In 1978, Bickelhaupt and co-workers reported the first phosphaalkene bearing solely carbon substituents, $MesP{=}CPh_2$ (**5**; Mes = 2,4,6-Me_3-C_6H_2) (Figure 2).[8] These pioneering developments ignited a rapid expansion in the field of phosphaalkene chemistry, as evidenced by the number of recent reviews dedicated to the subject.[9-15]

1.1.1 Electronic Structure of Phosphaalkene

In terms of their coordination properties, phoshaalkenes (PAs) can be compared to imines ($HN{=}CH_2$), however, their electronic structures differ significantly. Natural bond analysis carried out on geometries optimized at the B3PW91/6-311++G(3df, 2p) level of theory, on parent $H_2C{=}PH$ revealed that the lone pair of electrons (LP) on phosphorus is rather low in energy and best represented by HOMO-1, featuring a high 3s character (66%) (Figure 3)[11] This contrasts imines, in which the LP on the N atom is represented in the HOMO and resides in a nearly perfect sp^2 orbital. This clearly indicates the diminished hybridization at P in phosphaalkenes when compared to imines. The high s-character in the phosphorus LP in PAs affects the σ donation capacity and, consequently, the directionality of the LP. Experimentally, the high s-character of the lone pair, and therefore the low s-character of the σ-bonds, is supported by the reduced angle (between 100º and 107º) formed by the substituent at phosphorus and the carbon atom compared to classical sp^2 C- and N-based systems.[16] Consequently, the bond length of P=C double bonds is typically between 1.63 Å and 1.71 Å.

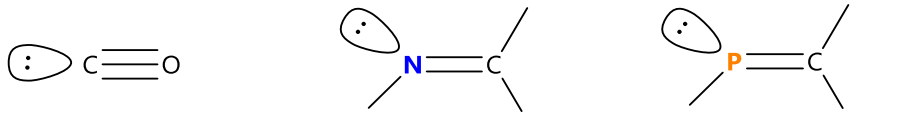

2s (s-character): 50%	2s (s-character): 39%	3s (s-character): 66%
2p (p-character): 50%	2p (p-character): 61%	3p (p-character): 34%

Figure 3. Lone pair molecular orbital compositions in CO, $HN{=}CH_2$ and $HP{=}CH_2$.

Furthermore, NBO calculations are clearly in line with an inverse polarity of the P=C bond in PAs with respect to imines as calculations reveal a positive charge of +0.42 e at the P atom, whereas in case of imines the N atom has a negative net charge of −0.59 e.[11] This slight polarization of the P−C σ-bond towards the C atom is also supported by the Pauling electronegativity scale as P (2.1) is more electropositive than C (2.5) and N (3.0). Additionally, most of the isolated phosphaalkenes need significant kinetic stabilization, which contrasts C=C and N=C olefinic systems. This can be attributed to the π-bond strength of the P=C bond (45 $kcal{\cdot}mol^{-1}$) in phosphaalkenes in comparison to the C=C bond olefins (65 $kcal{\cdot}mol^{-1}$).[17-18] Consequently, PAs show a great dimerization or oligomerization tendency, a direct result from inefficient P=C π-overlap.[19-21] The

analogy of PAs can be extended to carbon monoxide, CO. As the LP in PAs have high s-character (66% 3s), they are better σ-donors when compared to CO (sp hybrid orbital, 50% 2s). The P atom of PAs is electropositive, rendering the π* orbital in PAs rather low in energy, which is clearly in-line with the excellent π-accepting ability of PAs in transition metal complexes through back-bonding similar to CO.[22] Phosphaalkene based ligand systems are exciting to study due to their enhanced π-acceptor and rather unidirectional σ-donor properties in combination with their potential to fine tune the electronic and steric properties through the substituents.

1.1.2 Synthesis of Phosphaalkene

Literature reveals various synthetic routes towards phosphaalkenes. In 1976, Becker unveiled the synthesis of the first acyclic phosphaalkene (**6**) by isomerization of silylacylphosphines from their keto- to the corresponding enol-form via a P,O-silyl shift.[23] Furthermore, Bickelhaupt and co-workers later showed the first phosphaalkene with only C-substituents, MesP=CPh_2 (**7**), obtained in the base-assisted dehydrohalogenation of a benzhydrol-substituted chlorophosphine precursor (Scheme 1, ii).[8] As an alternative substrate, Mes*PH_2 (Mes* = 2,4,6-*t*Bu_3-C_6H_2) can also be converted to phosphaalkenes by reacting it with alkaline solutions of chloroform or bromoform (Scheme 1, iii), most likely through a carbene-type mechanism.[24] Moreover, "phospha-Peterson" and "phospha-Wittig" reactions have been used to construct P=C bonds recently.

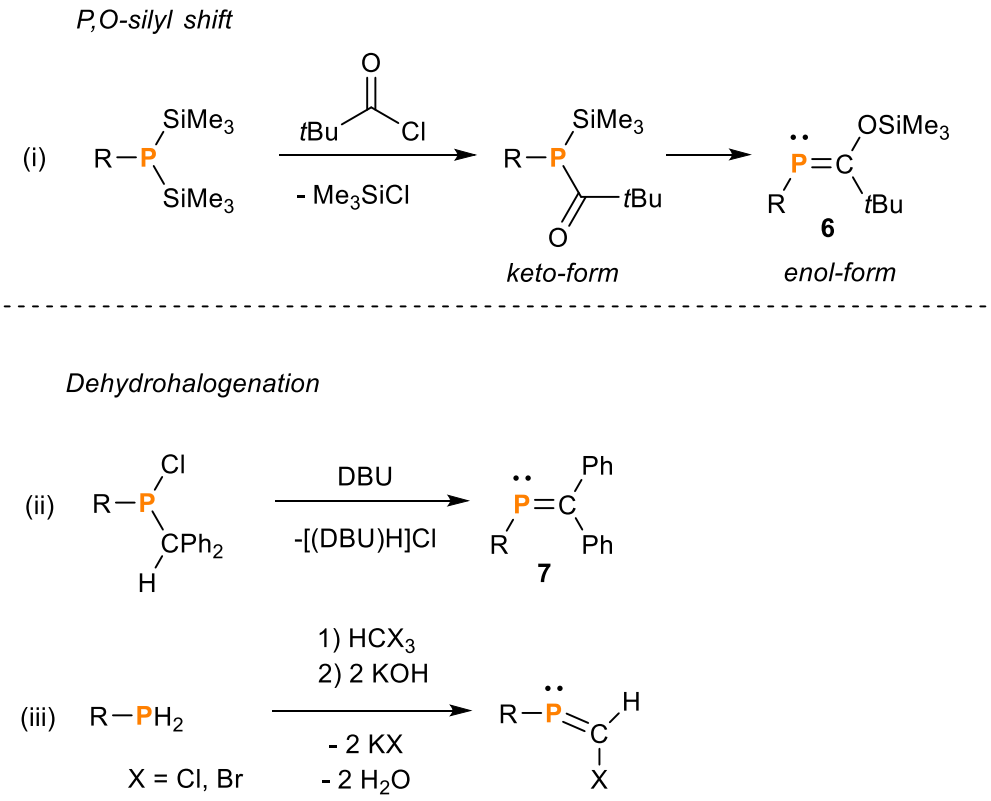

Scheme 1. Various synthetic routes towards phosphaalkene.

1.1.2.1 The phospha-Peterson Reaction

The phospha-Peterson route was initially reported by Bernardinelli and co-workers in the early 1990s,[25] and was then later applied by Yoshifuji and co-workers.[26] The phospha-Peterson reaction is based on the reaction of a silylated anion $RP^{(-)}Si(t\text{-}Bu)Me_2$ with an aldehyde to yield kinetically protected mono-, di- (**8**), and tridentate (**9**) phosphaalkene ligands (Scheme 2, top). Later this route was further developed by the Gates group, where they used bis(silyl)phosphines in the reaction with MeLi to form the reactive silyl phosphide intermediate *in situ*, which in turn reacted with various aldehydes to give phosphaalkenes selectively. They have shown that starting from $MesP(SiMe_3)_2$, a variety of mesityl-substituted phosphaalkenes could be isolated, among them the P,N-type ligand MesP=C(Ph)(2-pyridyl) (**10**). [27] In some cases, due to the difficulty in preparing the phospha-Peterson reagents, like EIND-P($SiMe_3$)Li (EIND = 1,1,3,3,5,5,7,7-octaethyl-1,2,3,5,6,7-hexahydro-*s*-indacen-4-yl), the phospha-Wittig pathway is considered a better approach.[28]

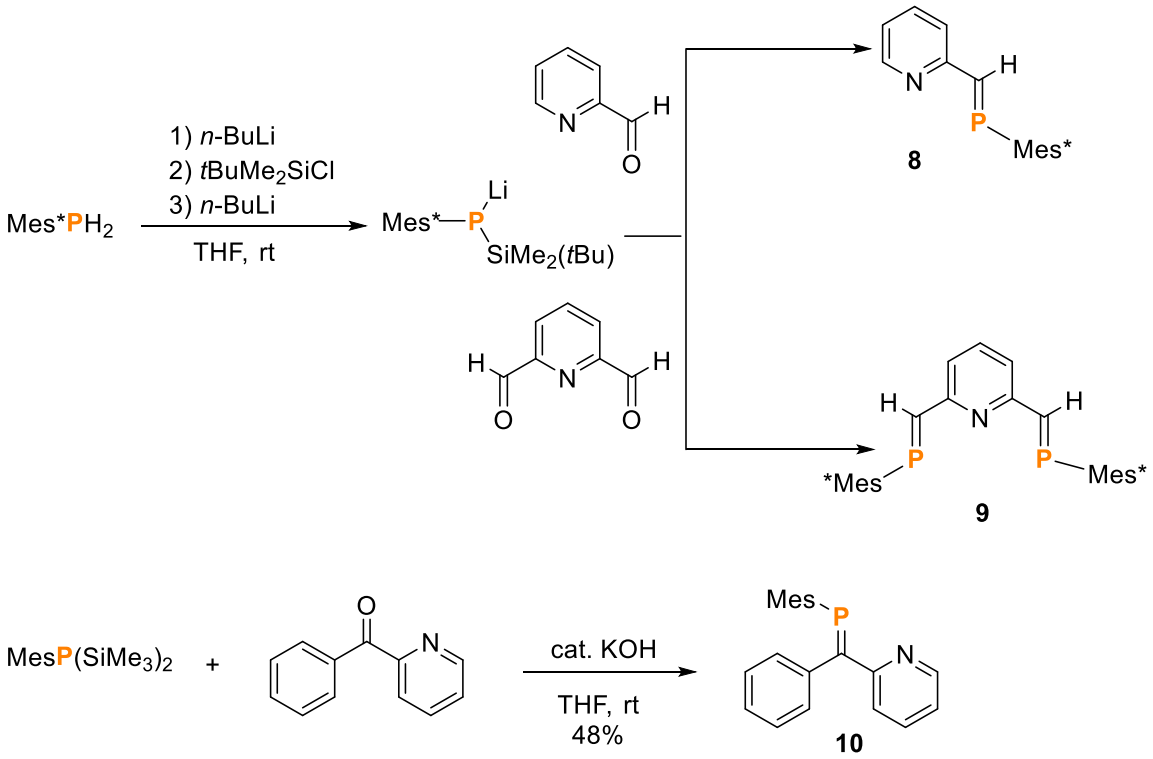

Scheme 2. Synthesis of pyridyl phosphaalkenes (**8**, **9** and **10**).

1.1.2.2 The Phospha-Wittig Reaction

The "phospha-Wittig" reaction was first introduced by Protasiewicz *et al.* utilizing phosphanylidene-σ^4-phosphoranes of the type Ar-P(PMe_3) (Ar = Mes*, ^{Mes}Ter = 2,6-(2,4,6-$Me_3C_6H_2$)-C_6H_3)[29] in reactions with different aldehydes to synthesize phosphaalkenes *E*-selectively with localized P=C double bonds (Scheme 3).[30] Since then this route has been a great tool to

synthesize a variety of phosphaalkene-based ligands *i.e.* P,N,P-,[31] P,P-, (**11**),[32] and P,P,P,P-type (**12**) ligands.[33] Furthermore, Ozawa and co-workers reported P,N,P-phosphaalkene ligands with sterically demanding Mes* or EIND (**13**) substituents utilizing the phospha-Wittig route (Figure 5).[28] EIND-PPEP (**13**; PPEP = 2-(phospholanylmethyl)-6-(2-phosphaethenyl)pyridine) was sufficiently stable against C-H activation due to steric protection from bulky EIND substituents in contrast to PPEP containing Mes* substituents.[28]

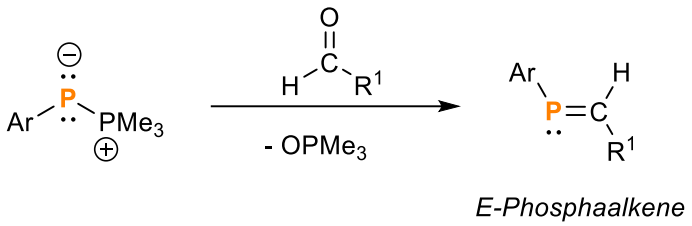

Scheme 3. Phosphaalkene synthesis through phospha-Wittig reaction.

Cain and co-workers also reported a series of PA-ligands including phosphine-phosphaalkenes[32] (**11**) and pyridine based P,N-phosphaalkenes (**14**).[34] Recently, the groups of Beweries and Hering-Junghans reported the synthesis of a P,N-type quinoline-based phosphaalkene ligand (2-quin)(H)C=PMes* using the phospha-Wittig route.[35]

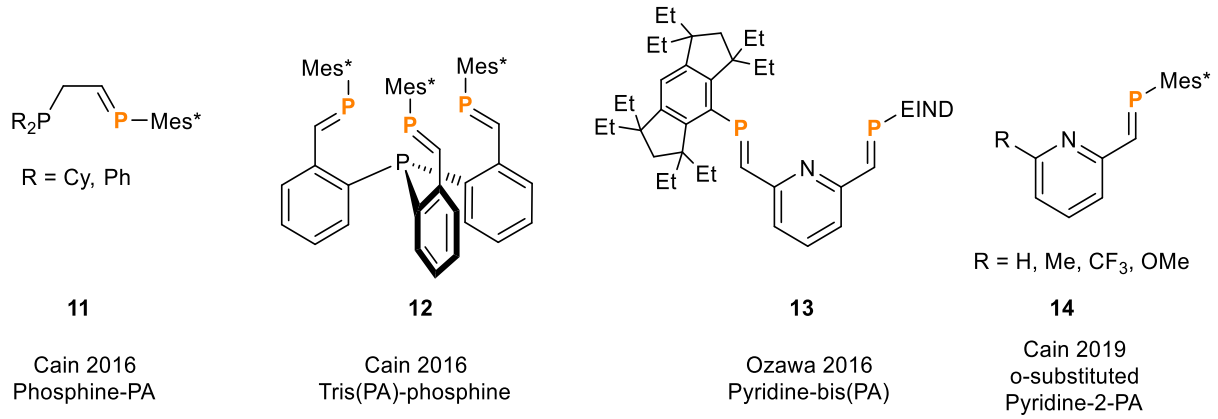

Figure 4. Known complexes obtained through the phospha-Wittig protocol.

Even with the undenied fact that phospha-Wittig reagents are a great tool to synthesize phosphaalkenes or phosphorus-carbon double bonds via so-called phospha-Wittig reaction, the reaction is limited to aldehydes. So, to expand the scope of P=C beyond aldehyde we moved in direction of ala-phospha-Wittig reactions. The section 1.2 of this thesis is dedicated to pnictatrielenes and more specifically, phosphaalumenes.

1.1.3 Coordination Properties of Phosphaalkene

Unlike traditional phosphines, the binding properties of phosphaalkenes are different due to the presence of both, a LP and a π bond on phosphorus. Hence, phosphaalkenes can engage in up to

five different coordination modes (Figure 5). The two most common metal binding modes of phosphaalkenes are the η^1-κ^P-coordination (**15**)[36] and η^2-$\kappa^{P,C}$-coordination (**16**) and due to the small energy gap between LP and π bond on phosphorus, the metal can easily interconvert between η^1- and η^2-coordination.[37] Sometimes more unusual coordination modes can be observed (Figure 5, **17**,**18**,**19**) for example when the metal is present in excess, η^1,η^2-coordination (**17**)[36, 38] has been reported or rarely, η^1-(μ_2-P)-coordination (**18**)[36, 39] can be detected as phosphorus has the capacity to become tetravalent. Another unusual η^1,η^2,μ_3-binding mode (**19**)[40] was observed when the phosphaalkene ligand was incorporated into a metal cluster. The first phosphaalkene complexes displaying PA η^1-κ^P-coordination were characterized by NMR spectroscopy as *cis*-M(CO)$_4$(η^1-MesP=CPh$_2$)$_2$ (M=Cr, Mo, W), *trans*-RhCl(PPh$_3$)$_2$(η^1-MesP=CPh$_2$), *trans*-RhCl(η^1-MesP=CPh$_2$)$_2$(CO), Rh(η^5-C$_9$H$_7$)(η^1-MesP=CPh$_2$)$_2$, *cis*-PtX$_2$(η^1-MesP=CPh$_2$)$_2$ (X=Cl, I, Me), and *cis*- and *trans*-PtCl$_2$(PEt$_3$)(η^1-MesP=CPh$_2$).[41] Each of these complexes exhibited binding through the phosphorus lone pair, and this was also confirmed crystallographically with the structural characterization of Cr(CO)$_5$(MesP=CPh$_2$) and *cis*-PtCl$_2$(PEt$_3$)(MesP=CPh$_2$).[42-43]

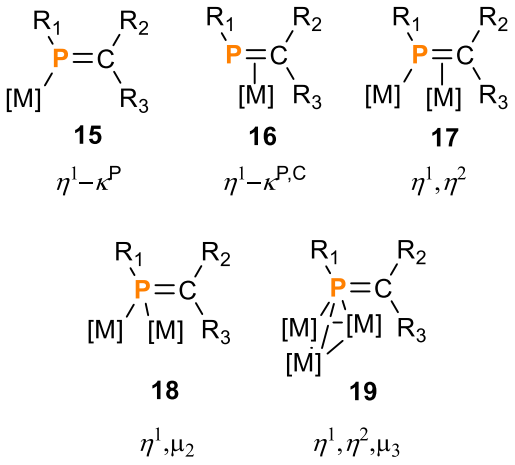

Figure 5. Different coordination modes of phosphaalkene ligands.

Typically, a metal center can bind to phosphaalkenes through the following orbital interactions: the LP at phosphorus donates electron density to an empty *d*-orbital of the metal (**20**), back-donation from a filled metal *d*-orbital into the π* orbital of the P=C bond (**21**). This interaction of metal with phosphaalkene brings the phosphorus atom of a phosphaalkene closer to an ideal sp^2 hybridized geometry, leading to an increase in the C–P=C angle to around 115° (**22**).

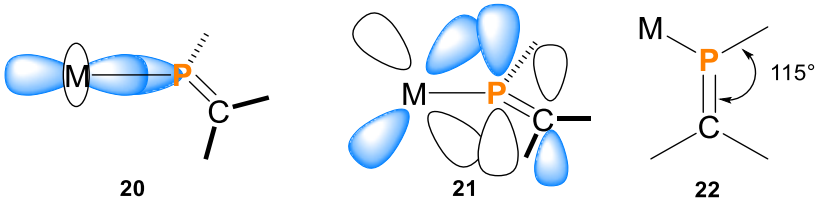

Figure 6. Orbitals involved in the coordination of phosphaalkenes.

This field is still growing and in our recently submitted manuscript we reported reactions of monoanionic PNP type bis-phosphaalkene ligands with $[Rh(cod)(Cl)]_2$ furnishing a dinuclear Rh(I) complex which shows the presence of three different phosphaalkene coordination modes (**15**, **16**, **17**) (refer section 2.4.1).[44]

1.1.2 Phosphaalkene Complexes

This section illustrates few examples of phosphaalkene coordination complexes rather than discussing all of them exhaustively. Ozawa and colleagues reported platinum(0) alkyne complexes (Scheme 4, **23**) featuring a 1,2-diphenyl-3,4-bis[(2,4,6-tri-*tert*-butylphenyl)phosphinidene] cyclobutene (DPCB) ligand with notable conjugative properties.[45] DFT studies demonstrated that the π-accepting nature of the phosphaalkene moiety creates an extended π-conjugated system with HOMO–LUMO gaps in the visible spectrum.[46] This behavior is unique among Pt(alkyne) complexes with other ligands.

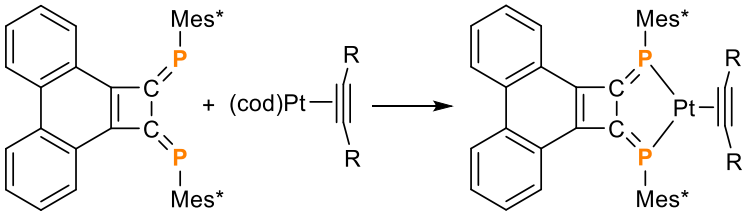

Scheme 4. DPCB Pt(alkyne) complexes.

Geoffrey *et al.* had previously prepared bis(phosphaethinyl)pyridines (BPEP) in the early 1990s via a route using Mes^*PH_2 and a silylated phosphide intermediate in a Peterson-type reaction.[25] Ozawa's group adapted this method to prepare Fe, Cu, and Ir complexes of these BPEP ligands. One-electron reduction of $FeBr_2$[BPEP-Ph] with $CoCp_2$ or Mes_2Mg yielded Fe(I) species FeBr[BPEP-Ph] (Scheme 5, **25**) and FeMes[BPEP-Ph] (Scheme 5, **26**). FeBr[BPEP-Ph] was confirmed as an Fe(I) (S=3/2) complex through Mössbauer and broken-symmetry DFT analysis.[47] Bonding analysis via NBO revealed effective dπ–pπ interaction between the metal and the low-lying π∗ orbital of the phosphaalkene. The Fe(I) center exhibited a rare distorted trigonal monopyramidal geometry. Notably, using a pyridinediimine ligand instead did not yield an Fe(I) species but led to ligand reduction with iron remaining as Fe(II).[47]

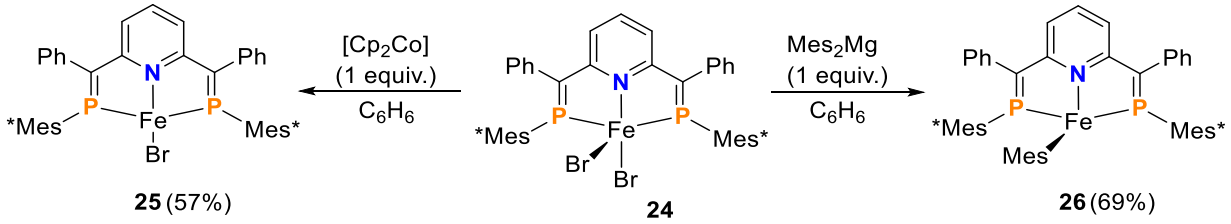

Scheme 5. $[FeBr_2$(BPEP-Ph)] complexes reduction to give Fe(I) complexes.

Cationic Cu(I) complexes were obtained by treating CuBr[BPEP-Ph] systems with Ag[EF_6] (E = P, Sb) or Ag[$B(C_6H_3(CF_3)_2)_4$], forming ion-separated salts (Scheme, **27**) in polar solvents as shown by ^{31}P NMR and X-ray analysis.[48] In non-polar solvents like toluene or benzene, contact ion pairs formed through Cu–F interactions; with PF_6, this led to a dinuclear complex bridged by PF_6 (Scheme 6, **28**), with typical Cu–F distances (~2.1 Å) and the dimeric structure persisting in solution even with MeCN or CO present. The authors attributed the unexpected F-affinity of BPEP–Cu systems to the strong π-accepting character of the ligand.[49] Complexes [Cu(BPEP-Ph)][EF_6] (E = P, Sb) (Scheme 6, **30**) showed Me_3SiCN activation under mild conditions.

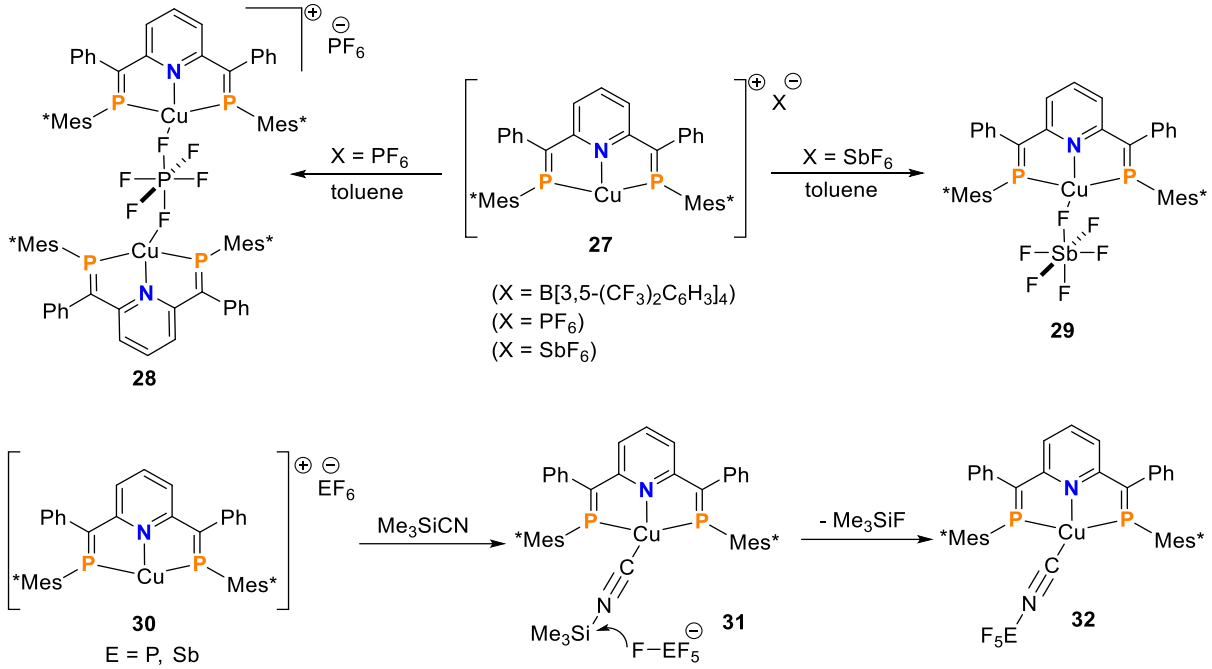

Scheme 6. Top: Cu(I) BPEP-Ph complexes. Bottom: Cu(I) BPEP-Ph complexes promoted bond activation of Me_3CN.

In another study, Ozawa's group observed metal–ligand cooperativity in a mixed Ir(I) P,N,P-complex containing phosphaalkene[50] and phosphaindane units. Heating [Ir(Cl)(BPEP-H)] (BPEP = 2,6-bis[2-(2,4,6-tri-*tert*-butylphenyl)-2 phosphaethenyl]pyridines) (Scheme 7, **33**) in toluene overnight induced selective cyclization of one *t*Bu group on the Mes* unit with phosphorus via Ir-mediated C–H activation and P–C elimination, yielding a PPEP-type ligand (Scheme 7, **34**). Subsequent addition of KO*t*Bu caused dearomatization of the central pyridine by deprotonating the benzylic position, forming anionic complexes of type K[Ir(Cl)(PPEP*)] (Scheme 7, **35**).[51] In **35**, a notably elongated P–C bond (1.701(12) Å) indicated enhanced π-backdonation compared to neutral BPEP. This complex displayed remarkable reactivity for cooperative activation of N–H bonds in NH_3 (1 atm), *n*-$C_6H_{13}NH_2$, and $C_6H_4NH_2$ (Scheme 7, **36**), proceeding rapidly at room temperature to quantitatively form amido complexes. In contrast, Rh(I) analogues could not be obtained due to successive C–H addition/cyclization at both Mes*P=C(R)H groups, leading to full

loss of the P=C bonds. Cain and co-workers recently reported Ru P,N-phosphaalkene complexes that exhibited intramolecular C–H activation at Mes* groups to form phosphaindane structures.[34]

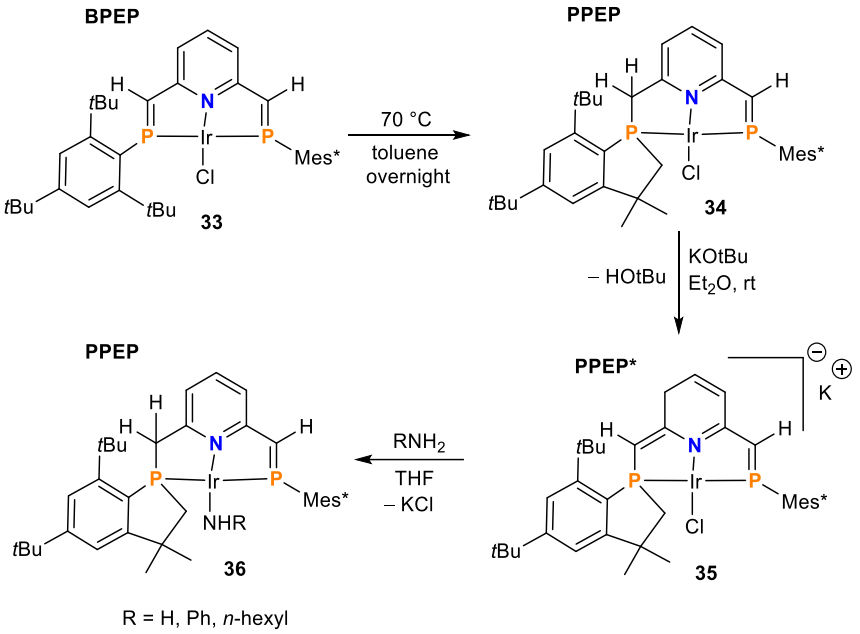

Scheme 7. Synthesis of Ir(I) PPEP and PPEP* complexes along with N–H bond cleavage.

In 2022, Hering-Junghans, Beweries and co-workers presented the synthesis and characterization of the P,N-type quinoline-based phosphaalkene ligand 2-quinC=PMes* (Scheme 8, **37**).[35] When coordinated to Rh(I), this ligand showed versatile coordination behavior, which upon heating undergoes twofold C-H bond activation at the *o*-*t*Bu grups of the Mes* substituents to yield the cationic bis(phosphaindane)Rh(I) complex (Scheme 8, **39**).

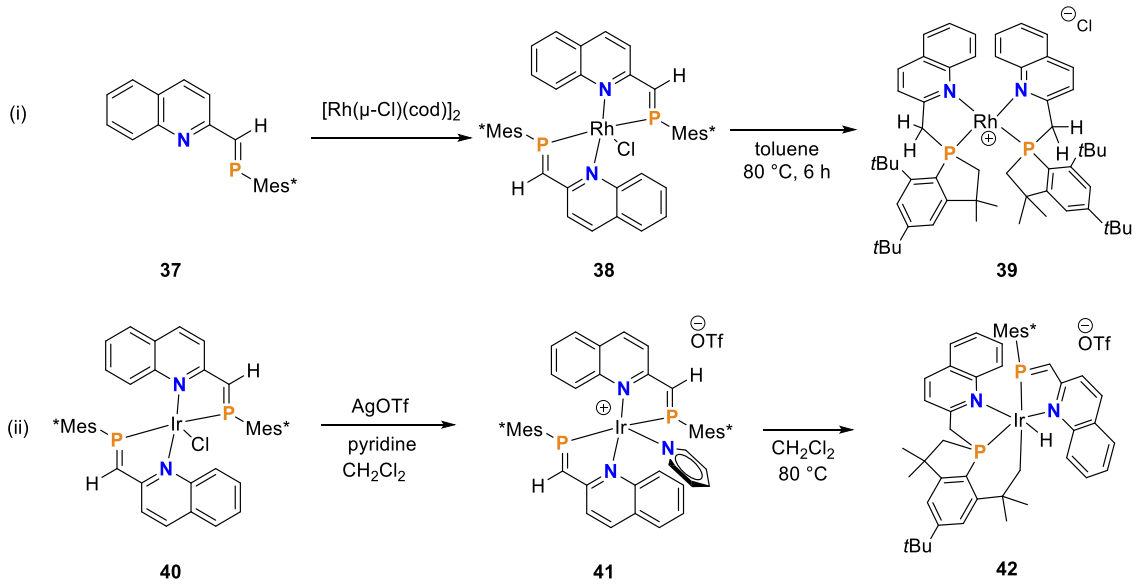

Scheme 8. Synthesis Rh(I) and Ir(I) P,N-phosphaalkene complexes.

More recently, using the same ligand Hering-Junghans, Beweries and co-workers reported an iridium complex (Scheme 8, **40**) which upon reaction with AgOTf in the presence of pyridine afforded pyridine coordinated cationic Ir(I) complex, $[(quin\text{-}CH{=}PMes^*)_2Ir(py)][OTf]$ (Scheme 8, **41**).[52] The Complex **41** on further heating at 80 °C, undergoes a C-H bond cleavage at both *o*-*t*Bu substituents of Mes* group. One hydrogen atom migrates to the carbon atom of the P=C bond, forming a phosphaindane moiety, while the second *t*Bu group undergoes cyclometallation with the iridium center to yield an Ir(III) hydride complex (Scheme 8, **2**). Complexes **40** and **41** were found to be active towards *N*-alkylation of aniline with benzyl alcohol (Scheme 9, (i)) and complex **40** was an active pre-catalyst for upgrading ethanol and methanol to *iso*-butanol (Scheme 9, (ii)).

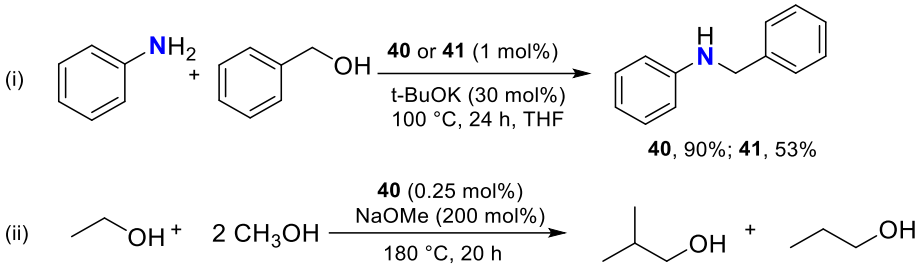

Scheme 9. Catalysis using iridium complexes **40** and **41**.

In a recently submitted paper, our group described the reaction of a monoanionic P,N,P-type bis-phosphaalkene ligand with $[Rh(cod)Cl]_2$, affording two dinuclear Rh(I) complexes among them one dinuclear Rh(I) complex displays C–H activation at both the *o*-*t*Bu substituents of Mes* group alongside a unique Rh–Rh donor–acceptor interaction.(refer section 2.4.1).[44] Overall, these examples illustrate the diverse coordination chemistry of phosphaalkene ligands, which can stabilize metals in unusual geometries and enhance conjugationfeatures that promise rich reactivity in catalysis.

1.2 Pnictatrielenes

Related to this concept, pnictatrielenes are compounds, which contain multiple bonding between a group 13 (triele, E13) and a group 15 element (pnictogen, E15). The synthesis of these compounds is challenging, especially when it comes to heavier base-free multiple bonds between P and B or Al due to intrinsic weakness of the π-bond.[53] Recently Liu *et al.* reported the first base-free phosphaborene $[(CH_2)(NDipp)]_2B\text{-}P{=}B\text{-}NC[(NDipp)(CH)]_2$ (Figure 7, **43**, Dipp = 2,6-*i*Pr_2-C_6H_3) stabilized by push-pull substitution at the B and P atoms, respectively.[54] Prior to this report there have been extensive studies on base-stabilized,[55-58] and especially NHC-stabilized phosphaborenes with small silyl-substituents (Figure 7, **44**). Particularly silyl-substituted NHC-stabilized phosphaborenes have been shown to undergo metathesis reactions through Me_3Si-halide elimination.[58] More recent examples include the phospha-bora-Wittig reaction involving the transient phosphaborene $Mes^*P{=}B{-}NR_2$ which reacts with carbonyl compounds to form 1,2,3-phosphaboraoxetanes, analogues to the oxaphosphetane intermediates in the classical Wittig

reaction. 1,2,3-Phosphaboraoxetanes undergo thermal or Lewis acid-promoted cycloreversion, yielding phosphaalkenes.[59]

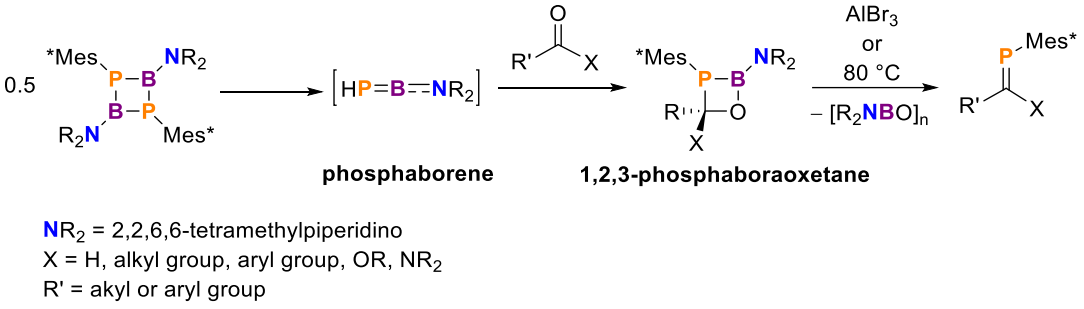

Scheme 10. Phospha-bora-Wittig reaction.

Furthermore, our group reported on the synthesis of pnictaalumenes using phosphanylidenephosphoranes of the type ArP(PMe$_3$) (Ar = sterically demanding aryl group) as phospha-Wittig reagents, by substitution of PMe$_3$ with stronger Lewis bases, in this case monovalent E13 species.[60-61] The first examples of phosphaalumenes ^{Ar}TerP=AlCp* (Figure 7, **45**, **46**) were afforded in the reaction of ^{Ar}TerP(PMe$_3$) (Ar = Dipp, Tipp) with (Cp*Al)$_4$ (a source of monomeric Cp*Al) as violet compounds with a highly polarized P–Al multiple bond.[62-63]

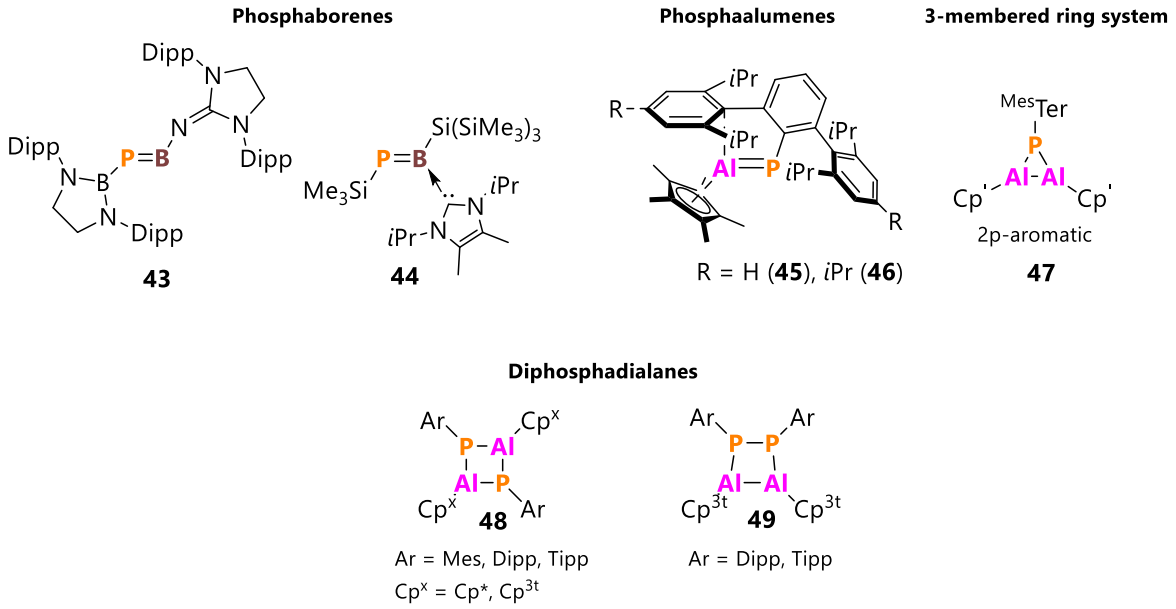

Figure 7. Isolable phosphaborenes/alumenes and dimers of phosphaalumenes.

Additionally, literature reports show that the size of the aryl groups at the P atom are crucial for the stabilization of phosphaalumenes. Using sterically less demanding ^{Mes}TerP(PMe$_3$), cyclic 2π-aromatic three-membered species of the type ^{Mes}TerP(AlCp')$_2$ (Cp' = Cp*, Cp^{3t} with Cp^{3t} = 1,2,4-*t*Bu$_3$; Figure 7, **47**) were obtained.[63] The reaction of triphosphiranes Ar$_3$P$_3$ (Ar = Mes, Dipp, Tipp) with Cp^{3t}Al or (Cp*Al)$_4$ afforded the dimers of phosphaalumenes, so-called base-free 1,3-

diphospha-2,4-dialanes.[64-65] These two products can exist in two distinct isomeric forms , either the 1,3-isomers (Figure 7, **48**), four-membered ring with alternating P and Al atoms, or the 1,2-isomers (Figure 7, **49**), four-membered rings containing P−P and Al−Al bonds.

Pnictatrielenes show a diverse reactivity with small, rather unreactive molecules. The diphosphadiboretane [Mes*PB(Tmp)]$_2$ (Scheme 11, **50**) (Tmp = 2,2,6,6-tetramethylpiperidyl) which generate the phosphaborene, [Mes*PB(Tmp)] intermediate *in situ*, reacts with phenylacetylene to give the corresponding [2+2]-cycloaddition product.[57] The isolated push-pull stabilized phosphaborene (Scheme 11, **51**) shows similar reactivity with *p*-methyl-benzaldehyde and when it was reacted with *p*-fluoroacetophenone C-H activation along the P=B bond was observed.[54]

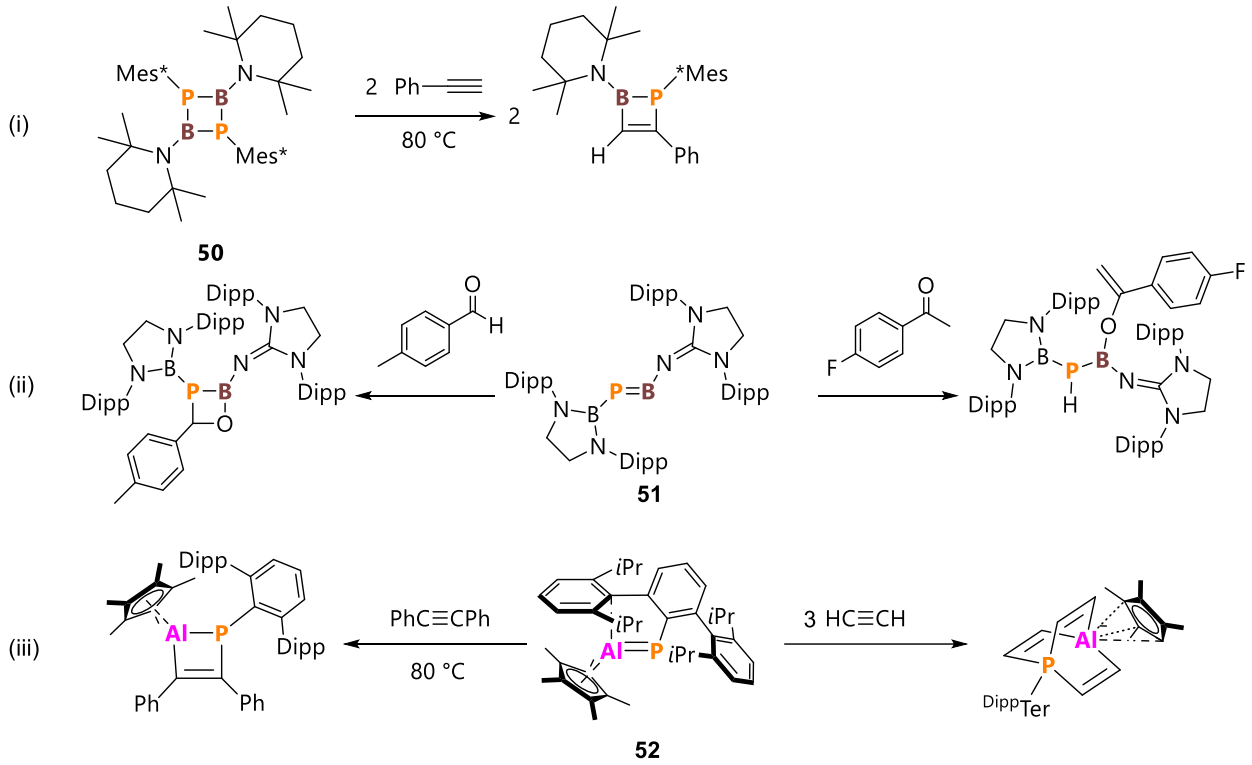

Scheme 11. Reactivity of phosphaborenes/alumenes.

The phosphaalumene (Scheme 11, **52**) was found to give P,Al-heterocycles and cage-type P,Al-barrelenes after undergoing initial [2+2]-cycloaddition along the P=Al double bond. Furthermore, to enable the formation of P=C bonds incorporating the Mes* substituent, we aimed to synthesize phosphaalumene species of the type RAl=P(Mes*), which could extend the scope of traditional phospha-Wittig reactivity beyond aldehydes. The choice of the Mes* group was intentional, as it is less sterically hindered than previously studied ^{Dipp}Ter substituents in ^{Dipp}TerP=AlCp* systems, which had been already reported by the Hering-Junghans group. The less encumbered Mes* substituent was expected to facilitate access to a wider range of substrates. Additionally, the polarized Al–P bond in RAl=P(Mes*) was designed to exploit cooperative activation: the Lewis acidic Al center would coordinate to the carbonyl oxygen, increasing electrophilicity, while the

nucleophilic phosphorus attacks the carbonyl carbon. This dual activation strategy was envisioned to lower the barrier for addition even to less reactive carbonyls such as ketones or esters, enabling the reaction to proceed under milder conditions. By harnessing this Lewis acid–base synergy, our goal was to establish a new Wittig-type transformation, termed the ala-phospha-Wittig reaction (Scheme 12), capable of delivering phosphaalkenes from a broader set of carbonyl precursors than previously achievable.

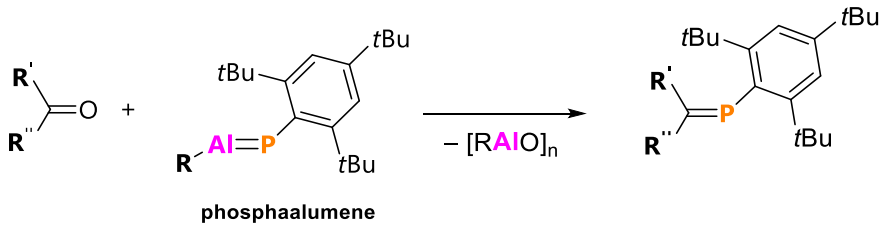

Scheme 12. Ala-phospha-Wittig reaction.

In this thesis we outline attempts to synthesize phosphaalumenes, using phospha-Wittig reagent Mes*P(PMe_3) and different Al(I) sources. These phosphaalumenes could potentially act as a tool to access phosphaalkenes, in a formal ala-phospha-Wittig reaction. In the Result and Discussion (Section 2.2) it is highlighted that attempts to make base-free phosphaalumenes with Mes*P(PMe_3) and different Al(I) precursor did not result in the isolation of phosphaalumenes. Instead, the intermediately formed phosphaalumene dimerizes in one case, or deactivates through C-H activation of on *o*-*t*Bu-group of the Mes* substituent (refer section 2.2).[66] Hence, the synthesis of phosphaalkene-based ligands was continued using the phospha-Wittig reaction.

1.3 Wittig Reaction and Modifications of Wittig Type Reactions

Element-element double bond formation is one of the most fundamental organic transformations. In this context one of the most popular reactions is the Wittig reaction used to form olefins from the reaction of carbonyl compounds with phosphorus ylides.[67] Over the years many modifications of Wittig-type reactivity have been explored. For example, In 1972, Rathke and Kow reported a borata-Wittig reaction where boron-stabilized carbanions reacted with *cyclo*-hexanone yielding the corresponding olefin.[68] Later the scope of the reaction was expanded by Tomioka[69-70], Morken[71-73], Pelter[74-77] and others[78-81]. Furthermore, in 1998, Protasiewicz *et al.* reported the phospha-Wittig reaction to synthesize P=C double bonds, *vide supra*.[30] Even before Wittig's seminal report on the Wittig reaction, Staudinger noted that iminophosphoranes $R_3P{=}NR'$ form imines when reacted with ketones or aldehydes to construct C=N double bonds, a so-called aza-Wittig reaction.[82] Moreover, mechanistic investigations on the reaction of azides with phosphines, revealed that azidophosphoranes $RN_3PR'_3$ were formed as intermediates. These can undergo N_2-elimination via a four-membered transition state to give the respective iminophosphoranes. However, these intermediates of the aza-Wittig reaction can be isolated when electron-rich or sterically demanding phosphines are used.[83]

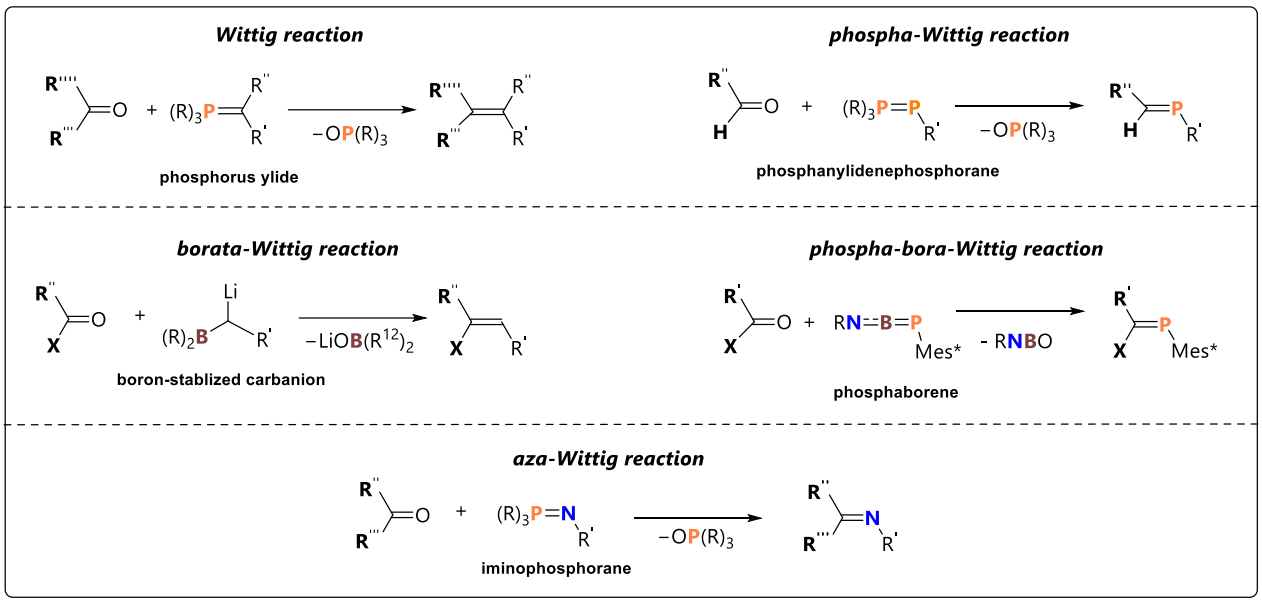

Scheme 13. General reaction scheme for Wittig reaction and modified Wittig reactions (R, R′, R″, R‴, R⁗ = alkyl or aryl groups).

1.4 Azidophosphoranes

Until the 1980s, azidophosphoranes (also termed phosphazides) were known to be transient species which form during the Staudinger reaction and were considered unstable with respect to N_2-elimination to give iminophosphorane below or at room temperature (Scheme 14).

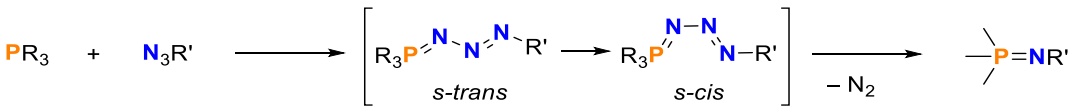

Scheme 14. Iminophopshorane formation via the elimination of N_2 from phosphazides.

However, it has since been reported that sterically demanding groups and electron withdrawing group introduction at the nitrogen atom could be utilized to stabilize azidophosphoranes, eventually rendering them isolable. In 1984, Kukhar's group extensively studied open chain phosphazides, in which they examined the effects of the substituents at the P and N atoms (Figure 8, **53**-**56**).[84-85]

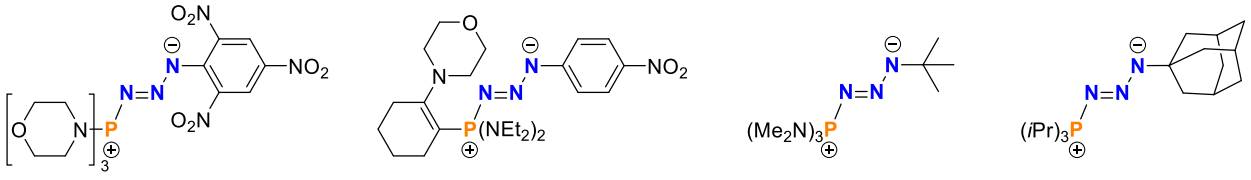

53 **54** **55** **56**

Figure 8. Some examples of electronically and sterically stabilized phosphazides.

They found that two strongly electron withdrawing groups in the *ortho*-positions of the aryl group on the N_α atom and morpholine-substituted phosphines greatly stabilized the corresponding phosphazides and allowed their isolation at room temperature (Figure 8). Hence, this study combined with Struchkov's findings on phosphazides (Figure 8, **53**) formed in the reaction of tris(morpholino) phosphine and 2,4,6-trinitrophenylazide, paved the way for studying the chemistry of free phosphazides. Phosphazides are best described by at least three resonance structures (Figure 9, **57**, **58**, **59**). Furthermore, it is evident from the resonance scheme that negative charge is accumulated at the N_α and N_γ atoms. The nucleophilicity of azidophosphoranes was also verified experimentally, through the reaction with $[Et_3O][BF_4]$ giving the N_α alkylation product. This clearly indicates that the N_α atom in these systems is the most nucleophilic site.

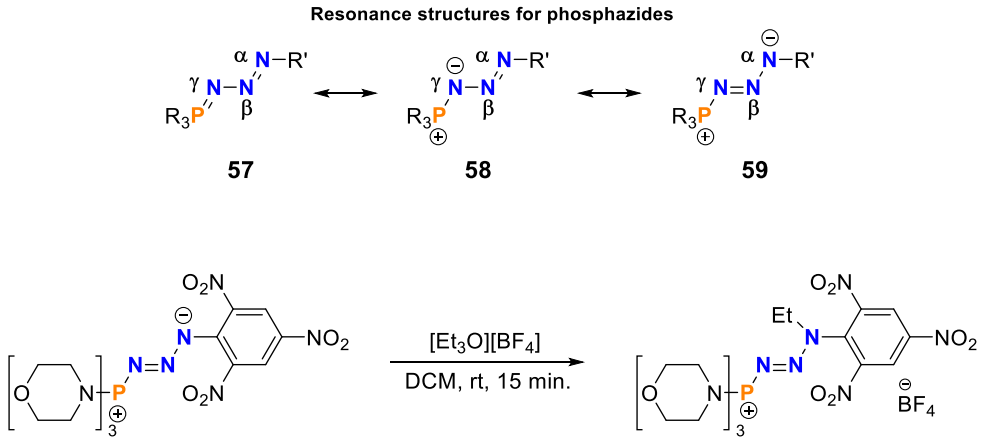

Figure 9. Resonance structures for phosphazides (top) and experimental identification of the most nucleophilic nitrogen atom (bottom).

Later other open chain azidophosphoranes (Figure 10, **60**) were isolated, based on cage phosphines, so-called proazaphosphatranes, pioneered by Verkade.[86] Over the years different types of phosphazides were isolated and characterized, for example, cyclic-[87-88], macrocyclic-[89-97], main group-[98-106], and transition metal[107-109] based phosphazides.

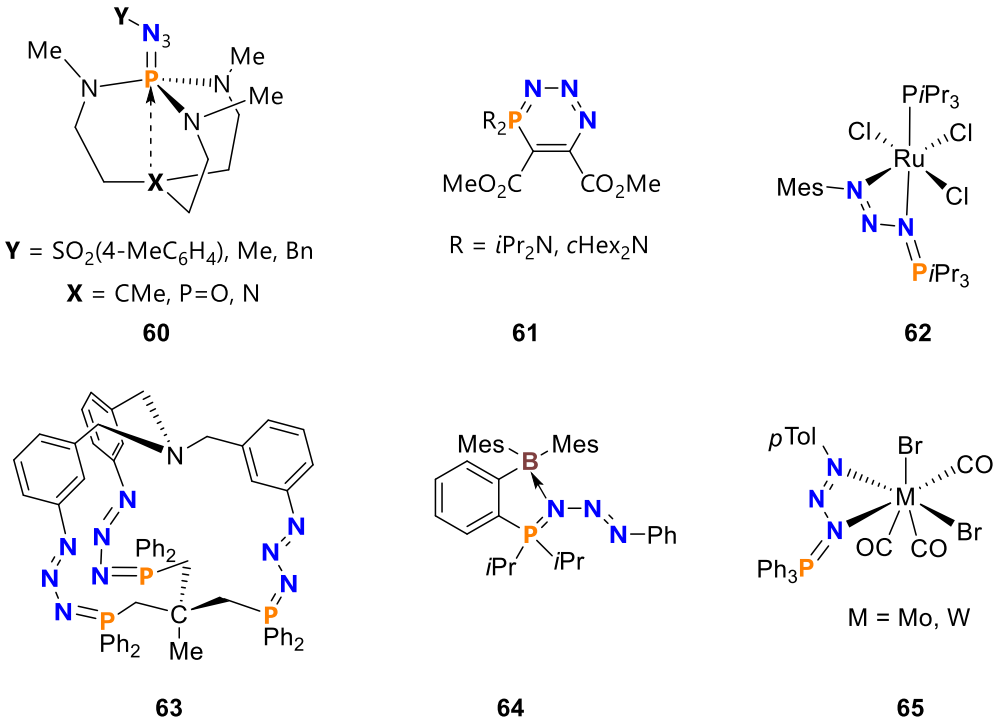

Figure 10. Some examples of proazaphosphatranes-, cyclic-, macrocyclic-, main group-, and transition metal based phosphazides.

1.5 Triazabutadienes

Triazabutadienes or π-conjugated triazenes are defined in the literature as conjugated dienes with three nitrogen atoms.[110-112] In 1965, Winberg and Coffmann first introduced triazabutadienes formed in the reaction of a bis(imidazolidine) with tosyl-, *p*-nitrophenyl, and diphenyl phosphonyl azide at 0 °C (Figure 11).[113] Interestingly, only in 1981 this class of π-conjugated triazenes reappeared in the literature when benzothiazole-based triazabutadiene systems were introduced by Fanghänel and co-workers. These were synthesized in a base-assisted coupling of diazonium salts with 3-methyl-2-iminobenzthiazoline (Figure 11).[114] Furthermore, a more facile single step synthetic route towards N-heterocyclic carbene (NHC) based triazabutadienes was reported by the Bielawski group utilizing imidazolium salts as NHC-precursors, from which the NHC was generated *in-situ* by addition of a base, and subsequent addition of azides (Figure 11).[115] Additionally, the groups of Katritzky, Burgarin, and Jewett also contributed towards the synthesis of NHC-based triazabutadienes.[116-120] More recently, reports from Beweries, Hering-Junghans and co-workers described a new organic transformation that stabilizes the reactive intermediates of the aza-Wittig reaction, namely azidophosphoranes, and treats them with various aldehydes to readily form triazabutadienes. They termed this novel approach the "azide-Wittig reaction" (refer to Section 2.3).[121]

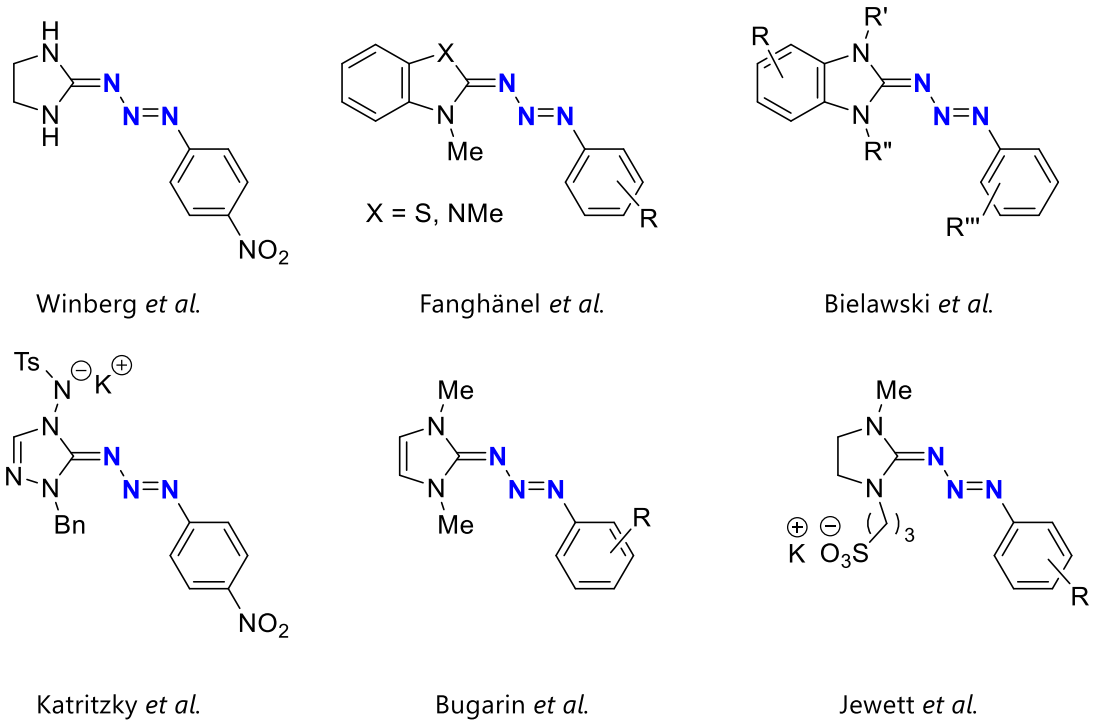

Figure 11. Contribution of various groups towards the synthesis of triazabutadienes.

In the contemporary literature various applications of triazabutadienes are outlined. In 2009, Lyapkalo and co-workers developed a two-step route towards guanidinium salts, where different NHCs were reacted with azides to generate π-conjugated triazene as intermediates, which upon

acidic workup furnished their guanidine adducts (Scheme 16).[122] Similarly, other guanidinium salts and free guanidines were reported by Tamm and co-workers.[123] Beside guanidine formation, triazabutadienes find application as diazo- or azide-transfer reagents, respectively, as developed by Kitamura and co-workers (Scheme 15).[124-125]

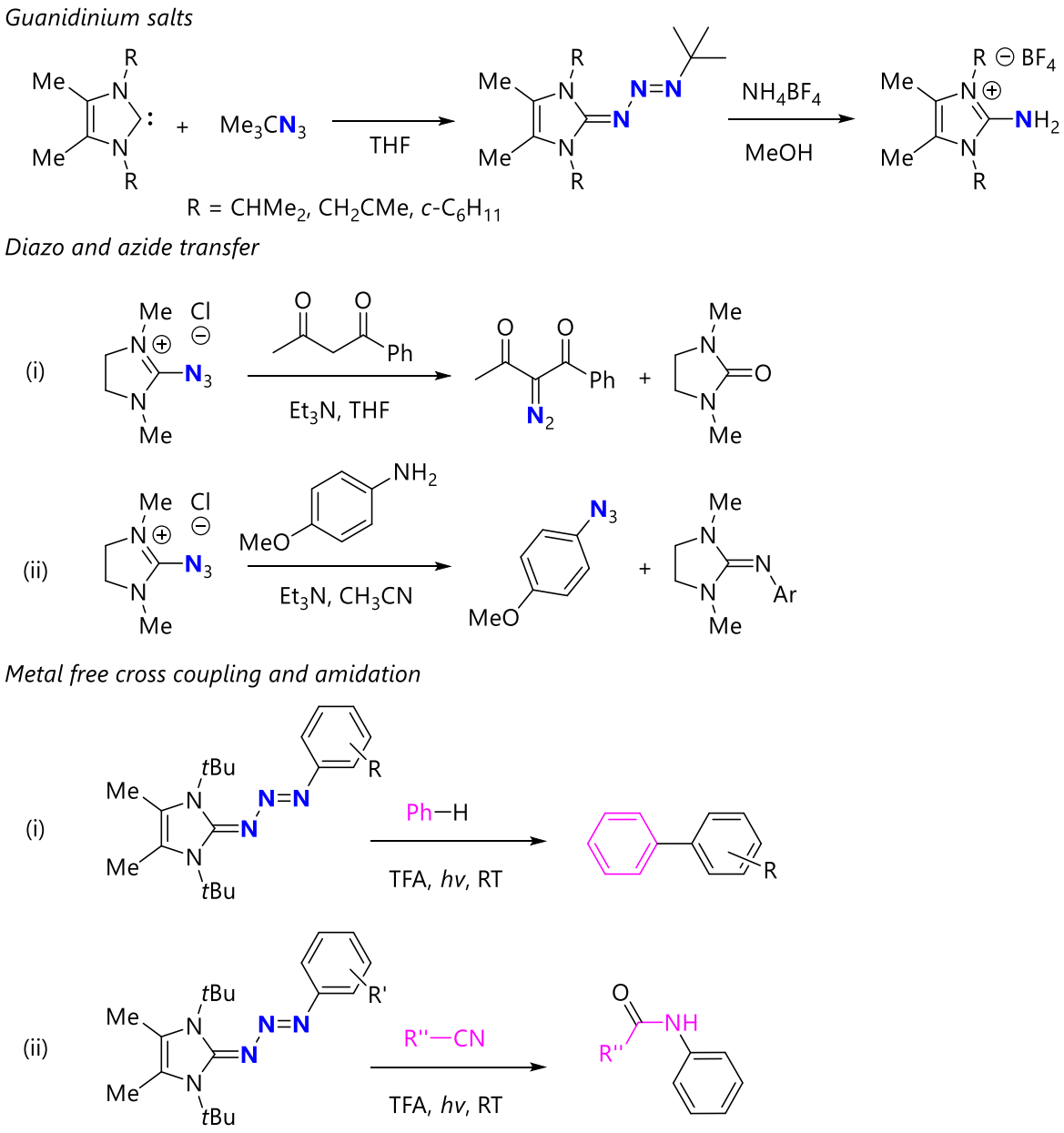

Scheme 15. Applications of triazabutadienes.

Interestingly, Bielawski and co-workers synthesized triazabutadiene-containing polymers from the reaction of polystyrene-derived azides with readily available NHCs (Scheme 16).[126-127] Moreover, Arnold and co-workers reported insertion of adamantyl azide into the metal-carbene bond of lanthanide complexes, which suggests that triazabutadienes ligands can effectively stabilize heavy metal (Y, Ce) ions (Scheme 16).[128-131] Additionally, NHC-based triazabutadiene can undergo metal-

free cross-coupling with unactivated arenes or nitriles via photoactivation of π-conjugated triazenes to give the corresponding aryl-aryl coupling product or anilides (Scheme 15).[132-133] Furthermore, Jewett and co-workers highlighted NHC-modified triazabutadienes that can deliver aryl diazonium ions to fluorescently labeled proteins by tyrosine-selective modification. The labeling can be triggered by low-pH-induced liberation of the diazonium species. (Scheme 16).[115, 134]

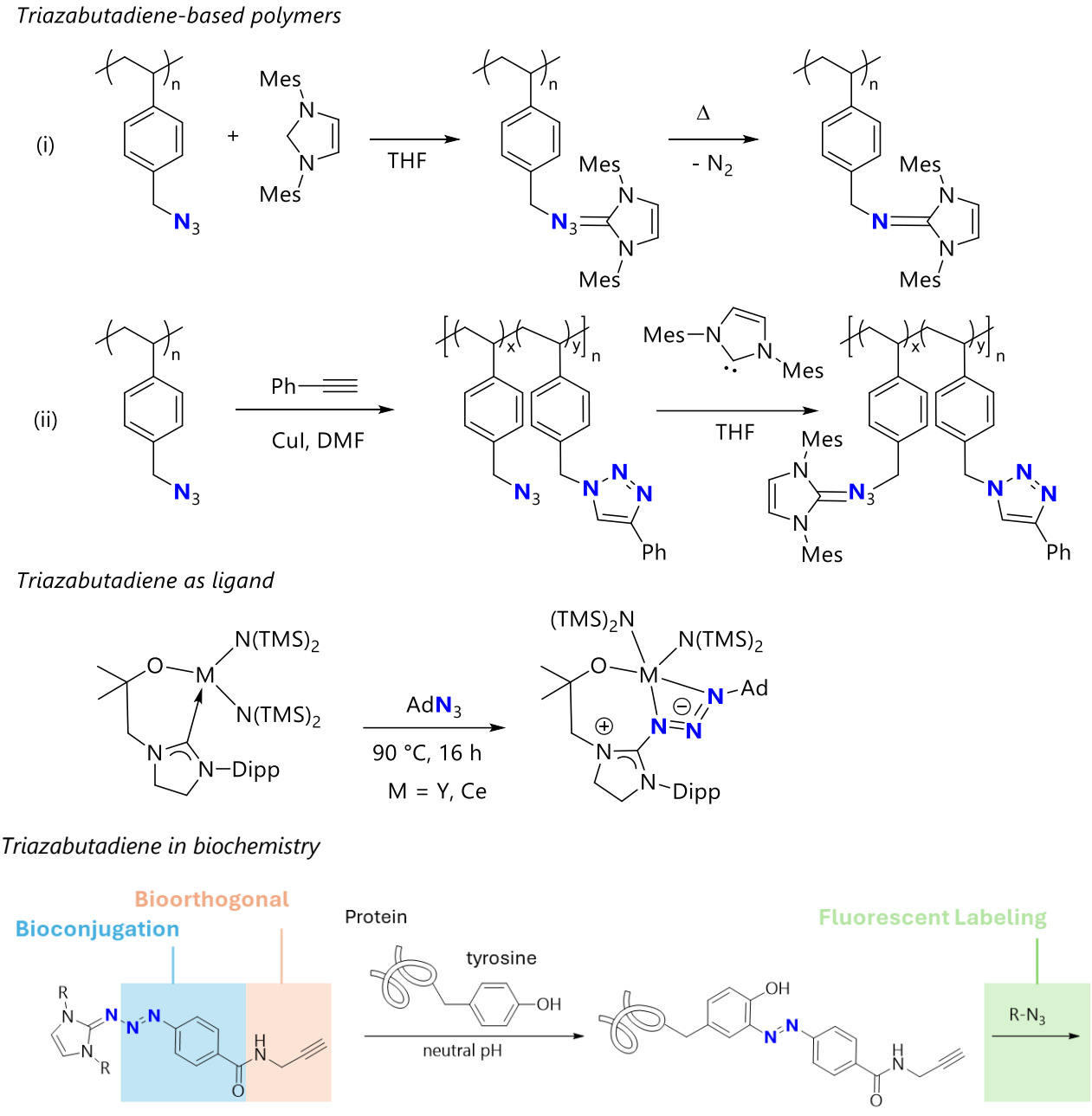

Scheme 16. Applications of triazabutadienes.

2 Result and Discussion

2.1 Overview

The initial objective of this thesis was to develop transition metal complexes for the activation of small molecules incorporating P,N,P-type phosphaalkene ligands. This investigation began with an effort to investigate whether phosphaalumenes can act as ala-phospha-Wittig reagents. This aimed to overcome the conventional constraints associated with phospha-Wittig chemistry, particularly its restriction to aldehyde substrates. To generate phosphaalumenes, the phosphinidene transfer reagent Mes*P(PMe_3) was employed in combination with various aluminum(I) precursors, namely ^{Dipp}NacNacAl, $(Cp^*Al)_4$, and $Cp^{3t}Al$. While the direct isolation of phosphaalumenes was unsuccessful in all cases, spectroscopic and crystallographic evidence supported their transient existence. This was illustrated by the formation of a dimeric species, $[Cp^*Al(\mu\text{-}PMes^*)]_2$, and by isolation of C–H activation products such as 1,2-P,Al-tetrahydronaphthalene derivatives. These observations highlighted the importance of steric protection at the phosphorus center to kinetically stabilize the reactive P=Al bond. Given the limited success in stabilizing phosphaalumenes with a Mes*-substituent at the P atom, the attention was turned to phospha-Wittig reagents to synthesize phosphaalkenes through suitable aldehyde substrates. Previously reported routes were scaled up successfully to produce gram-scale quantities of Mes*P(PMe_3). With these in hand, the synthesis of phosphaalkene-containing P,N,P-type ligands was pursued using diarylamine scaffolds such as carbazole and diphenylamine, functionalized with two aldehyde groups. When the model system 2,2′-iminobisbenzaldehyde was reacted with two equivalents of Mes*P(PMe_3) a mono-phosphaalkene product bearing an unreacted aldehyde moiety was obtained. Unexpectedly, this intermediate could be further converted into a triazabutadiene (TBD) framework upon reaction with Mes^*N_3 in the presence of PMe_3, bypassing the traditional aza-Wittig pathway. This transformation, termed the “azide-Wittig” reaction, provides facile access to structurally diverse TBDs from aldehydes and azides under mild conditions. The protocol tolerates a broad range of substituents and thus constitutes a versatile synthetic tool. Additionally, the reaction of two equivalents of Mes*P(PMe_3) with 3,6-dimethyl-9H-carbazole-1,8-dicarbaldehyde afforded the target P,N,P-type bis-phosphaalkene ligand in good yield. This ligand enabled subsequent metalation reactions. Notably, its alkali metal salts [$^{Mes^*2}$PNP]M (M = Na, K) were accessed using $M[N(SiMe_3)_2]$ bases, producing highly basic monoanionic amido species. Coordination of this ligand to Rh using $[Rh(cod)Cl]_2$, afforded two distinct dinuclear Rh(I) species. One of these demonstrated a rare case of C–H activation at the Mes* group adjacent to the phosphaalkene units and another revealed three different phosphaalkene coordination modes within a single complex. The study also includes the synthesis and structural characterization of the mononuclear Rh(I) carbonyl complex demonstrating the ligand's ability to stabilize square-planar Rh(I) centers.

2.2 Phoshaalumene

2.2.1 ^{Dipp}NacnacAl as Al(I) Source

Efforts to access phosphaalumenes commenced with the reaction between the phosphinidene transfer reagent Mes*P(PMe$_3$) and the low-valent aluminum(I) species ^{Dipp}NacnacAl in C_6D_6. At room temperature, no reactivity was observed by NMR spectroscopy. However, upon heating to 60 °C for 2 h, a new ^{31}P NMR signal at –158.7 ppm (splitting into a doublet upon ^{1}H decoupling) and a doublet at 3.48 ppm in the ^{1}H NMR spectrum indicated the formation of a novel P–H containing product (Scheme 8, **66**).

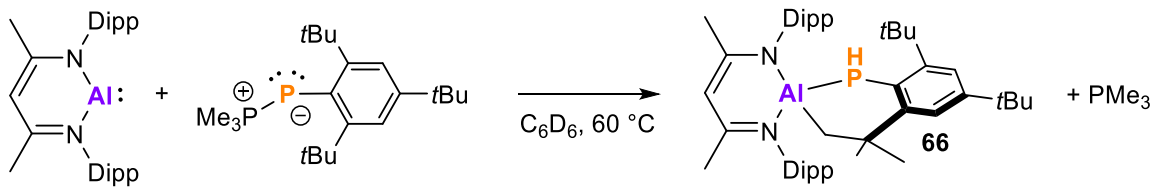

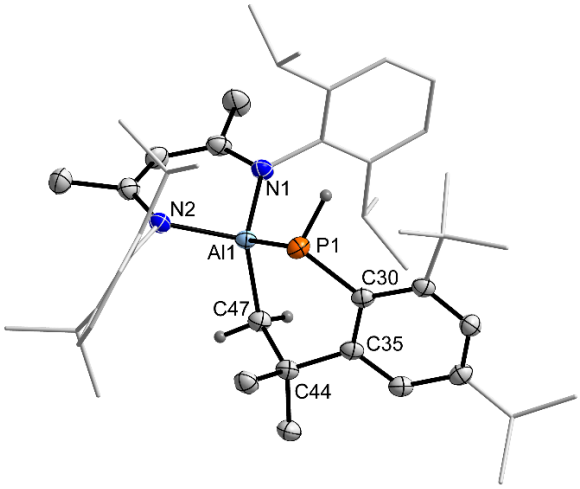

Figure 12. Synthesis of a P,Al-tetrahydronapthalene derivative and molecular structure of **66** with Ellipsoids drawn at 50% with C-H-atoms (except those on C47 and P1) omitted, Dipp- and *t*Bu-groups rendered as wireframe for clarity.

Crystallization from *n*-hexane yielded single crystals suitable for X-ray diffraction experiments (Figure 12). The molecular structure revealed a six-membered heterocycle containing Al and P in a 1,2-arrangement, consistent with C–H activation at one of the *o*-*t*Bu substituents of the Mes* group. While the desired phosphaalumene could not be isolated, the structural data provided clear evidence of its transient formation and subsequent transformation to the thermodynamically more stable C-H deactivation product. However, when free phosphinidene species Mes*–P are generated intermediately, they often undergo C–H bond activation at the *ortho*-*t*Bu group, resulting in the formation of cyclic phosphaindane derivatives.[135-137] To further understand the outcome, quantum chemical calculations were performed at DLPNO-CCSD(T)/def2-TZVP//PBE0-

D3/def2-SVP level of theory to compare the relative energetics of possible reaction pathways. The data indicate that although the formation of the phosphaalumene intermediate is slightly exergonic ($\Delta_R G°$ = –70.9 kJ/mol), the subsequent intramolecular C–H activation is significantly more favorable ($\Delta_R G°$ = –119.4 kJ/mol). This explains the isolation of the activation product and highlights the necessity to kinetically protect the reactive Al=P bond and avoid undesired activation pathways.

2.2.2 $(Cp^*Al)_4$ as Al(I) Source

Following the challenges in stabilizing phosphaalumenes with ^{Dipp}NacnacAl, we turned to the tetrameric low-valent aluminum species $(Cp^*Al)_4$ as an alternative Al(I) source. Heating Mes*P(PMe_3) with $(Cp^*Al)_4$ in a 4:1 ratio in benzene at 80 °C led to the formation of yellow crystalline material, from which the four-membered [Cp*Al(μ-PMes*)]$_2$ dimer (**67**) was isolated and structurally characterized (Scheme 17). This centrosymmetric species features P atoms in distorted pyramidal environments and Al–P bond lengths typical of single bonds, reflecting dimerization of the transient phosphaalumene Mes*P=AlCp*. As with the ^{Dipp}NacnacAl system, the desired monomeric phosphaalumene was not isolable, instead reacting under thermodynamic control to yield more stable aggregates. ^{31}P NMR spectroscopy of the reaction mixture revealed additional species, including a signal at –107.6 ppm, indicative of a three-membered compound. Recrystallization from *n*-pentane afforded Mes*P(AlCp*)$_2$ (Scheme 17, **68**), a 2π-aromatic heterocycle derived from further Al incorporation at the phosphaalumene in a formal [2+1]-cyclization.

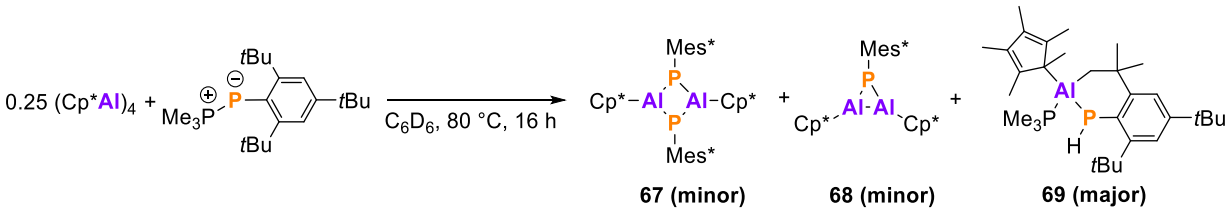

Scheme 17. Reaction of Mes*P(PMe_3) with $(Cp^*Al)_4$.

DFT calculations at the DLPNO-CCSD(T)/def2-TZVP//PBE0-D3/def2-SVP level of theory supported the observed reactivity, showing that dimerization of the intermediate, monomeric Mes*P=AlCp* ($\Delta_R G°$ = –14.3 kJ/mol) to form **67** ($\Delta_R G°$ = –75.0 kJ/mol), or its reaction with an additional equivalent of Cp*Al to give **68** ($\Delta_R G°$ = –66.1 kJ/mol), are both exergonic. These data suggest that without sufficient steric hindrance, the monomer cannot be kinetically stabilized. After removing the dimeric and trimeric species, the remaining solution yielded a third product upon slow cooling: compound **69**, identified as a C–H activation product (Scheme 17). Similar to compound **66**, this species results from intramolecular activation of a *t*Bu group on the Mes* substituent along the Al=P bond. ^{31}P and ^{1}H NMR spectroscopy revealed a PH-coupled signal and an IR band at 2335 cm^{-1}, confirming the presence of a P–H bond. X-ray crystallography showed that Al is coordinated to both a PMe_3 and a PH-Mes* fragment in a distorted tetrahedral geometry (Figure

13). Thermodynamic analysis again confirmed that compound **69** is the most stable product, forming from the phosphaalumene intermediate via C–H activation in a strongly exergonic process.

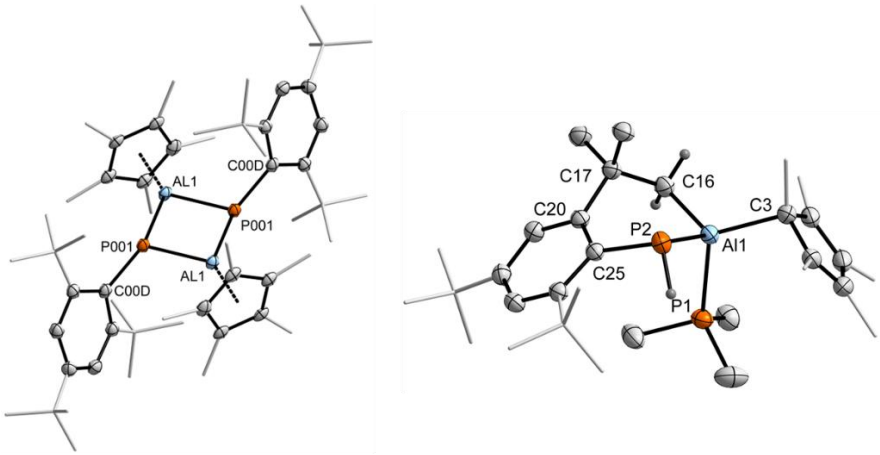

Figure 13. Molecular structures of **67** (left) and **69** (right). Ellipsoids drawn at 50% with C-H-atoms (except those on C16 and P2 for **69**) omitted, *t*Bu-, Cp*-, Me- and Tip- groups rendered as wireframe for clarity.

2.2.3 $Cp^{3t}Al$ as Al(I) Source

To further investigate the influence of the Al(I) source and substitution pattern on the phosphaalumene formation, $Cp^{3t}Al$ was employed in a final set of experiments. When Mes*P(PMe_3) and $Cp^{3t}Al$ were combined in a 1:1 ratio in C_6D_6 at room temperature, ^{31}P NMR spectroscopy indicated partial conversion, with signals corresponding to both the desired product and unreacted Mes*P(PMe_3).

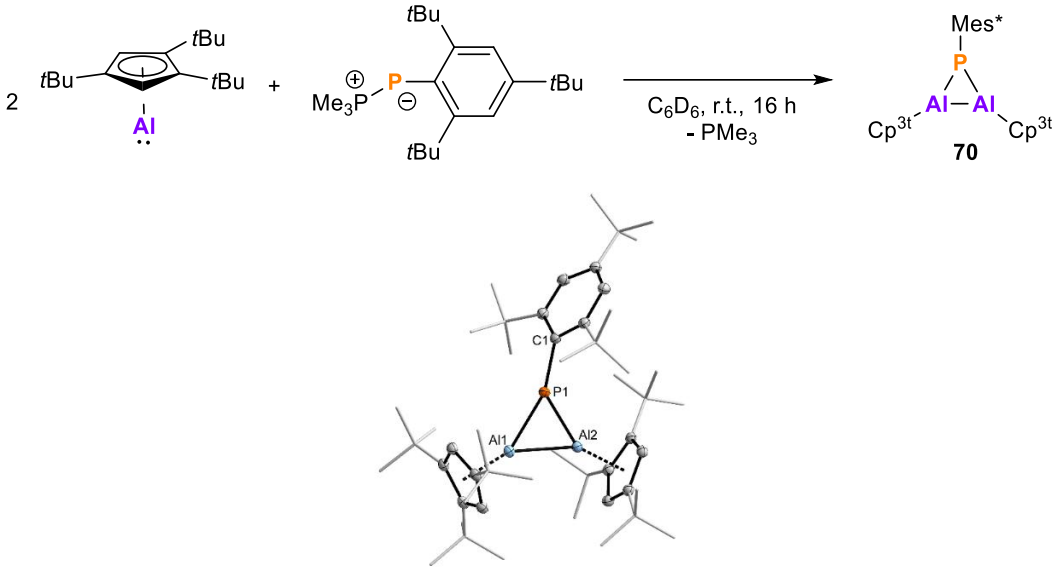

Figure 14. Synthesis of Mes*P($AlCp^{3t}$)$_2$ and molecular structure of **70** with ellipsoids drawn at 50% with C-H-atoms omitted, *t*Bu groups rendered as wireframe for clarity.

To drive the reaction to completion, the experiment was repeated with a slight excess of $Cp^{3t}Al$ and extended heating, leading to the formation of a new species, $Mes^*P(AlCp^{3t})_2$ (**70**) (Figure 14, top), which crystallized as a pale yellow solid from an *n*-pentane solution. The ^{27}Al NMR spectrum revealed a broad singlet at –43 ppm, which was in the range of $Cp^{3t}AlBr_2$ ($\delta(^{27}Al)$ = –46 ppm),[138] characteristic of aluminum centers in strained environment, and consistent with the presence of two $AlCp^{3t}$ units coordinated to a single phosphorus center. SC-XRD experiments confirmed the molecular structure of **70** as a three-membered PAl_2 ring in which the P atom adopts a planar coordination geometry (Figure 14, bottom). The Al–P bond distances fall within the typical range for P–Al interactions, and the geometry of the ring is consistent with a slightly distorted 2π-aromatic system.

2.3 The azide-Wittig Reaction

Following the limited success in isolating base-free phosphaalumenes and to potentially use them in ala-phospha-Wittig reactions, the research direction was shifted toward designing bis-aldehydes to be used in the assembly of PA-containing ligands using the phospha-Wittig approach. These frameworks offer dual functionalization sites. In particular, diphenylamine and carbazole-derived scaffolds were functionalized to carry two aldehyde groups (Figure 15, **71** and **72**) using literature-established methods,[139] enabling subsequent formation of multidentate phosphaalkene-type ligands.

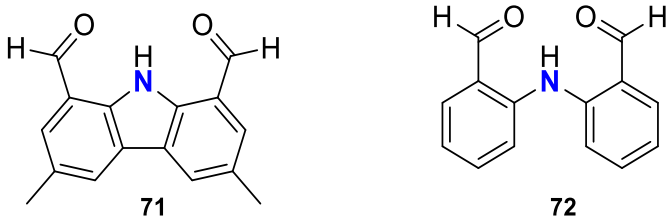

Figure 15. 3,6-dimethyl-9H-carbazole-1,8-dicarbaldehyde (**71**) and 2,2′-iminobisbenzaldehyde (**72**)

2.3.1 Serendipitous Formation of PN_4 Ligand

While attempting to generate a P,N,P-type phosphaalkene ligand, the reaction between $Mes^*P(PMe_3)$ and 2,2′-iminobisbenzaldehyde in a 2:1 ratio in C_6D_6 at 50 °C yielded a mono-functionalized product (Figure 16, **73**). Interestingly, only one of the two aldehyde groups was converted to a phosphaalkene moiety, leaving the second formyl unit available for further functionalization. The resulting P,N,O-type compound **73** was treated with Mes^*N_3 and PMe_3 in toluene under mild conditions, leading, after workup and crystallization compound **74**, a triazabutadiene (TBD) derivative (Figure 16, **74**). SC-XRD analysis revealed that this transformation proceeds via a formal azide-to-carbonyl transfer in a Wittig-type reaction, producing an *E*-configured TBD arm with three conjugated nitrogen atoms. NMR and IR data confirmed the presence of both phosphaalkene and imine functionalities in **74**. This reaction represents a previously unreported organic transformation and was therefore termed as the "azide-Wittig"

reaction. Unlike in the classical aza-Wittig reaction, which typically proceeds through iminophosphorane intermediates, the pathway discovered here allows direct formation of triazabutadienes (TBDs) under kinetically controlled conditions.

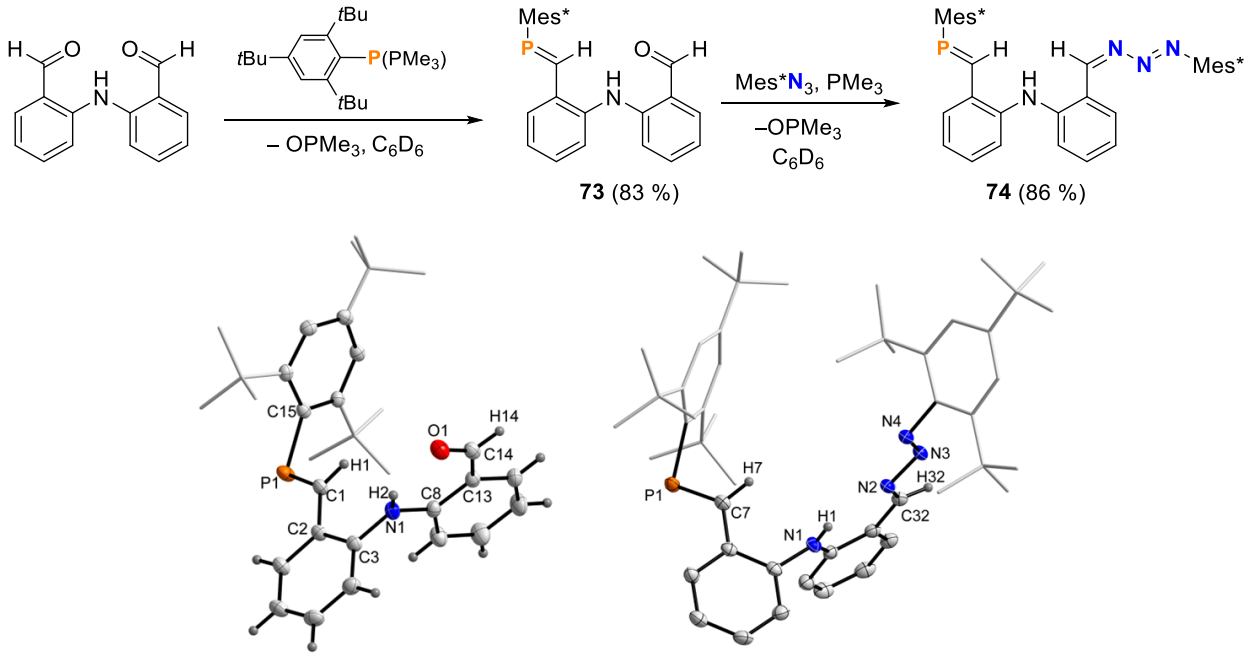

Figure 16. Synthetic pathway to TBD **74** along with molecular structure of **73** (left), **74** (right) and ellipsoids drawn at 50% (C-H protons are omitted and *t*Bu (left) and Mes* (right) groups rendered as wireframe for clarity).

To better understand the mechanistic features, the Staudinger reaction of Mes*N_3 with PMe_3 was monitored in situ by ^{31}P NMR spectroscopy, which revealed two species at 29.3 and -22.1 ppm in a 97:3 ratio within 15 min of reaction progress. Two distinct species were observed, with calculated ^{31}P NMR shifts confirming their assignment as azidophosphorane Mes*N_3(PMe_3) and iminophosphorane Mes*N(PMe_3), respectively. DFT calculations supported a reaction pathway involving a low-energy *cis–trans* isomerization followed by nitrogen extrusion through a four-membered transition state, forming the final triazabutadiene product. The energetics of this transformation were consistent with experimental outcomes, establishing how kinetic control can significantly alter the reaction pathway, thereby switching from an aza-Wittig to an azide-Wittig regime.

2.3.2 Aldehyde Scope in Case of Mes*N_3 Azide

Having established the azide-Wittig transformation for the formation of triazabutadiene (TBD) frameworks, the next step focused on exploring the aldehyde substrate scope using Mes*N_3 and PMe_3 in the presence of varying aldehydes. In the model reaction with benzaldehyde, performed at 0 °C, ^1H NMR spectroscopy confirmed the clean formation of the *E*-configured TBD product

Mes*N_3C(H)Ph (Figure 17, **75**), which crystallized from MeCN upon cooling. Structural analysis revealed that the central phenyl ring of the Mes*-substituent and the planar $PhCHN_3$ units were nearly orthogonal, which might be due to steric repulsion. Encouraged by this result, a range of *para*-substituted benzaldehydes were tested.

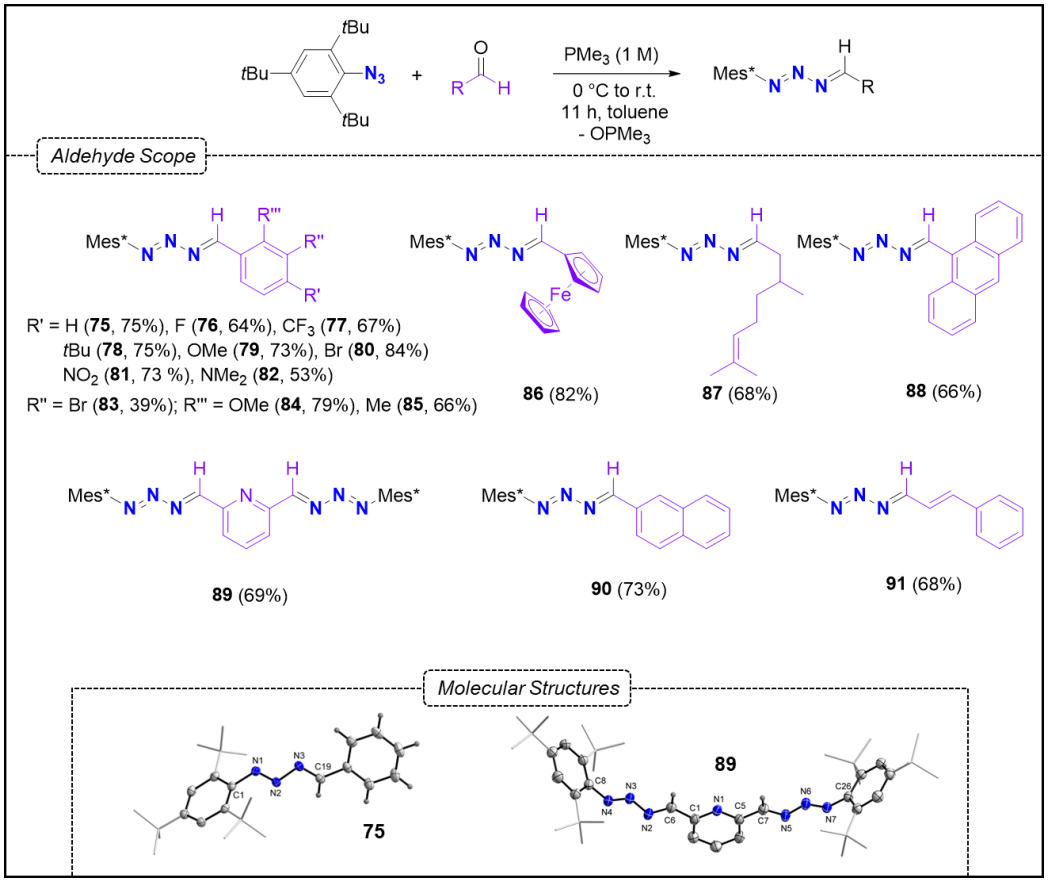

Figure 17. Top: Aldehyde scope using PMe_3 and the percentage given corresponds to isolated yields. Bottom: Molecular structure of **75** and **89**, and ellipsoids drawn at 50% (C-H protons are omitted and *t*Bu groups rendered as wireframe for clarity).

Electron-withdrawing groups such as CF_3, F, and Br afforded the corresponding TBDs (**77**, **76**, **80**) in good yields after work-up. Substrates with strongly electron-donating or synthetically sensitive groups, such as 4-NO_2 and 4-NMe_2, gave lower isolated yields (**81**, **82**), likely due to incomplete conversion or side-product formation during reaction. Substrates possessing substituents in the *ortho*-position, including 2-OMe and 2-Me, also participated efficiently in the reaction, delivering the products (**84**, **85**) in high yields. Additionally, bulky aromatic systems such as ferrocenyl (**86**), anthracenyl (**88**), and naphthyl (**90**) were successfully incorporated. These results demonstrate the broad tolerance of the azide-Wittig reaction to sterically and electronically diverse aldehydes. The transformation was also extended to heteroaromatic aldehydes. Notably, reaction with 2,6-pyridinedicarbaldehyde afforded a bis-TBD-functionalized pyridine derivative (**89**), which crystallized with nearly planar triazabutadiene arms. Single-crystal X-ray structures of **76** and **89**

confirmed the molecular connectivity and configuration of the triazabutadiene motifs (Figure 17, bottom). Furthermore, the reaction accommodated conjugated systems. For example, reaction with *E*-cinnamaldehyde yielded a triazahexatriene derivative (**91**) with three conjugated double bonds in the *E*-configuration. Similarly, the aliphatic aldehyde (*R*)-(+)-citronellal was converted to the corresponding TBD (**87**) as a yellow oil. In summary, this aldehyde screening confirms that the azide-Wittig protocol is a general and efficient method for synthesizing structurally diverse TBDs under mild conditions. Most substrates gave quantitative conversion as verified by NMR spectroscopy, with minor losses in isolated yield attributable to work-up or solubility limitations.

2.3.3 Azide Scope

To further explore the versatility of the azide-Wittig reaction, attention was turned to the effect of different organic azides and phosphines on the transformation. The stability and reactivity of various azidophosphoranes were first investigated using a combination of DFT calculations and variable temperature NMR spectroscopy (VT NMR). Theoretical studies indicated that nitrogen extrusion from azidophosphoranes is thermally accessible, with calculated activation barriers ranging from ~44 to 77 kJ·mol^{-1} depending on the azide and phosphine substituents.

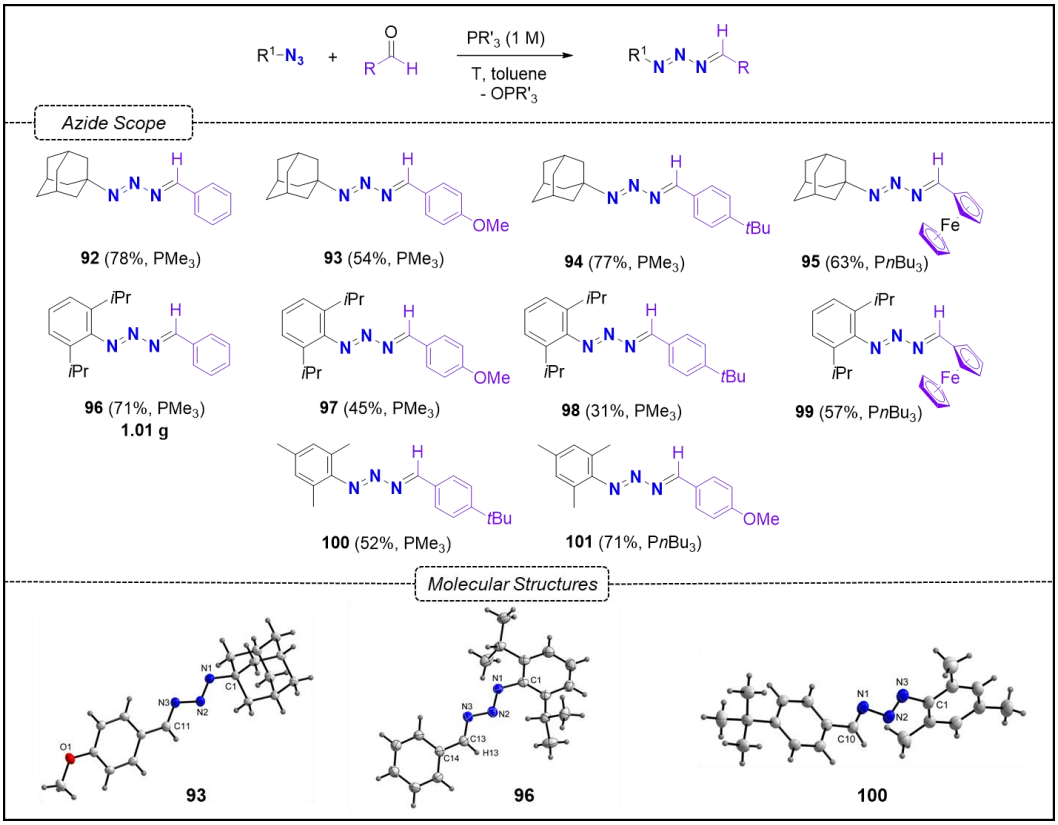

Figure 18. Top: Azide scope of azide-Wittig reaction along with the respective phosphine used. Bottom: Molecular structure of **93**, **96**, and **100** with ellipsoids drawn at 50%.

These results suggested that lower reaction temperatures could suppress premature decomposition and enable clean triazabutadiene formation. Experimental confirmation was completed using AdN_3 and PMe_3 in toluene-d_8. VT ^{31}P NMR studies revealed a thermally stable *trans*-azidophosphorane at –20 °C, which slowly isomerized to its *cis*-form near –10 °C. Subsequent reaction of AdN_3 with benzaldehyde and PMe_3 (1:1:1) at –78 °C, followed by gradual warming, yielded the triazabutadiene **92** in good yield (Figure 18). Related substrates, including 4-OMe and 4-*t*Bu benzaldehydes, formed TBDs **93** and **94** respectively in 54% and 77% yields. Notably, **94** exhibited limited thermal stability, when heated to 80 °C in benzene, it underwent decomposition to form 4-*t*Butylbenzonitrile and this thermal decomposition process parallels recent reports of Cu-catalyzed methods for converting ketones into benzonitriles.[140] When FcCHO was used, P*n*Bu_3 was selected as phosphine due to solubility limitations, leading to **95** in 63% yield. Next, reactions were performed using $DippN_3$ as the azide source. When combined with benzaldehyde and PMe_3 at –35 °C, followed by slow warming, the desired product **96** was isolated as an orange crystalline solid in 71% yield (Figure 18). X-ray analysis revealed that the plane of the Dipp group and $PhC(H)N_3$ units were rotated against each other by ca. 45° (Figure 18, bottom). The scalability of this reaction was demonstrated with a gram-scale synthesis of **96**. Additional benzaldehyde derivatives, such as 4-OMe and 4-*t*Bu, furnished TBDs **97** and **98** in moderate yields. For FcCHO, again, P*n*Bu_3 was required so that the formed OP*n*Bu_3 during the reaction could be washed away with hexane, leading to TBD **99** in 57% yield. Finally, the scope was extended using $MesN_3$. Reaction with PMe_3 and 4-*t*Bu-benzaldehyde yielded compound **100**, while the corresponding 4-OMe-benzaldehyde reaction gave **101**, which was easily crystallized from *n*-pentane (Figure 18, bottom). Both reactions provided satisfactory isolated yields, reinforcing the compatibility of Mes-based azides with the azide-Wittig methodology. Altogether, this scope study demonstrates the robustness of the azide-Wittig reaction across a wide range of azides and aldehydes. Yields were consistently good when low temperatures and appropriate phosphines were employed. In conclusion, this study showed a facile route towards triazabutadiene termed the "azide-Wittig" reaction, which has been overlooked since Staudinger's seminal report, a century ago.

2.4 Rh(I) P,N,P-Phosphaalkene Complexes

In the final stage of this research, the focus shifted to designing metal complexes based on newly developed P,N,P-type bis-phosphaalkene ligands. A key structural component was the 3,6-dimethyl-9H-carbazole-1,8-dicarbaldehyde backbone, chosen for its rigidity and symmetric bifunctionality. Following successful ligand synthesis, its deprotonation using non-nucleophilic alkali metal bases enabled access to monoanionic P,N,P systems, which were subsequently reacted with $[Rh(cod)Cl]_2$ to exemplarily explore their transition metal coordination behavior. The rationale behind synthesizing the Rh(I) complex was to stabilize a 14-electron T-shaped species bearing a cyclooctadiene ligand, which could serve as a potential platform for small-molecule activation.

2.4.1 Synthesis of Highly Basic Monoanionic P,N,P-type Bis-phosphaalkene Ligand

The bis-phosphaalkene ligands were synthesized by reacting two equivalents of Mes*P(PMe$_3$)[61] with the 3,6-dimethyl-9H-carbazole-1,8-dicarbaldehyde (**102**) under mild thermal conditions. The resulting compound, ^{Mes*2}PNP (Scheme 18, **103**), was obtained in high yield and exhibited a ^{31}P NMR signal at 249.9 ppm, which was on the lower end of the typical range for Mes*-substituted phosphaalkenes,[32, 34-35, 47] suggesting electronic delocalization from the carbazole unit to π* orbitals of the P=C unit of the phosphaalkene. An analogous ligand (Scheme 18, **104**) incorporating bulky ^{Dipp}Ter groups was synthesized via a similar approach but required extended reaction time of 14 days at elevated temperatures. Alongside **104**, a mono-phosphaalkene by-product (**105**) was also identified,[121] as evidenced by distinct ^{1}H NMR resonances including a deshielded N*H* doublet and characteristic signals for aldehyde and P=C(*H)* protons. These results confirm the previously mentioned stepwise formation of the bis-phosphaalkene and mono-functionalized PNO-type species under different stoichiometries and reaction conditions. Single-crystal X-ray diffraction of **103** and **104** confirmed the *E*-configuration of both P=C units (Figure 19). In the case of **103**, intramolecular hydrogen bonding was observed between the central NH and both phosphorus atoms. For **104**, the large ^{Dipp}Ter groups induced asymmetric orientation of the two phosphaalkene arms, yet both P=C bonds remained coplanar with the carbazole core.

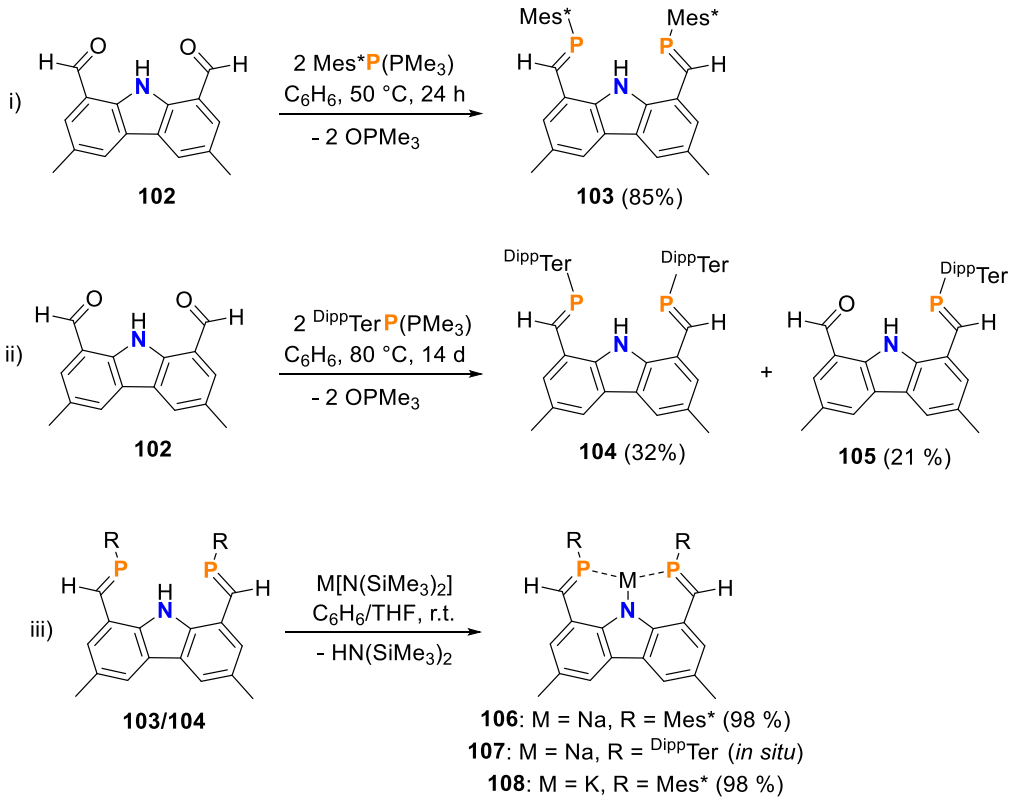

Scheme 18. a) Synthesis of novel ^{R2}PNP phosphaalkene ligands **103** and **104**.[a] Conditions for **103**: C_6H_6, 50 °C, 24 h; for **104**: C_6H_6, 80 °C, 14 d. b) Synthesis of M[^{Mes*2}PNP] (M = Na (**106**), K (**108**)) and Na[^{DippTer}PNP] (**107**).

To enable further reactivity, the acidic N*H* proton of **103** was removed using non-nucleophilic bases M[N(SiMe$_3$)$_2$] (M = Na, K), yielding the corresponding alkali metal salts **106** (Na) and **108** (K) in quantitative yields. Deprotonation was confirmed by the disappearance of the N*H* signal in the ^{1}H NMR spectrum and its associated IR band. The ^{31}P NMR signals of the salts [**106** ($\delta(^{31}P)$ = 228.4 ppm); **108** ($\delta(^{31}P)$ = 236.8 ppm)] were shifted significantly upfield compared to the neutral ligand ($\delta(^{31}P)$ = 249.9 ppm), consistent with increased electron density at phosphorus following metalation. Crystallographic analysis of **106** revealed a distorted seesaw coordination geometry around Na$^+$, coordinated by the PNP backbone and an Et$_2$O solvent molecule (Figure 19). The Na–N and Na–P bond distances were in expected ranges for ionic interactions, and the complex geometry supported the formulation of a monoanionic, strongly basic P,N,P-type phosphaalkene ligand.

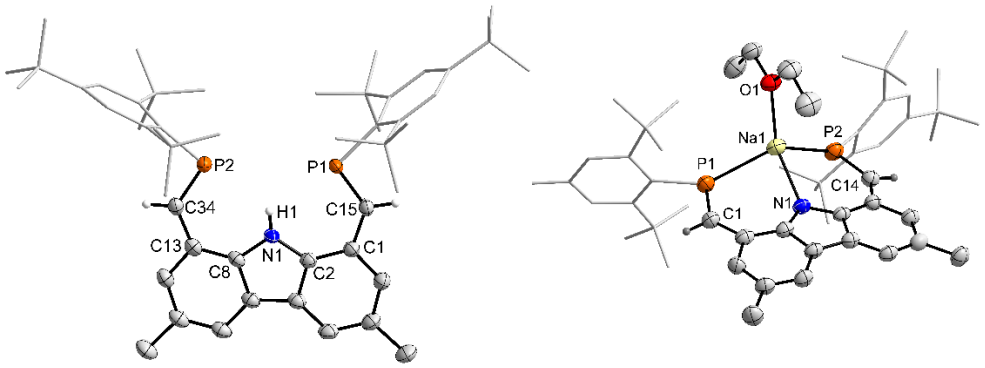

Figure 19. Molecular structures of **103** (left) and **106** (right). Ellipsoids drawn at 50% probability. H atoms (except N*H* and RP=C*H*R) omitted and Mes* groups rendered as wireframe for clarity.

This set of ligands and their alkali metal derivatives represent a versatile platform for further metal coordination chemistry, particularly due to their high basicity, making them ideal candidates for engaging in transition metal complexation as shown in the subsequent studies of Rh(I) complexes.

2.4.1 Synthesis of Mononuclear and Dinuclear Rh(I) Complexes

To investigate the coordination behavior of the monoanionic P,N,P-type phosphaalkene ligand, reactions were carried out between sodium salt **106** and [Rh(cod)Cl]$_2$ in a 2:1 ratio, ^{31}P NMR spectroscopy revealed the formation of two major species: a singlet at 249.9 ppm, corresponding to free ^{Mes*2}PNP ligand, and a doublet at 46.7 ppm ($^1J_{P–Rh}$ = 132 Hz), suggesting successful coordination to Rh(I) and formation of a new complex (Scheme 19, **109**).

a) Formation of a phosphaindane

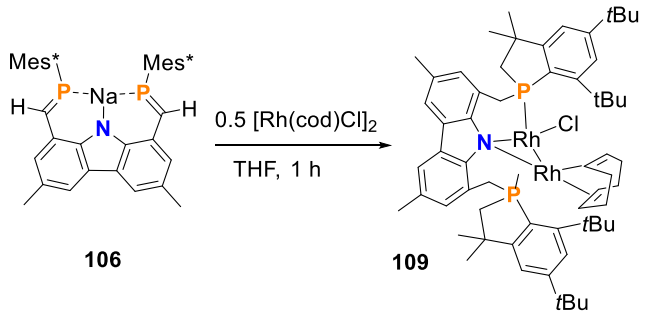

b) Phosphaindane and phophaalkene complex

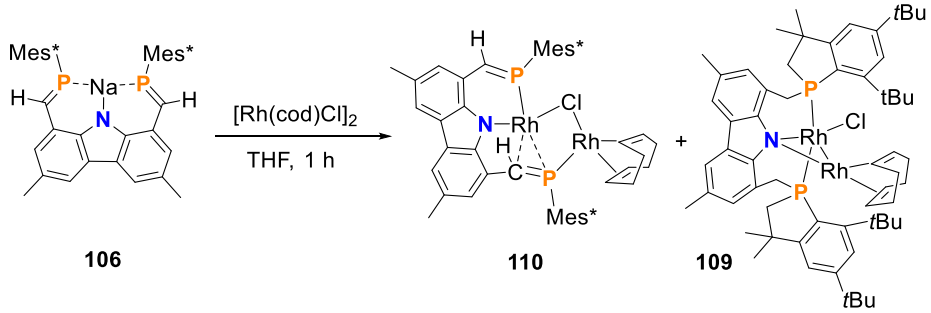

Scheme 19. Reactions of **106** with one or two equivalent of $[Rh(cod)(Cl)]_2$.

In the ^{1}H NMR spectrum, multiple sets of doublets were observed, characteristic of C–H activation at the phosphaalkene unit. This transformation resembles reported cyclometalation reactions in PN-type systems[28, 34-35] and results in the formation of a phosphaindane-type structure. Single-crystal X-ray diffraction confirmed that complex **109** features a dinuclear Rh(I) core (Figure 20), with the central nitrogen of the carbazole as bridging atom between the rhodium centres. Rh1 adopts a square-planar geometry, while Rh2 displays a trigonal pyramidal arrangement (when not considering the Rh-Rh interaction).

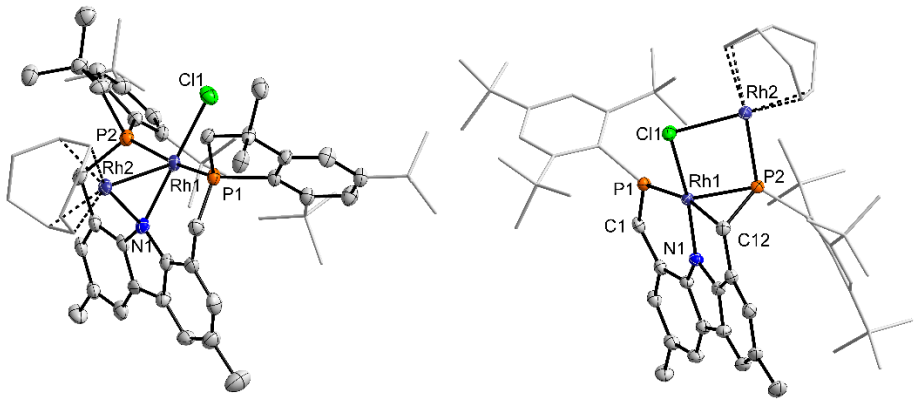

Figure 20. Molecular structures of complexes **109** (left) and **110** (right). Ellipsoids drawn at 50% probability. Hydrogen atoms are omitted and cod, *t*Bu (left) and Mes* (right) groups rendered as wireframe for clarity.

The two Rh centers are positioned at a distance of 2.6334(9) Å, indicative of a potential metal–metal interaction (cf. $\Sigma_{r(cov)}$(Rh–Rh) = 2.50 Å).[141] Additionally, Rh1 in complex **109**, can be best described as a 16-valence electron square planar Rh(I) centre (excluding Rh-Rh interaction) and both metal centers were bridged by carbazole N atom (Rh2–N1 = (2.094(6) Å; Rh1–N1 = (2.149(7) Å). To better understand the nature of this Rh–Rh interaction, DFT calculations were conducted. The HOMO was found to be a non-bonding orbital with *d*-character contributions from both Rh centers, while the HOMO–1 illustrated donation from a dz^2 orbital at Rh1 to a *d*-orbital at Rh2 and the LUMO, in contrast, was metal-centered. This is consistent with TD-DFT studies, where the HOMO–LUMO transition interpreted as a metal-to-metal charge transfer ($\lambda_{max,exp}$ = 652 nm; $\lambda_{max,calc}$ = 609 nm). Natural bond orbital (NBO) and intrinsic bonding orbital (IBO) analyses revealed delocalization of the lone pair on Rh1 across to Rh2, with complementary localization of electron density visualized by electron localization function (ELF) analysis (Figure 22). Additionally, lone pairs on the carbazole nitrogen were delocalized into the Rh centers, contributing further to the coordination environment.

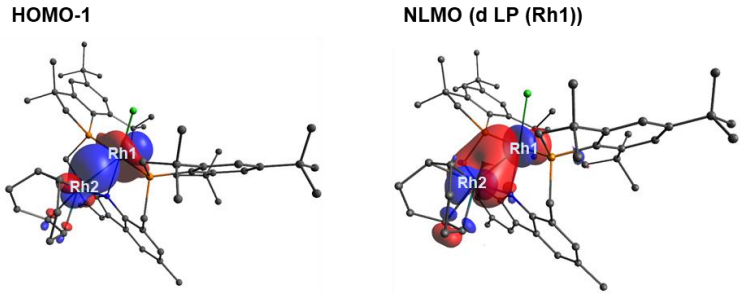

Figure 21. In complex **109** Rh-Rh interaction: HOMO-1 (PBE0-D3/def2-SVP) and NLMO (dz^2 type lone pair (LP) on Rh1).

In a parallel study, **106** was reacted with $[Rh(cod)Cl]_2$ in a 1:1 ratio to examine whether full ligand consumption could be achieved. The ^{31}P NMR spectrum in this case showed new sets of signals: a doublet at 169.2 ppm ($^1J_{P–Rh}$ = 152 Hz) and a doublet of doublets at 125 ppm ($^1J_{P–Rh}$ = 157.7 Hz), consistent with the formation of a distinct dinuclear Rh(I) complex (**110**) featuring a more complex coordination behavior. X-ray analysis of complex **110** revealed an unprecedented arrangement in which both Rh centers are bridged by a chloride and one phosphaalkene unit, which simultaneously coordinates in two distinct modes: side-on η^2 to Rh1 and end-on η^1-κ^P to Rh2 (Figure 20). The bond metrics supported this interpretation, with the P2–C12 bond (1.765(3) Å) elongated due to η^2-coordination, and the P1–C1 bond (1.694(2) Å) remaining relatively short, characteristic of P=C bonds. Complex **110** represents the first synthetically confirmed example of dual η^1/η^2 coordination modes in a single phosphaalkene ligand. TD-DFT simulations identified a strong HOMO–LUMO transition at 796 nm ($\lambda_{max,calc}$ = 735 nm), interpreted as intraframework charge redistribution within the PNP scaffold with limited Rh contribution. The next prominent transition at 564 nm was attributed to a metal-to-ligand charge transfer (MLCT) (HOMO-1 to LUMO). The HOMO-1 and HOMO-5 described the side-on coordination of the P2-C12 arm, while

in the NBO picture this interaction was reflected in a Rh−P bonding orbital which was best described as an interaction of a Rh-centred d-orbital with the P=C π* orbital.

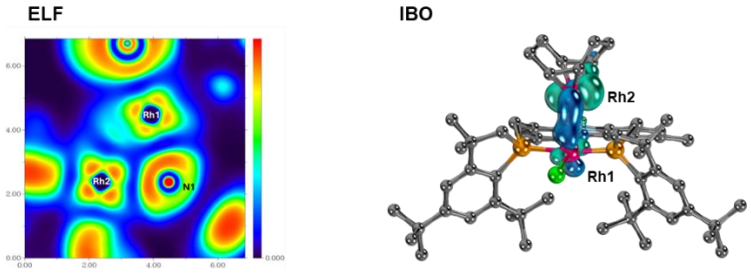

Figure 22. In complex **109** Rh-Rh interaction: Electron localisation function (ELF, PBE0-D3/def2-SVP) and IBO of Rh−Rh interaction (r2SCAN-3c//PBE0-D3/def2-SVP).

Control experiments with other Rh(I) precursors such as $[Rh(nbd)Cl]_2$, $[Ir(cod)Cl]_2$, and $[Rh(coe)_2Cl]_2$ did not lead to comparable product formation, highlighting the unique reactivity of $[Rh(cod)Cl]_2$ in accessing these dinuclear complexes. However, our approach to stabilize mononuclear Rh(I) complex with cod ligand proved largely unproductive, as the steric bulk of the cod ligand hindered proper accommodation within the ligand pocket. Nevertheless, our results showed that cod was indeed able to stabilize single Rh center which was outside the ligand pocket in the final complexes. It appears that the steric demands of the system prevented formation of a mononuclear species and instead favoured dimerization. Mechanistically, the formation of the complexes **109** and **110** is proposed to proceed via a reactive, tricoordinate Rh(I) 14-electron intermediate, a species that has recently been authenticated by Gade *et al.* and shown to be highly reactive.[142] We propose that this transient 14-electron Rh(I) species may have, either underwent C–H activation of the *tert*-butyl groups followed by attack on another equivalent of $[Rh(cod)Cl]_2$ to yield the dinuclear complex **109**, or bypassed C–H activation and directly formed complex **110** via a similar dimerization pathway. To overcome the steric limitations of cod, a more compact and strongly binding ligand such as CO was then employed to investigate whether a mononuclear square-planar Rh(I) complex could be stabilized. To investigate this, $[Rh(\mu\text{-}Cl)(CO)_2]_2$ was reacted with **106** in THF at room temperature, producing a brown solution. The ^{31}P NMR spectroscopy revealed a doublet at 181.7 ppm ($^1J_{Rh-P}$ = 163.6 Hz), indicating the formation of a Rh(I)-coordinated species.

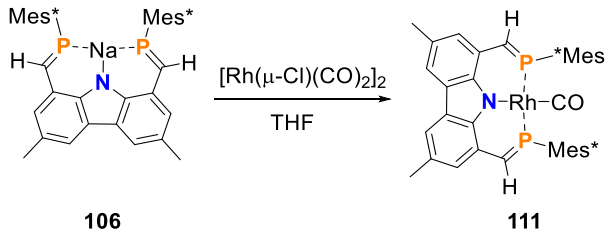

106 **111**

Scheme 20. Reactions of **106** with one or two equivalent of $[Rh(cod)(Cl)]_2$.

Crystallization of the compound yielded [Rh(CO)(^{Mes*2}PNP)] (Scheme 20, **111**), confirmed by single-crystal X-ray diffraction as a C_{2v}-symmetric complex with intact phosphaalkene units and a distorted square-planar geometry. The IR spectroscopy showed a CO stretching vibration at 1996 cm^{-1}, while the UV–vis absorption at 505 nm matched TD-DFT calculated corresponds to a π-π^* transition. These results demonstrate the ability of the phosphaalkene ligand **102** to form well-defined mononuclear Rh(I) carbonyl complexes. These results showcase the ability of phosphaalkene ligands to support diverse and previously unobserved metal coordination geometries, offering new avenues for Rh–Rh bimetallic chemistry and added novel dimension to coordination chemistry of phosphaalkenes.

3 Summary

This thesis explored the design and reactivity of phosphaalkene-based ligands and their integration into transition metal complexes, advancing the understanding of phosphorus–main group and phosphorus–transition metal chemistry. Initially, synthetic efforts focused on accessing phosphaalumenes using Mes*P(PMe_3) and a series of low-valent Al(I) reagents. Although direct isolation of monomeric phosphaalumenes was unsuccessful, spectroscopic and crystallographic characterization confirmed their transient formation and revealed competing deactivation pathways via dimerization or intramolecular C–H activation. These studies provided new structural insights into base-free Al=P bonding motifs and underscored the challenges of stabilizing such highly reactive species. Recognizing these limitations, the research pivoted toward employing the phospha-Wittig strategy to synthesize novel phosphaalkene-containing P,N,P-type ligands derived from carbazole framework and P,N,N3-type ligands from diphenylamine framework. A significant outcome was the discovery of the "azide-Wittig" reaction: a new synthetic route for forming triazabutadienes (TBDs) from azides and aldehydes under mild conditions. This transformation displayed broad substrate scope, offered practical access to diverse TBD frameworks, and demonstrated the utility of azidophosphorane intermediates in organic synthesis. Finally, the newly developed bis-phosphaalkene ligands were shown to act as highly basic, monoanionic P,N,P donors. Their coordination to Rh(I) yielded dinuclear complexes with unique structural features, including rare phosphaalkene coordination modes and intramolecular C–H activation products. Computational analyses revealed unusual Rh–Rh donor–acceptor interactions and metal-to-metal charge-transfer characteristics, expanding the known coordination chemistry of phosphaalkene systems. Complementing these results study also demonstrate that phosphaalkene systems can stablize mononuclear Rh(I) carbonyl complex, which further show the ligand's ability to stabilize well-defined square-planar Rh(I) centers.

Collectively, this work provides new synthetic methodologies and fundamental reactivity insights that broaden the scope of phospha-Wittig reagents, establish versatile ligand platforms for transition metal complexation, and highlight new strategies for main-group multiple-bond activation. These findings lay an important groundwork for further exploration in catalysis, small-molecule activation, and organophosphorus ligand design.

4 List of Publication

The following chapter contains the original papers in which the presented results were published. The own contribution of the author of the dissertation to each publication is highlighted separately.

In paper 4.1, I have contributed to the synthesis and characterization of parts of the compounds

In paper 4.2, I carried out most of the experiments and analyzed the characterization data. In addition, the supporting information corresponding to the paper was written by me.

In paper 4.3, the work I undertook is synthesizing the ligand and the metal complexes along with the supporting information writing. In addition, I have drafted the manuscript.

4.1 On the Reactivity of Mes*P(PMe3) towards Aluminum(I) Compounds – Evidence for the Intermediate Formation of Phosphaalumenes

Dr. Samuel Nees, Dr. Henrik Beer, Philip Just, Leon M. Teichmeier, Leif E. Christoffer, Ailina Guljam, Kushik, Prof. Dr. Holger Braunschweig, Dr. Christian Hering-Junghans

ChemPlusChem ***2023****, 88, e202300078*.

DOI: 10.1002/cplu.202300078

Contribution to this paper is 15%

Check for updates

ChemPlusChem

Research Article
doi.org/10.1002/cplu.202300078

Chemistry Europe
European Chemical Societies Publishing

www.chempluschem.org

Special Collection

On the Reactivity of Mes*P(PMe$_3$) towards Aluminum(I) Compounds – Evidence for the Intermediate Formation of Phosphaalumenes

Samuel Nees,[a, b] Henrik Beer,[c] Philip Just,[d] Leon M. Teichmeier,[d] Leif E. Christoffer,[d] Ailina Guljam,[d] Kushik,[c] Holger Braunschweig,[a, b] and Christian Hering-Junghans*[c]

Dedicated to Evamarie Hey-Hawkins on the occasion of her 65th birthday.

Phosphaalumenes are the heavier isoelectronic analogs of alkynes and have eluded facile synthesis until recently. We have reported that the combination of a phosphinidene transfer agent, ^{Ar}TerP(PMe$_3$) (^{Ar}Ter = 2,6-Ar$_2$-C$_6$H$_3$), with (Cp*Al)$_4$ (Cp* = C$_5$(CH$_3$)$_5$) afforded the phosphaalumenes ^{Ar}TerPAlCp* as isolable, violet, thermally stable compounds. In here we describe attempts to utilize Mes*P(PMe$_3$) (Mes* = 2,4,6-*t*Bu$_3$-C$_6$H$_2$) as a phosphinidene source in combination with different Al(I) precursors, namely ^{Dip}NacnacAl (^{Dip}Nacnac = HC[C(Me)NDip]$_2$, Dip = 2,6-*i*Pr$_2$-C$_6$H$_3$), (Cp*Al)$_4$ and Cp^{3t}Al (Cp^{3t} = 1,2,4-*t*Bu$_3$-C$_5$H$_2$). In all cases the formation of phosphaalumenes was not observed, however, their intermediate formation is indicated by formation of the dimer [Cp*Al(μ-PMes*)]$_2$ (**2**) and C–H-bond activation products along the putative P=Al bond, giving unusual 1,2-P,Al-tetrahydronaphtalene derivatives **1** and **4**, clearly underlining the role the sterically demanding group on phosphorus plays in these transformations. The reactivity studies are supported by theoretical studies, demonstrating a thermodynamic preference for the C–H activation products. Additionally, we show that there are potential pitfalls in the synthesis of Cp*$_2$AlH, the precursor to make (Cp*Al)$_4$ and give recommendations how to circumvent these.

Introduction

Multiple bonding between trielenes (group 13 elements, E^{13}) and pnictogens (E^{15}) is of general interest due to the isovalence electronic relationship with C–C multiple bonds. Nevertheless, the synthesis of such compounds is challenging, which can be attributed to the intrinsic weakness of the π-bond between E^{13}–E^{15} elements. Moreover, adjacent Lewis acidic group 13 and Lewis basic group 15 elements result in a pronounced oligomerization tendency of pnictatrielenes.[1] Especially the heavier base-free multiple bonds between P and B, Al or Ga have eluded facile synthesis until recently. Only last year Liu and co-workers described the synthesis of the first free boraphosphene [(CH$_2$)(NDip)]$_2$B–P=B–NC[(NDip)(CH)]$_2$ (**A**, Figure 1, Dip = 2,6-*i*Pr$_2$-C$_6$H$_3$), enabled through push-pull substitution at the B and P atoms, respectively.[2] Base-stabilized acyclic boraphosphenes have been studied in detail,[3] and NHC-stabilized phosphaborenes with small silyl-substituents (**B**, Figure 1) have been described, that can engage in metathesis reactions through Me$_3$Si-halide elimination.[3d] Our group has used phosphanylidenephosphoranes of the type ArP(PMe$_3$) (Ar = sterically demanding aryl group),[4] so-called phospha-Wittig reagents,[5] as phosphinidene transfer reagents, by substitution of PMe$_3$ with stronger Lewis bases.[6] The reaction of ^{Ar}TerP(PMe$_3$) (Ar=Dip (**C**), Tip (**D**) 2,4,6-*i*Pr$_3$-C$_6$H$_2$; ^{Ar}Ter = 2,6-Ar$_2$-C$_6$H$_3$, Figure 1) with (Cp*Al)$_4$ (Cp* = C$_5$(CH$_3$)$_5$) afforded the first examples of phosphaalumenes ^{Ar}TerP=AlCp*, as violet compounds with a highly polarized P–Al multiple bond.[7] The size of the aryl group is important for the stabilization of phosphaalumenes, and using the minimally less demanding ^{Mes}TerP(PMe$_3$) (^{Mes}Ter = 2,6-(2,4,6-Me$_3$-C$_6$H$_2$)-C$_6$H$_3$), the three-membered species ^{Mes}TerP(AlCp^x)$_2$ (**E**, Cp^x = Cp*, Cp^{3t} 1,2,4-*t*Bu$_3$-C$_5$H$_2$; Figure 1) was obtained,[7b] which according to theoretical aromaticity descriptors is a 2π-aromatic system.[8] Attempts to use triphosphiranes Ar$_3$P$_3$ (Ar=Mes, Dip, Tip)[9] in conjunction with Cp^{3t}Al or (Cp*Al)$_4$ afforded base-free diphosphadialanes, the formal dimers of the free phosphaalumenes.[10] Depending on the aryl-group and the Cp-substituent on Al either the 1,3-isomers (**F**, Figure 1), with alternating P and Al atoms in the four-membered ring, or the 1,2 isomers (**F'**, Figure 1) with P–P and Al–Al bonds, were formed. Phosphagallenes were synthes-

[a] Dr. S. Nees, Prof. Dr. H. Braunschweig
Institut für Anorganische Chemie
Julius-Maximilians-Universität Würzburg
Am Hubland, 97074 Würzburg (Germany)
[b] Dr. S. Nees, Prof. Dr. H. Braunschweig
Institute for Sustainable Chemistry & Catalysis with Boron
Julius-Maximilians-Universität Würzburg
Am Hubland, 97074 Würzburg (Germany)
[c] Dr. H. Beer, Kushik, Dr. C. Hering-Junghans
Leibniz-Institut für Katalyse e.V. (LIKAT)
Albert-Einstein-Straße 29a, 18059 Rostock (Germany)
E-mail: christian.hering-junghans@catalysis.de
[d] P. Just, L. M. Teichmeier, L. E. Christoffer, A. Guljam
Institute of Chemistry
University of Rostock
Albert-Einstein-Straße 3a, 18059 Rostock (Germany)

Supporting information for this article is available on the WWW under https://doi.org/10.1002/cplu.202300078

Part of a Special Collection: "From Light to Heavy: Advancing the Chemistry of Pnictogen Compounds"

ChemPlusChem
Research Article
doi.org/10.1002/cplu.202300078
Chemistry Europe
European Chemical Societies Publishing

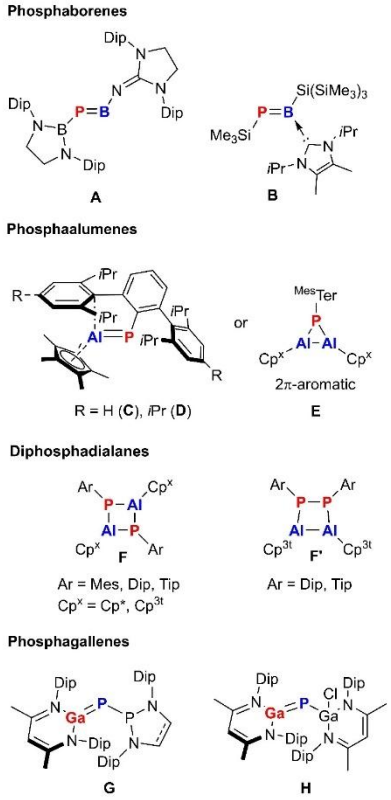

Figure 1. Overview of isolable phosphatrielenes (**A**, **C**, **D**, **G**, **H**), along with dimers of phosphaalumenes (**F**, **F'**) and three-membered PAl_2-species (**E**).

ised by Goicoechea and Schulz using phosphanyl- or gallaphosphaketenes, respectively. Both groups utilized the readily available Ga(I) precursor (^{Dip}Nacnac)Ga (^{Dip}Nacnac = HC[C(Me)NDip]$_2$) in conjunction with the phosphaketenes [(S)P]–PCO ([(S)P] = (H_nCNDip)$_2$P; n = 1, 2) or (^{Dip}Nacnac)Ga(Cl)–PCO facilitating CO cleavage and formation of [(S)P]–P=Ga(^{Dip}Nacnac) (**G**, Figure 1),[11] or (^{Dip}Nacnac)Ga=P–Ga(Cl)(^{Dip}Nacnac) (**H**, Figure 1),[12] respectively. Early attempts to generate monomeric phosphagallenes, revealed the formation of the trimeric species [(2,4,6-Ph_3-C_6H_2)GaP*c*Hex]$_3$ when (2,4,6-Ph_3-C_6H_2)$GaCl_2$ was treated with Li_2P*c*Hex (*c*Hex = *cyclo*-C_6H_{11}) in a 1 : 1 molar ratio.[13] Similarly, when von Hänisch and co-workers utilized NHC-stabilized (NHC=N-heterocyclic carbene) metal silylphosphanides of the general formula (IMes)R_2MP(H)Si*t*BuPh_2 (M=Al–In; R=Et, *i*Pr; IMes = {HCN(2,4,6-$Me_3C_6H_2$)}$_2$C:), oligomerization occurred and heterocubane structures, formally the tetramers of the phosphatrielenes, were obtained upon thermal intramolecular alkane (RH) elimination, rather than the corresponding NHC-stabilized phosphatrielenes (IMes)RM=PSi*t*BuPh_2.[14] The formation of dimers,[3c,15] trimers,[16] and heterocubanes[17] as oligomerization products of putative [RE^{13}=$E^{15}R'$] is well documented in the literature and underlines the importance of kinetic protection through sterically demanding groups and electronic effects invoked by the substituents.

Reactivity studies on phosphatrielenes have revealed a diverse reactivity towards small molecules. The in situ generated phosphaborene [Mes*PB(Tmp)] (Mes* = 2,4,6-*t*Bu_3-C_6H_2; Tmp = 2,2,6,6-tetramethylpiperidyl) was shown to react with phenyl acetylene in [2+2] cycloadditions,[3c] and to enable a bora-phospha-Wittig type chemistry, giving straightforward access to a variety of phosphaalkenes.[18] A similar reactivity was reported for **A** with *p*-methyl-benzaldehyde, while *p*-fluoroacetophenone reacted in C–H bond activation of the Me-group along the P=B fragment.[2] Phosphaalumenes **C** and **D** were found to react with alkynes, alkenes and butadiene, to give P,Al-heterocycles and P,Al-barrelenes, after initial [2+2] cycloaddition reactions at the P–Al double bond. Phosphanylphosphagallenes (**G**), mainly show 1,3-dipolar reactivity, akin to frustrated Lewis pairs (FLP), towards a range of protic substrates, with the anionic group being added to Ga, while the phosphanyl P atom is protonated.[11,19] **H** mainly reacts at the P–Ga double bond in 1,2-additions,[20] and the reversible activation of carbodiimides and CO_2 was reported.[21] When attempting to generate the iminoalane ^{Dip}NacnacAl=N^{Ar}Ter (Ar=Mes, Dip), Power, Roesky and co-workers observed CH-activation of one of the *i*Pr-groups of the Dip-substituents in the ^{Dip}Nacnac-moiety, with the N atom being protonated and the carbanion binding to Al.[22] This serves as another reminder that the correct choice of substituents on the group 13 and 15 elements is crucial to access pnictatrielenes.

In this manuscript we outline our attempts to synthesize phosphaalumenes using the phospha-Wittig reagent Mes*P-(PMe_3) and different Al(I) sources. These studies clearly show that the Mes*-substituent is not ideal for the stabilization of highly reactive Al–P multiple bonds, as it is prone to be C–H activated at one of the *o*-*t*Bu-groups, which has been documented on various occasions in the literature. Nevertheless, these studies show that unusual 6-membered heterocycles can be formed in selective fashion.

The intermediate formation of phosphaalumenes was authenticated by isolation of its dimer in one case and theoretical studies show a preference for *t*Bu-activation along the putative Al=P bond. Moreover, we outline some practical recommendations in the synthesis of $(Cp^*Al)_4$, which is a versatile and recently re-emerging Al(I) precursor.[23]

Results and Discussion

We started our exploration of Mes*P(PMe_3) as Ar–P transfer reagent towards Al(I) precursors by combining it with ^{Dip}-NacnacAl. Treatment of ^{Dip}NacnacAl with Mes*P(PMe_3) in C_6D_6 gave no discernable reaction at room temperature according to NMR spectroscopy. The mixture was thus heated to 60 °C for 2 h, which gave clean conversion into a new species, P,Al-tetrahydronaphtalene derivative **1**, with a $^{31}P\{^1H\}$ NMR signal at −158.7 ppm, which split into a doublet upon proton coupling

ChemPlusChem
Research Article
doi.org/10.1002/cplu.202300078
Chemistry Europe
European Chemical Societies Publishing

($^1J_{PH}$ = 209 Hz), with a corresponding doublet signal in the ^{1}H NMR spectrum at 3.48 ppm, indicating a PH-containing species. Evaporation of the solvent and recrystallization of the crude product from *n*-hexane afforded crystals suitable for SC-XRD, which revealed the formation of compound **1** (Scheme 1), which can be described as the deactivation product of the desired phosphaalumene ^{Dip}NacnacAl=PMes* (**1'**), through activation of one of the *o*-*t*Bu-groups along the putative Al=P bond. C–H bond activation of the *o*-*t*Bu-group has been observed in many cases when the free phosphinidene Mes*–P has been generated intermediately, giving cyclic phosphaindane species.[24] A rather rigid framework in **1** is indicated by four doublet resonances for the *i*Pr methyl groups, as well as two septets for the corresponding methine protons for the ^{Dip}Nacnac substituent. The C–H bond activation of the Mes*-substituent is indicated by multiple signals for the *t*Bu-groups as well as by two signals for the *m*-C_{ArH} of the central aryl ring. The PH-functionality is further corroborated by the asymmetric P–H stretching mode in the IR spectrum at 2367 cm^{-1}, which agrees with the theoretically predicted value (calc. 2363 cm^{-1}).

1 crystallizes in the monoclinic spacegroup $P2_1/c$ with four molecules in the unit cell (Figure 2). The P–Al bond (2.3275(6) Å) is rather short for a single bond (Σr_{cov}(P–Al) = 2.37 Å,[25] (cf. {$(Me_3Si)_2CH$}$_2$Al–PPh_2 2.3367(16) Å).[26] The central $AlPC_4$ six-membered ring adopts a butterfly conformation, with a fold angle along the P1–C44 axis of 127.93(8)° and the Al atom is located above the ^{Dip}Nacnac plane (18.2(2)°). The

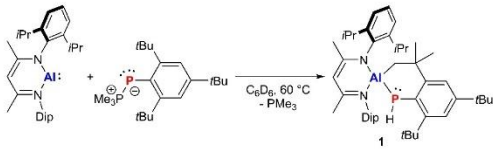

Scheme 1. Synthesis of P,Al-tetrahydronaphtalene derivative **1**.

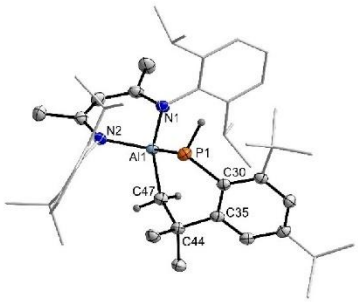

Figure 2. Molecular structure of **1**. Ellipsoids drawn at 50% with C-*H*-atoms (except those on C47 and P1) omitted, Dip- and *t*Bu-groups rendered as wire-frame for clarity. Selected bond lengths [Å] and angles [°], **4**: Al1–P1 2.3275(6), Al1–N1 1.9021(12), Al1–N2 1.9297(13), P1–C30 1.8587(14), Al1–C47 1.9580(15); C30–P1–Al1 100.72(5), C30–P1–H1 99.2(9), Al1–P1–H1 98.8(8), Al1–C16 1.973(2); C16–Al1–C3 118.26(9), C3–Al1–P2 113.89(7), C25–P2–Al1 96.83(7), N1–Al1–C47 118.84(6), N1–Al1–P1 117.00(4), Al1–C41 2.1603(18), C1–P1–Al1 112.00(5); Al1–P1–C30–C35–43.93(11).

Al1–C47 distance of 1.9580(15) Å indicates a single bond, while the P1–C30 distance of 1.8587(14) Å is in the typical range of P–C_{Ar} distances (cf. Mes*$_2$$P_2$ 1.862(2) Å).[27] The P–H was identified in the difference fourier map, thus allowing to discuss the angles at P, which shows a distorted trigonal pyramidal coordination environment ($\Sigma(\angle P)$ = 298.72(7)°), whereas according to a τ_4-value of 0.88, Al is in a minimally distorted tetrahedral coordination mode.[28]

Theoretical studies at the DLPNO-CCSD(T)/def2-TZVP[29] using the PBE0-D3/def2-SVP[30] optimized geometries for obtaining the corrections to the free enthalpy, revealed that the formation of **1** is strongly exergonic (Scheme 2, iii).[31] The intermediate formation of phosphaalumene **1'** was considered, which is also exergonic, however, only by −70.9 kJ·mol^{-1} (Scheme 2, i). The C–H bond activation along the Al=P double bond was found to be strongly exergonic ($\Delta_R G°$ = −119.4 kJ·mol^{-1}; Scheme 2, ii), thus clearly explaining the observed formation of **1** being the sole product of this transformation as the thermodynamic product. The formation of **1** is noteworthy, as six-membered rings containing Al and P in 1,2-position are rare. Hydroalumination of bis-alkynylphosphines with Et_2AlH afforded $Al_2C_2P_2$ rings, which can be regarded as masked FLPs,[32] similar to reactivity observed for the six-membered species ($R_2PCH_2AlMe_2$)$_2$ (R=Me, Ph).[33] Considering the isoelectronic replacement of C by Al and P, compound **1** can be regarded as a 1,2-phosphaalumina-1,2,3,4-tetrahydronaphtalene derivative. By analogy to our recently described synthesis of the phosphaalumenes ^{Ar}TerPAlCp* (Ar=Dip, Tip) we next focused on the reaction of Mes*P(PMe_3) with (Cp*Al)$_4$ under thermal conditions.

The combination of Mes*P(PMe_3) and (Cp*Al)$_4$ in a 4:1 ratio in C_6H_6 afforded after heating to 80 °C without stirring for 16 h a clear yellow solution, from which a yellow crystalline solid precipitated after cooling to 8 °C (Scheme 3, top). ^{31}P NMR spectroscopy of the precipitate revealed the formation of the four-membered ring [Cp*Al(μ-PMes*)]$_2$ (**2**), a 1,3-diphospha-2,4-dialane with a characteristic ^{31}P NMR signal at −183.8 ppm ($\delta_{calc.}$(^{31}P) = −195.2 ppm). After work-up **2** was recovered in a yield of 9%, making this only a side-product. X-ray quality crystals of **2** were obtained directly from the cooled reaction mixture and confirmed the formation of **2** (Figure 3), as a centrosymmetric dimer of the phosphaalumene Mes*PAlCp*

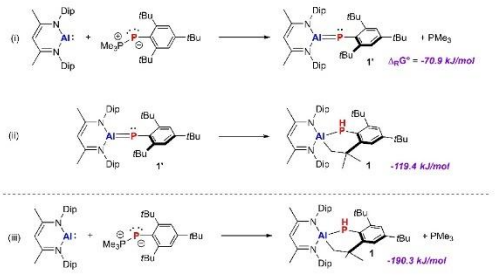

Scheme 2. Thermodynamic considerations for the formation of compound **1** at the DLPNO-CCSD(T)/def2-TZVP//PBE0-D3/def2-SVP level of theory.

ChemPlusChem
Research Article
doi.org/10.1002/cplu.202300078
Chemistry Europe
European Chemical Societies Publishing

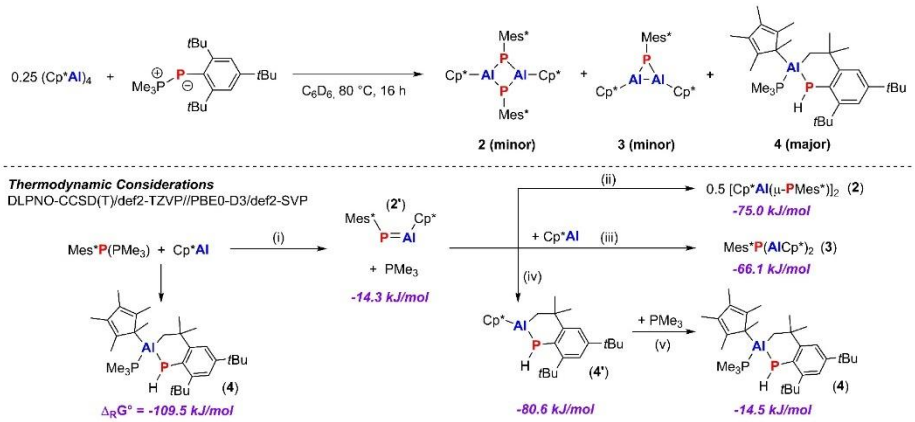

Scheme 3. Reaction of Mes*P(PMe$_3$) with (Cp*Al)$_4$ (top) and thermodynamic considerations to understand the preference for compound **4**.

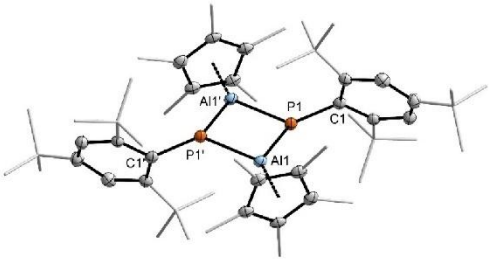

Figure 3. Molecular structure of **2**. Ellipsoids drawn at 50% with *C*-*H*-atoms omitted, *t*Bu- and Cp*-Me-groups rendered as wire-frame for clarity. Selected bond lengths [Å] and angles [°]: Al1–P1 2.3166(10), Al1–P1′ 2.3473(10), P1–C1 1.865(3), C1–P1–Al1 115.29(9), C1–P1–Al1′ 136.29(9), Al1–P1–Al1′ 92.95(4), P1–Al1–P1′ 87.05(4); Al1–P1–C1–C6 110.1(2), Al1–P1–Al1′–P1′ 0.000(35).

(**2′**), with a deltoid central four-membered ring (P–Al 2.3166(10), 2.3473(10) Å) with the P-atoms in a significantly flattened trigonal pyramidal coordination environment (Σ(∠P) = 344.53°) and nearly rectangular angles at Al (87.05(4)°) and P (92.95(4)°).The planarization at P is more pronounced than in the related [Cp*Al(μ-PTip)]$_2$ (cf. Σ(∠P) = 332.816°),[10] whereas the P–Al distances in **2** are similar (cf. 2.3099(6), 2.3395(6) Å) and also compare well with the six-membered species (Mes*PAlPh)$_3$ (cf. $d_{avg.}$ (P–Al) = 2.328(3) Å).[16b]

With **2** identified we turned to the supernatant solution, which revealed a broad singlet signal at −107.6 ppm and two additional major singlet signals at −48.6 and −163.6 ppm in the ^{31}P NMR spectrum before further work-up. Removal of C_6H_6 from the supernatant solution and addition of *n*-pentane, again gave a yellow precipitate, which was isolated by decantation of the mother liquor. This precipitate was identified as the 2π-aromatic three-membered species Mes*P(AlCp*)$_2$ by its characteristic ^{31}P NMR signal at −107.6 ppm ($\delta_{calc.}$(^{31}P) = −132.1 ppm; cf. ^{Mes}TerP(AlCp*)$_2$ −116.4 ppm)[7b] and a Mes* to Cp* ratio of 1 : 2 in the ^{1}H NMR spectrum. The formation of **2** and **3** can be understood when inspecting the thermodynamics of these transformations (Scheme 3, bottom). First the intermediate formation of the phosphaalumene **2′** was considered (Mes*P(PMe$_3$) + Cp*Al → Mes*PAlCp* + PMe$_3$; Scheme 3, i), which is exergonic by −14.3 kJ·mol^{-1} (note that the monomerization of (Cp*Al)$_4$ is endergonic, but it was shown that the monomer is present in solution at elevated temperatures).[34] Subsequent dimerization of **2′** to give half an equivalent of **2** is exergonic by −75.0 kJ·mol^{-1} (Scheme 3, ii). While the reaction of **2′** with a second equivalent of Cp*Al was found to be exergonic by −66.1 kJ·mol^{-1} (Scheme 3, iii). One more parameter to differentiate between four-membered species **2** and three-membered **3** are the different ring deformation stretching modes in the IR spectrum. For **2** there are two strong modes at 513 and 493 cm^{-1} (calc. 504 and 480 cm^{-1}), which according to DFT calculations correspond to the asymmetric deformation modes. In contrast **3** only shows a strong vibration at 470 cm^{-1} (calc. 461 cm^{-1}), clearly assigned as a ring deformation mode, in addition to a band at 544 cm^{-1} (calc. 545 cm^{-1}), which corresponds well with the theoretically predicted value for the Al–Al symmetric stretching vibration.

With **2** and **3** identified we were able to recover the main product in pure form by placing the *n*-pentane supernatant solution in the freezer at −30 °C for 24 h. This yielded pale yellow crystals, suitable for SC-XRD analysis and showed the formation of the C–H bond activation product **4** akin to **1**, in which one of the *o*-*t*Bu-groups was activated along the putative Al=P bond, while the Al-atom is coordinated by PMe$_3$. The ^{31}P NMR spectrum of isolated **4** showed two singlet resonances at −48.6 and −163.2 ppm, with no coupling between the phosphorus nuclei. Upon ^{1}H coupling the signal at −163.2 ppm split into a doublet, with a corresponding doublet in the ^{1}H NMR spectrum at 3.42 ppm ($^1J_{PH}$ = 197.7 Hz), signifying the PH-moiety. The CH$_2$-group attached to Al is shielded signifi-

ChemPlusChem
Research Article
doi.org/10.1002/cplu.202300078
Chemistry Europe
European Chemical Societies Publishing

cantly and gives a broad singlet at 0.47 ppm in the ^{1}H NMR spectrum with the $C(CH_3)_2$ part of the activated *t*Bu-group at 1.88 ppm. In the solid state the Cp*-substituent on Al is η^1-coordinated, whereas a singlet in the ^{1}H NMR spectrum indicates a fast sigmatropic shift on the NMR time scale. The PMe_3 coordinated to Al shows a deshielded signal in the ^{31}NMR spectrum, while the doublet in the ^{1}H NMR spectrum at 0.22 ppm is shielded compared to free PMe_3. The presence of the P–H group was further confirmed by IR spectroscopy, showing the P–H stretching mode at 2335 cm^{-1} (calc. 2346 cm^{-1}).

In the solid state **4** (Figure 4) adopts a similar butterfly structure as found in **1** (fold angle along the C17···P2 axis 126.84(16)°), with a P(H)–Al atom distance of 2.3440(8) Å, while the Al–P_{PMe3} distance is 2.4381(8), in line with a coordinative bond (cf. $Cl_3Al(PMe_3)_2$ 2.452(2), 2.459(2) Å).[35] Also the sum of angles at P ($\Sigma(\angle P) = 293.79°$) indicate a trigonal pyramidal coordination environment, whereas the coordination at Al is nearly tetrahedral ($\tau_4 = 0.91$).[28] The formation of **4** again points to the intermediate formation of the phosphaalumene **2'**, and to verify our assumption of a thermodynamically driven process we again turned to calculations on the DLPNO-CCSD(T)/def2-TZVP//PBE0-D3/def2-SVP level of theory. Starting from **2'** the C–H bond activation to give the PMe_3-free activation product **4'**, was found to be exergonic by −80.6 kJ·mol^{-1} (Scheme 3, iv), while the addition of PMe_3 to give **4** provided an additional energy gain of −14.5 kJ·mol^{-1} (Scheme 3, v). Considering that the reaction takes place at 80 °C the formation of **4** as the main product is clearly thermodynamically driven.

In a last series of experiments we investigated the reaction of Mes*P(PMe_3) with monomeric $Cp^{3t}Al$[36] in C_6D_6 at room temperature in a 1:1 ratio at first, giving one product with a ^{31}P{^{1}H} NMR signal at −104.5 ppm and unreacted Mes*P(PMe_3) in a 1:1 ratio, which is in line with the formation of Mes*P($AlCp^{3t}$)$_2$ (**5**) and full conversion was achieved when starting from a 1:2 mixture of Mes*P(PMe_3) and $Cp^{3t}Al$ after 16 h (Scheme 4). After slowly evaporating a *n*-pentane solution of **5**, pale yellow crystals suitable for SC-XRD experiments were obtained.

In the ^{1}H NMR spectrum the characteristic signals for the Cp^{3t}- and Mes*-substituent show the expected 2:1 ratio, with two singlet signals for the Cp^{3t} *t*Bu-groups at 1.45 and 1.43 ppm and two singlets for the *o*-*t*Bu and *p*-*t*Bu-groups of the Mes*-substituent at 2.00 and 1.37 ppm, respectively. The aromatic protons of the Mes*-group at 7.39 ppm and of the Cp^{3t}-group at 6.29 ppm show the expected 1:2 ratio. The ^{31}P{^{1}H} NMR shift of −104.5 ppm ($\delta_{calc.}(^{31}P) = -123.3$ ppm) compares well with that of **3** and is in the range of ^{Mes}TerP($AlCp^{3t}$)$_2$ (cf. −79.7 ppm). In case of **5** we were also able to determine the ^{27}Al NMR shift at −43 ppm as a broad singlet,[31] which is in the range of $Cp^{3t}AlBr_2$ ($\delta(^{27}Al) = -46$ ppm).[36] The Al_2P-ring in **5** is not isosceles (Figure 5) in contrast to previously reported ^{Mes}TerP($AlCp^{3t}$)$_2$ (cf. d(Al–P) = 2.3543(8), 2.3495(7) Å). The Al2–P1 (2.2965(4) Å) is considerably shorter than the Al1–P1 distance (2.3664(4) Å), while the Al1–Al2 distance (2.5464(5) Å) is only minimally longer than that in ^{Mes}TerP($AlCp^{3t}$)$_2$ (2.5265(9) Å) and compares well with Al–Al distance in strained cyclic dialanes.[37] The P atom in **5** is in a trigonal planar coordination environment ($\Sigma(\angle P) = 359.97°$), which again indicates a 2π-aromatic system as was shown for ^{Mes}TerP($AlCp^{3t}$)$_2$ and the isovalence electronic species $Na_2[^{Mes}Ter_3Al_3]$.[38] In the IR spectrum two characteristic modes for the PAl_2-ring were identified, with the mode at 528 cm^{-1} (calc. 519 cm^{-1}) showing the ring breathing, whereas the mode at 459 cm^{-1} (calc. 450 cm^{-1}) corresponds to ring deformation.

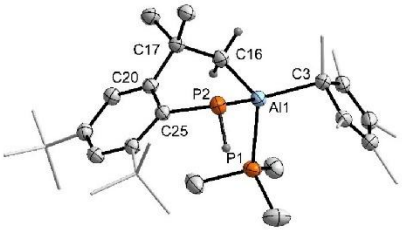

Figure 4. Molecular structure of **4**. Ellipsoids drawn at 50% with C-*H*-atoms (except those on C16 and P2) omitted, Tip-groups rendered as wire-frame for clarity. Selected bond lengths [Å] and angles [°], **4**: Al1–P1 2.4381(8), Al1–P2 2.3440(8), P2–C25 1.867(2), Al1–C3 2.032(2), Al1–C16 1.973(2); C16–Al1–C3 118.26(9), C3–Al1–P2 113.89(7), C25–P2–Al1 96.83(7), Al1–C41 2.1603(18), C1–P1–Al1 112.00(5); Al1–P2–C25–C20 −43.16(16).

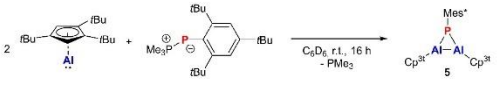

Scheme 4. Synthesis of compound **5**.

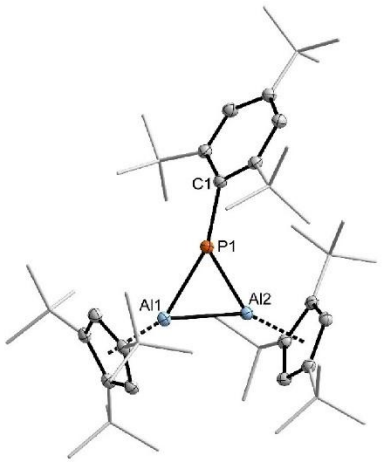

Figure 5. Molecular structure of **5**. Ellipsoids drawn at 50% with C-*H*-atoms omitted, *t*Bu-groups rendered as wire-frame for clarity. Selected bond lengths [Å] and angles [°], **5**: Al1–P1 2.3664(4), Al2–P1 2.2965(4), P1–C1 1.8862(11), Al1–Al2 2.5464(5); C1–P1–Al2 134.62(4), C1–P1–Al1 159.17(4), Al2–P1–Al1 66.177(14), P1–Al1–Al2 55.594(12), P1–Al2–Al1 58.229(13).

ChemPlusChem
Research Article
doi.org/10.1002/cplu.202300078
Chemistry Europe
European Chemical Societies Publishing

For the synthesis of ^{Dip}NacnacAl we have used a modified synthesis that was recently described by Kretschmer and co-workers.[39] This route is based on the reaction of ^{Dip}NacnacNa with $(Cp^*Al)_4$ and gave ^{Dip}NacnacAl (under formation of NaCp*) in reasonable, reproduceable yields when strictly following the literature procedure. However, we have encountered some challenges when preparing $(Cp^*Al)_4$, which we want to disclose here. Two pathways for $(Cp^*Al)_4$ are described in the latest edition of *Inorganic Syntheses*,[40] and we use the reductive elimination approach originally outlined by Fischer et al., using the thermal elimination of Cp*H from Cp^*_2AlH, which gives $(Cp^*Al)_4$ in pure form in a high yielding process.[41] During the synthesis of Cp^*_2AlH we have observed two potential pitfalls, which we want to report here. Firstly, the preparation of Cp*K is based on the reaction of Cp*H with KH in THF,[42] using an excess of Cp*H, which can be removed afterwards by filtration. While stating that Cp*K is obtained in pure form after decantation of the supernatant THF-solution, washing with THF and careful drying, we have found that this can result in some remaining THF in the thus-prepared Cp*K. THF was found to interfere with the following reaction of Cl_2AlH and by fractional crystallization [Cp*AlHCl(thf)] (**6**) was identified as an undesired by-product (Scheme 5, top), by re-crystallization from Et_2O. In the ^{1}H NMR spectrum in C_6D_6 **6** was identified by three signals, with a singlet signal for the Cp*-substituent at 2.06 ppm, as well as two broad signals at 1.01 and 3.50 ppm for the coordinated THF molecule. To the best of our knowledge **6** is the first mixed chloride/hydride AlCp* derivative, in which the SC-XRD analysis revealed the Cp* substituent to be on the continuum of being η^1 and η^3-coordinated, with one short Al–C3 (2.1032(18) Å) and two longer Al–C2 (2.3763(17) Å) and Al–C4 (2.3151(17) Å) (Figure 6, left). In contrast, the Cp*-substituent in the related $[Cp^*AlCl_2(thf)]$ complex is η^1-coordinated (Al–C 2.009(2) Å) and the Al–O_{thf} in **6** is considerably longer compared to $[Cp^*AlCl_2(thf)]$ (1.8332(15) Å),[43] in line with a less Lewis acidic Al-center in the mixed hydride/chloride **6**. When extracting the reaction mixture of Cp^*_2AlH with *n*-hexane and concentrating the filtrate **6** crystallizes first. After removal of the supernatant solution from **6** the desired Cp^*_2AlH crystallized in analytically pure form from this solution. To circumvent the formation of **6** during the preparation of Cp^*_2AlH we recommend washing the Cp*K with *n*-pentane rather than using only THF. Since adapting the *n*-pentane washing step we have not encountered the formation of **6** anymore.

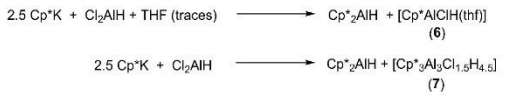

Scheme 5. Pitfalls in the synthesis of Cp^*_2AlH, which afforded the side-products **6** and **7**.

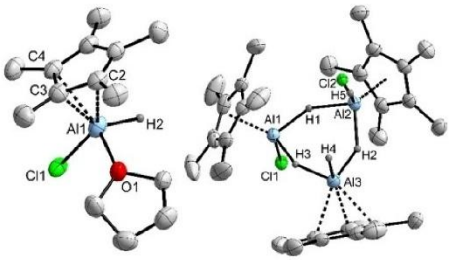

Figure 6. Molecular structure of **6** (left) and **7** (right). Ellipsoids drawn at 50% with C-*H*-atoms (except H on Al) omitted. Selected bond lengths [Å] and angles [°], **6**: Cl1–Al1 2.1935(8), Al1–O1 1.9209(13), Al1–C3 2.1032(18), Al1–C4 2.3151(17), Al1–C2 2.3763(17), Al1–H2 1.703(17); Cl1–Al1–H2 103.3(5), O1–Al1–Cl1 95.30(5), O1–Al1–H2 100.6(5). **7**: Al1–Cl1 2.1743(8), Al1–H3 1.674(18), Al1–H1 1.657(18), Al2–H1 1.752(17), Al2–H2 1.725(17), Al3–H4 1.689(17), Al3–H3 1.722(18), Al3–H2 1.782(17).

Another potential pitfall was identified when skipping a step in the literature procedure. According to this, after the reaction of Cp*K with Cl_2AlH the reaction mixture in Et_2O is filtered, then the filtrate is dried and this filtrate is again extracted with *n*-hexane and filtered to give Cp^*_2AlH after recrystallization at −30 °C (Scheme 5, bottom). We attempted to directly dry the reaction mixture in Et_2O and then extract with *n*-hexane and filter afterwards, thereby skipping one filtration. This however resulted in the isolation of another undesired by-product, which was identified as a trimeric mixed $Cp^*_3Al_3Cl_{1.5}H_{4.5}$ (**7**) species by SC-XRD analysis (Figure 6, right), which is in line with ^{1}H NMR spectroscopy, showing a singlet at 1.94 ppm for the Cp*-substituent in C_6D_6 solution along with a broad resonance for the hydrides in a 45:4.3 ratio, which agrees well with the ratio obtained from SC-XRD analysis (45:4.42). We note that there is probably fast exchange between $[Cp^*_3Al_3Cl_2H_4]$ and $[Cp^*_3Al_3ClH_5]$ in solution, thus giving the observed singlet resonance for the Cp*-groups in the ^{1}H NMR spectrum. In the solid state three hydrides were found to be μ-bridging, whereas Cl and the additional hydrides occupy end-on positions on Al, with the Cp*-substituents being η^5-coordinated on Al1 and Al2, and showing a rather unsymmetric coordination on Al3 in line with a η^3-coordination mode. The Al–(μ-H)–Al distances range from 1.65–1.75 Å, which agrees with the Al–H distances in the dimeric $(ArAlH_2)_2$ (1.60–1.72 Å, Ar = 2,6-$(CH(SiMe_3)_2)_2$-4-*t*Bu-C_6H_2).[44] Again, after removal of the supernatant solution from **7**, the desired Cp^*_2AlH was isolated in good yields by crystallization. We have not encountered the formation of **7** when strictly following the literature procedure for Cp^*_2AlH.

Conclusion

Using the phospha-Wittig reagent Mes*P(PMe_3) the synthesis of phosphaalumenes was attempted. With the Al(I) precursor ^{Dip}NacnacAl the 1,2-phosphaalumina-1,2,3,4-tetrahydronaphtalene derivative **1** was obtained, which signifies the intermediate formation ^{Dip}NacnacAl=PMes*. However, the C–H-activation of an *o*-*t*Bu-group of the Mes*-substituent along the putative Al=P bond occurred in a thermodynamically driven process. A similar outcome was observed for the reaction of Mes*P(PMe_3) with $(Cp^*Al)_4$, which gave C–H-activation product **4** as the main species. However, in this case the dimer of a putative phosphaalumene, the four-membered species **2**, as well as the

ChemPlusChem | Research Article doi.org/10.1002/cplu.202300078 | Chemistry Europe European Chemical Societies Publishing

three-membered ring system **3** were identified as by-products. The formation of **4** as the main product is again thermodynamically driven. Lastly, the selective formation the 2π-aromatic system **5** was achieved when Mes*P(PMe_3) was treated with the monomeric $Cp^{3t}Al$ at room temperature. All this evidence points to the effect the sterically demanding group on P plays, and in particular the Mes*-group is shown to be not an ideal candidate as it is prone to C–H-activation of the *o*-*t*Bu-groups. Moreover, the isolation of **2** clearly shows that the steric bulk of Mes* is not sufficient to stabilize a monomeric phosphaalumene. In addition, we have identified two potential side-products when preparing Cp*AlH, the direct precursor of $(Cp^*Al)_4$, which is an essential starting material for the synthesis of low-valent aluminum species. Future work will focus on further fine tuning the sterically demanding groups on phosphorus and aluminium to access novel phosphaalumenes and to exploit their reactivity.

Experimental Section

If not stated otherwise, all manipulations were carried out under oxygen- and moisture-free conditions under an inert atmosphere of argon using standard Schlenk or Drybox techniques. All glassware was heated three times *in vacuo* using a heat gun and cooled under argon atmosphere. Solvents were transferred using syringes, which were purged three times with argon prior to use. Solvents and reactants were either obtained from commercial sources or synthesized as detailed in Table S1.[31] NMR spectra were recorded on Bruker spectrometers (AVANCE 300, AVANCE 400 or Fourier 300) and were referenced internally to the deuterated solvent (C_6D_6 δ_{ref} = 128.06 ppm), to protic impurities in the deuterated solvent (C_6HD_5 δ_{ref} = 7.16 ppm) or externally (^{31}P: 85 % H_3PO_4 δ_{ref} = 0 ppm). The broad resonance at δ = 70 ppm observed in the ^{27}Al NMR spectrum corresponds to a background from Al-nuclei in the probe head. All measurements were carried out at ambient temperature unless denoted otherwise. NMR signals were assigned using experimental data (e.g. chemical shifts, coupling constants, integrals where applicable) in conjunction with computed NMR data (GIAO method, *cf.* Computational details, p. S31 ff.).[31] IR spectra of crystalline samples were recorded on a Bruker Alpha II FT-IR spectrometer equipped with an ATR unit at ambient temperature under argon atmosphere. Relative intensities are reported according to the following intervals: very weak (vw, 0–10 %), weak (w, 10–30 %), medium (m, 30–60 %), strong (s, 60–90 %), very strong (vs, 90–100 %). Elemental analyses were obtained using a Leco Tru Spec elemental analyzer. *Important Note:* Suitable CHN values for compounds **2**–**7** were not obtained, with deviations in between 3 to 15 % for both C and H values. As CHN analysis is unfortunately already prone to manipulations[45] we decided to not provide any values because in our eyes there is no evidence beyond a reasonable doubt that the material is pure *at the point of measurement*. However, the state-of-the-art characterization such as with NMR spectroscopy (see displayed spectra in the ESI) demonstrates the existence and analytical pureness of the herein published compounds if not stated otherwise. Crystallographic details are given in the ESI (p. S4 ff).[31]

Synthesis of compound 1: ^{Dip}NacnacAl (0.045 mg, 0.1 mmol) and Mes*P(PMe_3) (0.036 g, 0.1 mmol) were combined in an NMR tube equipped with a J-Young valve and benzene-d_6 (0.6 mL) was added at room temperature. The NMR tube is sonicated until all solids have dissolved and the NMR tube is then placed in an oil bath set to 60 °C. The sample is heated to 60 °C over a period of 2 h resulting in a colour change from bright orange to yellow. After checking the reaction by ^{1}H and ^{31}P{1H} NMR spectroscopy the reaction mixture is transferred into a Schlenk tube and the volatiles are removed in vacuo. The yellow solid residue is then extracted with *n*-heptane (2 mL) and filtered through a canula fitted with a glass filter paper to give a clear yellow solution. This solution is then placed in a freezer at −30 °C and compound **1** is afforded as yellow crystalline solid after 48 h. Yield: 45 mg (0.062 mmol, 62 %). Single crystals suitable for X-ray diffraction can be grown from saturated *n*-hexane solution at 5 °C.

CHN calc. (found) in %: C 78.29 (78.09), H 9.79 (9.71), N 3.89 (3.70). **^{31}P{^{1}H} NMR** (C_6D_6, 162.01 MHz): δ = −158.7. **^{31}P NMR** (C_6D_6, 162.01 MHz): δ = −158.7 (d, $^1J_{PH}$ = 201.9 Hz). **^{1}H NMR** (C_6D_6, 400.1 MHz): δ = 0.47 (s, 2H, Al-C*H*$_2$(CMe$_2$)), 1.07 (d, $^3J_{HH}$ = 6.7 Hz, 6H, CH(C*H*$_3$)$_2$), 1.14 (d, $^3J_{HH}$ = 6.8 Hz, 6H, CH(C*H*$_3$)$_2$), 1.22 (d, $^3J_{HH}$ = 6.7 Hz, 6H, CH(C*H*$_3$)$_2$), 1.29-1.34 (m, 21 H, *o*-*t*Bu, Al-CH$_2$(C(C*H*$_3$)$_2$), CH(C*H*$_3$)$_2$)*, 1.54 (s, 6 H, C*H*$_3$-^{Dip}Nacnac), 1.75 (s, 9 H, *p*-*t*Bu), 3.25 (hept, $^3J_{HH}$ = 6.7 Hz, 2H, C*H*(CH$_3$)$_2$), 3.47 (hept, $^3J_{HH}$ = 6.7 Hz, 2H, C*H*(CH$_3$)$_2$), 3.48 (d, $^1J_{PH}$ = 202.3 Hz, P*H*), 4.85 (s, 1H, C*H*-^{Dip}Nacnac), 7.01-7.13 (m, 6H, C$_{Aryl}$*H*-Dip), 7.34 (m, 1 H, *m*-C$_{Aryl}$*H*), 7.45 (m, 1 H, *m*-C$_{Aryl}$*H*). **^{13}C{^{1}H} NMR** (C_6D_6, 100.6 MHz): δ = 23.9 (s (br), Al*C*H$_2$), 24.2 (s, *C*H$_3$-^{Dip}Nacnac), 24.8, 24.9 (d, J_{PC} = 7.4 Hz), 25.1, 25.3 (CH(*C*H$_3$)$_2$), (s, *C*H$_3$-^{Dip}Nacnac), 28.7 (s, *C*H(CH$_3$)$_2$), 29.3 (d, J_{PH} = 6.1, *C*H(CH$_3$)$_2$), 31.7 (s, *p*-C(*C*H$_3$)$_3$), 32.6 (d, J_{PC} = 6.2 Hz, *o*-C(*C*H$_3$)$_3$), 34.8 (s, *p*-*C*(CH$_3$)$_3$), 35.5 (d, J_{PC} = 10.5 Hz, *C*(CH$_3$)$_2$), 38.5 (*o*-*C*(CH$_3$)$_3$), 40.6 (*C*(CH$_3$)$_2$), 98.6 (H*C*(C-(CH$_3$)NDip)$_2$), 120.5, 121.6 (*C*H$_{aryl}$, Mes*), 124.4, 125.1 (*m*-*C*H$_{Dip}$), 127.6,* 128.6* (*o*-*C*H$_{Dip}$), 132.1 ($^1J_{PC}$ = 34.3 Hz, *C*$_{ipso}$), 141.0, 144.0, 145.0 (*C*$_{q,Dip}$), 145.4 (*p*-*C*$_{q,Mes*}$), 152.7 (d, $^2J_{PC}$ = 4.2 Hz, o-C$_{q,Mes*}$), 154.4 (d, $^2J_{PC}$ = 5.2 Hz, o-C$_{q,Mes*}$, activated *t*Bu-group), 170.9 (C$_q$, HC(*C*-(CH$_3$)NDip)$_2$). *overlap with the C_6D_6 signal, assigned via HSQC, and DEPT-135 spectra. **IR** (ATR, 32 scans, cm^{-1}): $\tilde{\nu}$ = 3067 (vw), 3057 (vw), 2956 (s), 2925 (m), 2867 (m), 2366 (vw), 1663 (vw), 1622 (vw), 1591 (w), 1550 (m), 1521 (s), 1515 (s), 1461 (m), 1435 (s), 1385 (vs), 1358 (s), 1315 (s), 1296 (m), 1253 (m), 1214 (w), 1208 (m), 1193 (w), 1173 (m), 1132 (w), 1105 (m), 1084 (m), 1053 (m), 1041 (m), 1016 (m), 969 (w), 936 (m), 884 (m), 872 (m), 860 (m), 822 (w), 794 (s), 759 (s), 726 (w), 711 (m), 678 (m), 653 (m), 641 (m), 610 (m), 596 (w), 557 (m), 528 (m), 495 (m), 474 (m), 443 (s).

Reaction of Mes*P(PMe_3) with $(Cp^*Al)_4$.

Isolation of compound 4: $(Cp^*Al)_4$ (0.162 mg, 0.25 mmol) and Mes*P(PMe_3) (0.353 g, 1.0 mmol) were combined in a Schlenk tube and benzene (3 mL) was added at room temperature. The Schlenk tube was then heated to 80 °C (oil bath). The sample was heated at 80 °C over a period of 16 h without stirring resulting in a clear yellow solution. Upon cooling to 8 °C a yellow crystalline solid precipitated (compound **2**, see below), from which the supernatant was removed via a canula fitted with a glass filter paper to give a clear yellow filtrate. From this filtrate the volatiles were removed *in vacuo* ($1\cdot10^{-3}$ mbar), giving a yellow solid. This solid was then extracted with *n*-pentane (2 mL), again giving a yellow precipitate (compound **3**, see below), and the supernatant solution was filtered and the filtrate was then concentrated to incipient crystallization and placed in a freezer at −30 °C. Compound **4** was afforded as a pale yellow crystalline solid after standing at −30 °C for 24 h and removal of the supernatant solution and drying *in vacuo* ($1\cdot10^{-3}$ mbar). Yield: 0.155 mg (0.030 mmol, 30 %; based on Mes*P(PMe_3)). Single crystals suitable for X-ray diffraction can be grown from a saturated *n*-pentane solution at −30 °C.

^{31}P{^{1}H} NMR (C_6D_6, 121.5 MHz): δ = −162.0 (*P*H), −48.6 (*P*Me$_3$). **^{31}P NMR** (C_6D_6, 121.5 MHz): −162.0 (d, $^1J_{PH}$ = 197.7 Hz, *P*H), −48.6 (decett, $^2J_{PH}$ = 7.7 Hz, *P*Me$_3$). **^{1}H NMR** (C_6D_6, 300.1 MHz): δ = 0.22 (d, $^2J_{PH}$ = 7.7 Hz, 9 H, P(C*H*$_3$)$_3$), 0.47 (s (br), Al*CH*$_2$), 1.34 (s, *p*-C(C*H*$_3$)$_3$), 1.81 (s, *o*-C(C*H*$_3$)$_3$), 1.88 (AlCH$_2$(C(C*H*$_3$)$_2$), 1.93 (s, C$_5$(C*H*$_3$)$_5$), 3.42 (d, $^1J_{PH}$ =

ChemPlusChem
Research Article
doi.org/10.1002/cplu.202300078
Chemistry Europe
European Chemical Societies Publishing

197.7 Hz), 7.50 (m, 1 H, *m*-C*H*), 7.52 (m, 1 H, m-C*H*). **^{13}C{^{1}H} NMR** (C_6D_6, 75.5 MHz): δ = 10.1 (d, $^{1}J_{PC}$ = 20.5 Hz, P(CH_3)$_3$), 12.3 (d, J_{PC} = 2.7 Hz, C_5(CH_3)$_5$), 24.5 (s (br), AlCH_2), 31.7 (s, *p*-C(CH_3)$_3$), 32.4 (d, J_{PC} = 4.6 Hz, *o*-(C(CH_3)$_3$), 34.8 (s, *p*-C(CH_3)$_3$), 36.1 (s (br), AlCH$_2$C(CH_3)$_2$), 38.5 (s, *o*-C(CH_3)$_3$), 41.3 (s (br), AlCH$_2$C(CH_3)$_2$), 117.8 (s, C_5(CH$_3$)$_5$), 121.0 (d, J_{PC} = 2.7 Hz, *m*-C, PAr), 121.8 (s, *m*-C, PAr), 133.6 (J_{PC} = 37.9 Hz, ipso-C, PAr), 145.8 (p-C, Ar), 152.2 (o-C, PAr), 154.2 (J_{PC} = 7.4 Hz, o-C (C(CH$_3$)$_2$CH$_2$Al), PAr). **IR** (ATR, 32 scans, cm^{-1}): $\tilde{\nu}$ = 2956 (s), 2906 (m), 2865 (m), 2853 (m), 2335 (w), 1593 (w), 1536 (w), 1476 (w), 1457 (m), 1445 (m), 1428 (w), 1414 (m), 1408 (m), 1391 (m), 1379 (m), 1358 (m), 1307 (w), 1284 (w), 1253 (m), 1239 (m), 1210 (m), 1183 (m), 1169 (w), 1130 (w), 1086 (w), 1041 (m), 961 (m), 946 (m), 903 (w), 890 (w), 874 (m), 843 (s), 824 (m), 804 (m), 748 (m), 699 (m), 658 (s), 641 (m), 631 (m), 589 (m), 561 (m), 542 (m), 534 (m), 493 (s), 466 (vs), 443 (s), 416 (m).

Isolation of compound 2: After heating a mixture (Cp*Al)$_4$ (0.162 mg, 0.25 mmol) and Mes*P(PMe$_3$) (0.353 g, 1.0 mmol) to 80 °C for 16 h and cooling to 8 °C the four-membered ring-species [Cp*Al(μ-PMes*)]$_2$ (**2**) (0.040 g, 0.045 mmol, 9% based on Mes*P-(PMe$_3$)), was obtained as a yellow precipitate, which was isolated by decantation of the supernatant solution. X-Ray quality crystals were obtained directly from the reaction mixture.

^{31}P{^{1}H} NMR (C_6D_6, 121.5 MHz): δ = −183.8. **^{1}H NMR** (C_6D_6, 300.1 MHz): δ = 1.37 (s, 9 H, *p*-*t*-Bu), 1.89 (s, 15 H, C_5(CH_3)$_5$), 2.00 (s, 18 H, *o*-*t*-Bu), 7.50 (s, 2 H, *m*-H). **^{13}C{^{1}H} NMR** (C_6D_6, 75.5 MHz): δ = 11.7 (s, C_5(CH_3)$_5$), 31.6 (s, *p*-C(CH_3)$_3$), 34.9 (s, *p*-C(CH$_3$)$_3$), 35.4 (s, *o*-C(CH_3)$_3$, PMes*), 40.0 (s, *o*-C(CH$_3$)$_3$), 116.8 (s, C_5Me$_5$), 122.3 (s, *m*-C, PMes*), 147.2 (s, *p*-C, PMes*), 156.9 (s, *o*-C, PMes*), *ipso*-C at PMes* not observed. **IR** (ATR, 32 scans, cm^{-1}): $\tilde{\nu}$ = 2956 (m), 2908 (m), 2867 (w), 1593 (w), 1542 (vw), 1534 (vw), 1521 (vw), 1476 (w), 1459 (w), 1408 (w), 1391 (w), 1381 (w), 1360 (m), 1309 (vw), 1278 (w), 1235 (m), 1210 (w), 1195 (w), 1165 (w), 1119 (w), 1107 (w), 1066 (w), 1020 (w), 998 (w), 983 (w), 921 (w), 901 (w), 876 (m), 831 (m), 814 (m), 802 (m), 752 (m), 730 (m), 709 (m), 680 (m), 672 (m), 662 (m), 645 (m), 625 (m), 612 (m), 596 (m), 513 (s), 493 (vs), 437 (s).

Isolation of compound 3: After heating a mixture (Cp*Al)$_4$ (0.162 mg, 0.25 mmol) and Mes*P(PMe$_3$) (0.353 g, 1.0 mmol) to 80 °C for 16 h and cooling to 8 °C the supernatant solution was removed from a yellow precipitate by decantation. From the supernatant solution the volatiles were removed in vacuo and *n*-pentane (2 mL) was added, resulting in the precipitation of a yellow solid. This yellow solid was isolated by decantation of the supernatant *n*-pentane solution and was identified as the three-membered ring species Mes*P(AlCp*)$_2$ (**3**, 0.030 g, 0.05 mmol, 5% based on Mes*P(PMe$_3$)). X-Ray quality crystals of **3** could not be obtained.

^{31}P{^{1}H} NMR (C_6D_6, 121.5 MHz): δ = −107.6. **^{1}H NMR** (C_6D_6, 300.1 MHz): δ = 1.30 (s, 9 H, *p*-*t*-Bu), 1.88 (s, 30 H, C_5(CH_3)$_5$), 2.14 (s, 18 H, *o*-*t*-Bu), 7.51 (s, 2 H, *m*-H). **^{13}C{^{1}H} NMR** (C_6D_6, 75.5 MHz): δ = 10.4 (d, J_{PC} = 2 Hz, C_5(CH_3)$_5$), 31.6 (s, *p*-C(CH_3)$_3$), 34.2 (d, J_{PC} = 5.3 Hz, *o*-C(CH_3)$_3$, PMes*), 35.1 (s, *p*-C(CH$_3$)$_3$), 38.2 (s, *o*-C(CH$_3$)$_3$), 114.0 (s, C_5Me$_5$), 121.2 (s, *m*-C, PMes*), 147.5 (s, *p*-C, PMes*), 154.1 (s, *o*-C, PMes*), *ipso*-C at PMes* not observed. **IR** (ATR, 32 scans, cm^{-1}): $\tilde{\nu}$ = 2954 (m), 2906 (m), 2865 (m), 1595 (w), 1546 (vw), 1529 (vw), 1459 (w), 1447 (w), 1410 (w), 1387 (w), 1377 (w), 1360 (m), 1280 (vw), 1237 (w), 1212 (w), 1189 (w), 1022 (w), 983 (w), 923 (w), 876 (m), 831 (m), 814 (m), 800 (m), 752 (m), 730 (m), 715 (m), 678 (m), 666 (m), 658 (m), 647 (m), 629 (m), 596 (m), 544 (s), 470 (vs), 437 (s), 420 (s).

Synthesis of compound 5: Cp^{3t}Al (0.030 g, 0.11 mmol) and Mes*PPMe$_3$ (20.0 mg, 0.056 mmol) were mixed in C_6H_6 (0.6 mL). While stirring for a day at room temperature, the solution turned orange. Benzene and the forming PMe$_3$ were removed under vacuum and the residue was extracted with *n*-pentane. Slow evaporation of the solvent at −30 °C yielded pale yellow crystals of Mes*P(AlCp^{3t})$_2$ (**6**), suitable for single crystal X-ray diffraction. Yield: 20.8 mg, 0.026 mmol (46%).

^{31}P{^{1}H} NMR (C_6D_6, 162MHz): δ = −104.5 ppm. **^{27}Al NMR** (C_6D_6, 104 MHz): δ = -43 (s, (br)) ppm. **^{1}H NMR** (C_6D_6, 400 MHz): δ = 1.37 (s, 9H, *p*-C(CH_3)$_3$), 1.42 (s, 18H, C(CH_3)$_3$, Cp^{3t}), 1.45 (s,36H, C(CH_3)$_3$, Cp^{3t}), 2.00 (s,18H, *o*-C(CH_3)$_3$), 6.29 (s, CH_{Cp}, 4H), 7.39 (s, 2H, CH_{Aryl}). **^{13}C{^{1}H} NMR** (C_6D_6, 101 MHz): δ = 31.7 (CH(CH_3)$_3$)), 31.9 (CH(CH_3)$_3$), 32.3 (CH(CH$_3$)$_3$), 33.9(CH(CH_3)$_3$), 34.1 (d, J_{PC} = 3.4 Hz, CH(CH_3)$_3$, *o*-*t*Bu), 34.9 (CH(CH$_3$)$_3$, p-*t*Bu), 38.5 (CH(CH$_3$)$_3$, *o*-*t*Bu), 107.2 (CH$_{Cp}$), 121.1 (CH$_{Aryl}$), 129.8 (C$_{q'Aryl}$), 131.3 (C$_{q,Aryl}$), 145.0 (d, JPC = 175.6 Hz, C$_{ipso}$), 146.9 (C$_{q,Aryl}$), 152.8 (C$_{q,Aryl}$). **IR** (ATR, 32 scans, cm^{-1}): $\tilde{\nu}$ = 2954 (vs), 2903 (m), 2866 (m), 2281 (vw),* 1624 (vw), 1587 (w), 1479 (m), 1459 (m), 1389 (m), 1361 (s), 1240 (s), 1204 (m), 1167 (m), 1124 (m), 1024 (m), 1006 (m), 965 (w), 953 (w), 922 (w), 902 (w), 871 (m), 838 (vs), 814 (m), 800 (m), 745 (m), 669 (m), 590 (m), 563 (m), 528 (m), 496 (m), 459 (vs), 420 (m), 408 (m). *artefact or minimal amounts of a C–H-activation product.

Isolation of compound 6: To AlCl$_3$ (1.506 g, 11.3 mmol) in a 100 mL Schlenk flask, which was cooled to −78 °C (EtOH/CO$_2$), was added Et$_2$O (50 mL). To this LiAlH$_4$ (4 M in Et2O, 0.94 mL, 3.76 mmol) was added dropwise over a period of 5 min. The reaction mixture is allowed to warm to room temperature over a period of 1 h and stirred for an additional hour at that temperature. Afterwards the now cloudy suspension (LiCl) is filtered via a canula equipped with a glass filter paper and from the filtrate the volatiles are removed *in vacuo*. The Schlenk flask containing the sticky white residue of Cl$_2$AlH is brought inside the glovebox and Cp*K (4.94 g, 28.3 mmol) are added and the mixture is then suspended in Et$_2$O (100 mL) and stirred at room temperature for 4 h. Afterwards the volatiles were removed in vacuo and to the sticky yellow residue *n*-hexane (50 mL) and Et$_2$O (5 mL) was added. The resulting suspension was filtered using a Schlenk-frit, giving a pale yellow, clear filtrate. After concentration of the filtrate to incipient crystallization and placement in the fridge at 6 °C for 16 h a first crop of crystals was afforded, which were identified as [Cp*Al(H)(thf)] (**6**) (0.760 g, 2.81 mmol, 24.9% based on AlCl$_3$).

^{1}H NMR (C_6D_6, 300.2 MHz): δ = 1.01 (t, $^{3}J_{HH}$ = 6.8 Hz, OCH$_2$CH_2), 2.06 (s, C_5(CH_3)$_5$), 3.50 (t, $^{3}J_{HH}$ = 6.8 Hz, OCH_2CH$_2$). **^{13}C{^{1}H} NMR** (C_6D_6, 75.5 MHz): δ = 11.7 (s, C_5(CH_3)$_5$), 24.9 (s, OCH$_2$CH_2), 71.3 (s, OCH_2CH$_2$), 115.3 (s, C_5(CH$_3$)$_5$).

The desired Cp*$_2$AlH then crystallized from the supernatant solution upon placement at −30 °C as a colourless crystalline solid (1.618 g, 5.42 mmol, 47.9% based on AlCl$_3$). Cp*$_2$AlH: **^{1}H NMR** (C_6D_6, 300 MHz): δ = 1.92 (s, C_5(CH_3)$_5$).

We want to note that THF in the side product (most likely) stems from the synthesis of Cp*K, which was afforded from the reaction of Cp*H with KH in THF as a white solid,[42] after drying in vacuo (10^{-3} mbar) for 4 h. *Consequently, we recommend to not only decant the supernatant solution of the Cp*H/KH reaction mixture, but to also wash the crude Cp*K with n-pentane (2x).*

Isolation of compound 7: To AlCl$_3$ (1.614 g, 12.0 mmol) in a 100 mL Schlenk flask, which was cooled to −78 °C (EtOH/CO$_2$), was added Et$_2$O (75 mL). To this LiAlH$_4$ (1 M in Et2O, 4 mL, 4 mmol) was added dropwise over a period of 5 min. The reaction mixture is allowed to warm to room temperature over a period of 1 h and stirred for an additional hour at that temperature. Afterwards the now cloudy suspension (LiCl) is filtered via a canula equipped with a glass filter paper and from the filtrate the volatiles are removed *in vacuo*. The Schlenk flask containing the sticky white residue of Cl$_2$AlH is brought inside the glovebox and Cp*K (5.23 g, 30 mmol) are added

ChemPlusChem

Research Article
doi.org/10.1002/cplu.202300078

Chemistry Europe
European Chemical Societies Publishing

and the mixture is then suspended in Et_2O (100 mL) and stirred at room temperature for 4 h. Afterwards the volatiles were removed in vacuo and to the sticky yellow residue *n*-hexane (60 mL) was added. The resulting suspension was filtered using a Schlenk-frit, giving a pale yellow, clear filtrate. After concentration of the filtrate (ca. 30 mL) an amorphous white precipitate formed, which was isolated by decantation of the supernatant solution via a cannula. The amorphous residue was identified as a mixture of $[Cp^*_3Al_3H_2(\mu\text{-}H)_3Cl]$ and $[Cp^*_3Al_3H(\mu\text{-}H)_3Cl_2]$ (**7**, ca. 1 : 1) and X-ray quality crystals were obtained by recrystallization from Et_2O at −30 °C (0.215 mg, 0.39 mmol, 9.7 % based on $AlCl_3$). **^{1}H NMR** (C_6D_6, 300.2 MHz): $\delta =$ 1.94 (s, $C_5(CH_3)_5$), 3.36 (s (br), Al*H*). **^{13}C{^{1}H} NMR** (C_6D_6, 75.5 MHz): $\delta =$ 10.7 (s, $C_5(\underline{C}H_3)_5$), 114.4 (s, $\underline{C}_5(CH_3)_5$).

The desired Cp^*_2AlH then crystallized from the supernatant solution upon placement at −30 °C as a colourless crystalline solid (2.6 g, 8.71 mmol, 73 % based on $AlCl_3$). We therefore recommend to strictly follow the synthesis of Cp^*_2AlH as outlined in *Inorganic Syntheses*,[40] which states that the reaction mixture of Cp*K and Cl_2AlH in Et_2O is first filtered, then dried and extracted with fresh *n*-hexane followed by a second filtration, instead of first removing the Et_2O directly from the reaction mixture before filtration.

Acknowledgements

He. Be. and C. H.-J. thank the Leibniz Association for funding within the scope of the Leibniz ScienceCampus Phosphorus Research Rostock (www.sciencecampus-rostock.de). We thank Till Brockmann for synthetic assistance, the technical and analytical staff at LIKAT for assistance, especially Dr. Anke Spannenberg for her support regarding X-ray analysis. We want to thank Prof. Dr. Torsten Beweries for helpful discussions. Ho. Br. wishes to acknowledge financial support by the Deutsche Forschungsgemeinschaft, DFG. Open Access funding enabled and organized by Projekt DEAL.

Conflict of Interest

The authors declare no conflict of interest.

Data Availability Statement

The data that support the findings of this study are available in the supplementary material of this article.

Keywords: Phosphaalumenes · Phosphorus · Aluminium · C–H-Bond Activation · Ring Systems

[1] F. Dankert, C. Hering-Junghans, *Chem. Commun.* **2022**, *58*, 1242–1262.
[2] J. Li, Z. Lu, L. L. Liu, *J. Am. Chem. Soc.* **2022**, *144*, 23691–23697.
[3] a) E. Rivard, W. A. Merrill, J. C. Fettinger, P. P. Power, *Chem. Commun.* **2006**, 3800–3802; b) A. N. Price, M. J. Cowley, *Chem. Eur. J.* **2016**, *22*, 6248–6252; c) A. N. Price, G. S. Nichol, M. J. Cowley, *Angew. Chem. Int. Ed.* **2017**, *56*, 9953–9957; *Angew. Chem.* **2017**, *129*, 10085–10089; d) A. Koner, B. Morgenstern, D. M. Andrada, *Angew. Chem. Int. Ed.* **2022**, *61*, e202203345.
[4] a) J. D. Protasiewicz, C. Hering-Junghans, in *Encyclopedia of Inorganic and Bioinorganic Chemistry*, **2022**, pp. 1–27; b) J. D. Protasiewicz, *Eur. J. Inorg. Chem.* **2012**, *2012*, 4539–4549.
[5] S. Shah, J. D. Protasiewicz, *Chem. Commun.* **1998**, 1585–1586.
[6] a) M. Fischer, C. Hering-Junghans, *Chem. Sci.* **2021**, *12*, 10279–10289; b) P. Gupta, J.-E. Siewert, T. Wellnitz, M. Fischer, W. Baumann, T. Beweries, C. Hering-Junghans, *Dalton Trans.* **2021**, *50*, 1838–1844.
[7] a) S. Nees, T. Wellnitz, F. Dankert, M. Härterich, S. Dotzauer, M. Feldt, H. Braunschweig, C. Hering-Junghans, *Angew. Chem. Int. Ed.* **2023**, *62*, e202215838; 9b) M. Fischer, S. Nees, T. Kupfer, J. T. Goettel, H. Braunschweig, C. Hering-Junghans, *J. Am. Chem. Soc.* **2021**, *143*, 4106–4111.
[8] K. Ota, R. Kinjo, *Chem. Soc. Rev.* **2021**, *50*, 10594–10673.
[9] A. Schumann, F. Reiß, H. Jiao, J. Rabeah, J.-E. Siewert, I. Krummenacher, H. Braunschweig, C. Hering-Junghans, *Chem. Sci.* **2019**, *10*, 7859–7867.
[10] S. Nees, F. Fantuzzi, T. Wellnitz, M. Fischer, J.-E. Siewert, J. T. Goettel, A. Hofmann, M. Härterich, H. Braunschweig, C. Hering-Junghans, *Angew. Chem. Int. Ed.* **2021**, *60*, 24318–24325; *Angew. Chem.* **2021**, *133*, 24520–24528.
[11] D. W. N. Wilson, J. Feld, J. M. Goicoechea, *Angew. Chem. Int. Ed.* **2020**, *59*, 20914–20918; *Angew. Chem.* **2020**, *132*, 21100–21104.
[12] M. K. Sharma, C. Wölper, G. Haberhauer, S. Schulz, *Angew. Chem. Int. Ed.* **2021**, *60*, 6784–6790; *Angew. Chem.* **2021**, *133*, 6859–6865.
[13] H. Hope, D. C. Pestana, P. P. Power, *Angew. Chem. Int. Ed. Engl.* **1991**, *30*, 691–693.
[14] M. Kapitein, C. von Hänisch, *Eur. J. Inorg. Chem.* **2015**, *2015*, 837–844.
[15] a) A. M. Arif, J. E. Boggs, A. H. Cowley, J. G. Lee, M. Pakulski, J. M. Power, *J. Am. Chem. Soc.* **1986**, *108*, 6083–6084; b) C. Couret, J. Escudie, B. Garrigues, M. Lazraq, J. Satge, *Can. J. Chem.* **1987**, *65*, 1230–1232.
[16] a) H. V. R. Dias, P. P. Power, *J. Am. Chem. Soc.* **1989**, *111*, 144–148; b) R. J. Wehmschulte, P. P. Power, *J. Am. Chem. Soc.* **1996**, *118*, 791–797.
[17] B. Kaufmann, N. Metzler, H. Nöth, R. T. Paine, *Chem. Ber.* **1994**, *127*, 825–827.
[18] A. M. Borys, E. F. Rice, G. S. Nichol, M. J. Cowley, *J. Am. Chem. Soc.* **2021**, *143*, 14065–14070.
[19] J. Feld, D. W. N. Wilson, J. M. Goicoechea, *Angew. Chem. Int. Ed.* **2021**, *60*, 22057–22061; *Angew. Chem.* **2021**, *133*, 22228–22232.
[20] M. K. Sharma, C. Wölper, S. Schulz, *Dalton Trans.* **2022**, *51*, 1612–1616.
[21] M. K. Sharma, C. Wölper, G. Haberhauer, S. Schulz, *Angew. Chem. Int. Ed.* **2021**, *60*, 21784–21788; *Angew. Chem.* **2021**, *133*, 21953–21957.
[22] H. Zhu, J. Chai, V. Chandrasekhar, H. W. Roesky, J. Magull, D. Vidovic, H.-G. Schmidt, M. Noltemeyer, P. P. Power, W. A. Merrill, *J. Am. Chem. Soc.* **2004**, *126*, 9472–9473.
[23] P. Dabringhaus, J. Willrett, I. Krossing, *Nat. Chem.* **2022**, *14*, 1151–1157.
[24] a) A. H. Cowley, F. Gabbai, R. Schluter, D. Atwood, *J. Am. Chem. Soc.* **1992**, *114*, 3142–3144; b) X. Li, D. Lei, M. Y. Chiang, P. P. Gaspar, *J. Am. Chem. Soc.* **1992**, *114*, 8526–8531; c) S. Shah, M. C. Simpson, R. C. Smith, J. D. Protasiewicz, *J. Am. Chem. Soc.* **2001**, *123*, 6925–6926.
[25] P. Pyykkö, M. Atsumi, *Chem. Eur. J.* **2009**, *15*, 12770–12779.
[26] W. Haider, M. D. Calvin-Brown, I.-A. Bischoff, V. Huch, B. Morgenstern, C. Müller, T. Sergeieva, D. M. Andrada, A. Schäfer, *Inorg. Chem.* **2022**, *61*, 1672–1684.
[27] M. Yoshifuji, I. Shima, N. Inamoto, K. Hirotsu, T. Higuchi, *J. Am. Chem. Soc.* **1981**, *103*, 4587–4589.
[28] L. Yang, D. R. Powell, R. P. Houser, *Dalton Trans.* **2007**, 955–964.
[29] a) C. Riplinger, F. Neese, *J. Chem. Phys.* **2013**, *138*, 034106; b) D. G. Liakos, M. Sparta, M. K. Kesharwani, J. M. L. Martin, F. Neese, *J. Chem. Theory Comput.* **2015**, *11*, 1525–1539; c) C. Riplinger, P. Pinski, U. Becker, E. F. Valeev, F. Neese, *J. Chem. Phys.* **2016**, *144*, 024109.
[30] a) J. P. Perdew, K. Burke, M. Ernzerhof, *Phys. Rev. Lett.* **1996**, *77*, 3865–3868; b) J. P. Perdew, K. Burke, M. Ernzerhof, *Phys. Rev. Lett.* **1997**, *78*, 1396–1396; c) C. Adamo, V. Barone, *J. Chem. Phys.* **1999**, *110*, 6158–6170; d) S. Grimme, J. Antony, S. Ehrlich, H. Krieg, *J. Chem. Phys.* **2010**, *132*, 154104; e) S. Grimme, S. Ehrlich, L. Goerigk, *J. Comput. Chem.* **2011**, *32*, 1456–1465; f) S. Grimme, S. Ehrlich, L. Goerigk, *J. Comput. Chem.* **2011**, *32*, 1456–1465.
[31] See Supporting Information for all experimental and computational details. CCDC 2239701–2239706 contain the crystallographic data for the structures reported in this paper. These can be obtained free of charge via www.ccdc.cam.ac.uk/data_request/cif.
[32] S. Roters, C. Appelt, H. Westenberg, A. Hepp, J. C. Slootweg, K. Lammertsma, W. Uhl, *Dalton Trans.* **2012**, *41*, 9033–9045.
[33] J. Boudreau, M.-A. Courtemanche, F.-G. Fontaine, *Chem. Commun.* **2011**, *47*, 11131–11133.

ChemPlusChem
Research Article
doi.org/10.1002/cplu.202300078
Chemistry Europe
European Chemical Societies Publishing

[34] H. Sitzmann, M. F. Lappert, C. Dohmeier, C. Üffing, H. Schnöckel, *J. Organomet. Chem.* **1998**, *561*, 203–208.
[35] a) J. Burt, W. Levason, M. E. Light, G. Reid, *Dalton Trans.* **2014**, *43*, 14600–14611; b) S. Mebs, J. Beckmann, *J. Phys. Chem. A* **2017**, *121*, 7717–7725.
[36] A. Hofmann, T. Tröster, T. Kupfer, H. Braunschweig, *Chem. Sci.* **2019**, *10*, 3421–3428.
[37] a) C. Cui, X. Li, C. Wang, J. Zhang, J. Cheng, X. Zhu, *Angew. Chem. Int. Ed.* **2006**, *45*, 2245–2247; *Angew. Chem.* **2006**, *118*, 2303–2305; b) K. Koshino, R. Kinjo, *J. Am. Chem. Soc.* **2021**, *143*, 18172–18180; c) P. Dabringhaus, S. Zedlitz, I. Krossing, *Chem. Commun.* **2023**, *59*, 187–190.
[38] R. J. Wright, M. Brynda, P. P. Power, *Angew. Chem. Int. Ed.* **2006**, *45*, 5953–5956; *Angew. Chem.* **2006**, *118*, 6099–6102.
[39] O. Kysliak, H. Görls, R. Kretschmer, *Dalton Trans.* **2020**, *49*, 6377–6383.
[40] A. M. Arif, B. L. Benac, A. H. Cowley, R. A. Jones, K. B. Kidd, C. M. Nunn, A. Kuckowski, S. Schulz, A. H. Cowley, R. A. Jones, P. R. Harris, D. A. Atwood, C. Knapp, C. Carmalt, J. Weßing, K. Freitag, G. Chelladurai, R. A. Fischer, J. Arnold, H. W. Roesky, K. Freitag, R. A. Fischer, G. S. Hair, A. H. Cowley, R. A. Jones, D. Barisic, R. Anwander, in *Inorganic Syntheses*, Vol. 37 (Eds: P. P. Power), John Wiley & Sons, Inc. **2018**, ch. 7, pp. 135–153.
[41] C. Ganesamoorthy, S. Loerke, C. Gemel, P. Jerabek, M. Winter, G. Frenking, R. A. Fischer, *Chem. Commun.* **2013**, *49*, 2858–2860.
[42] G. Rabe, H. W. Roesky, D. Stalke, F. Pauer, G. M. Sheldrick, *J. Organomet. Chem.* **1991**, *403*, 11–19.
[43] P. E. Romero, W. E. Piers, S. A. Decker, D. Chau, T. K. Woo, M. Parvez, *Organometallics* **2003**, *22*, 1266–1274.
[44] K. Nagata, T. Murosaki, T. Agou, T. Sasamori, T. Matsuo, N. Tokitoh, *Angew. Chem. Int. Ed.* **2016**, *55*, 12877–12880; *Angew. Chem.* **2016**, *128*, 13069–13072.
[45] a) W. Kandioller, J. Theiner, B. K. Keppler, C. R. Kowol, *Inorg. Chem. Front.* **2022**, *9*, 412–416; b) R. E. H. Kuveke, L. Barwise, Y. van Ingen, K. Vashisth, N. Roberts, S. S. Chitnis, J. L. Dutton, C. D. Martin, R. L. Melen, *ACS Cent. Sci.* **2022**, *8*, 855–863.

Manuscript received: February 7, 2023
Revised manuscript received: February 22, 2023
Accepted manuscript online: February 23, 2023

4.2 The Azide-Wittig Reaction

Kushik, Dr. A. Petrov, Dr. D. Ranieri, L. Edelmann, Prof. Dr. T. Beweries, Dr. C. Hering-Junghans

Angew. Chem. Int. Ed. 2024, 63, e202412982.

DOI: 10.1002/anie.202412982

Reprinted with permission from *Angew. Chem.*.

Contribution to this paper is 60%

GDCh Communication Angewandte International Edition Chemie www.angewandte.org
Check for updates
How to cite: *Angew. Chem. Int. Ed.* **2024**, *63*, e202412982
doi.org/10.1002/anie.202412982

Organic Synthesis

The Azide-Wittig Reaction

Kushik, A. Petrov, D. Ranieri, L. Edelmann, T. Beweries, and C. Hering-Junghans**

In memory of Ian Manners.

Abstract: The introduction of heteroatoms into conjugated organic molecules is an important strategy to tune their reactivity and physical properties. In this realm triazabutadienes (TBDs) of the general from $R_2C{=}N{-}N{=}NR'$ are an interesting class of compounds, however, general synthetic protocols for their generation are limited. Based on the serendipitous finding that the sterically encumbered azide Mes*N_3 (Mes* = 2,4,6-tBu$_3$C$_6$H$_2$) reacted with PMe_3 in the presence of an aromatic aldehyde to form a TBD, we now report on the "Azide-Wittig" reaction. This azide-Wittig reaction is shown to be a versatile tool for the synthesis of a variety of TBDs, tolerating a wide range of aldehydes and organic azides as coupling partners. The preference for azide-Wittig, rather than aza-Wittig reactivity was rationalized using computational methods. This study shows how kinetic control can significantly alter the reaction pathway, thereby switching from an aza-Wittig to an azide-Wittig regime.

C=C and C=N double bonds are ubiquitous structural motifs and efficient, chemoselective methodologies for their construction are valuable tools in organic synthesis. In this respect, the Wittig reaction remains one of the most important reactions yet discovered. In 1953 Wittig and Geissler noted that benzophenone reacted with methylene triphenylphosphorane to give 1,1-diphenyl-ethylene,[1] and follow-up studies[2] showed that the Wittig reaction is an indispensable synthetic tool in organic synthesis in academia and industry. Recent developments in the field include catalytic protocols,[3] and strategies for phosphine oxide recycling.[4] Meanwhile, other Wittig-type reactions have emerged. These include aza-, borata-,[5] phospha-,[6] or just recently bora-phospha-Wittig reactions.[7] Our group and others have utilized phospha-Wittig reactions for the synthesis of phosphaalkene-based ligands with P=C double bonds.[8]

Phospha-Wittig reagents of the general form RP(PR'$_3$) can be viewed as phosphine-stabilized phosphinidenes,[9] and are also used as a shuttle for phosphinidenes.[10]

Even before Wittig's seminal report, Staudinger noted that the iminophosphorane $Ph_3P{=}NPh$, derived from Ph–N_3 and PPh_3 (Figure 1A), reacted with benzaldehyde to imine

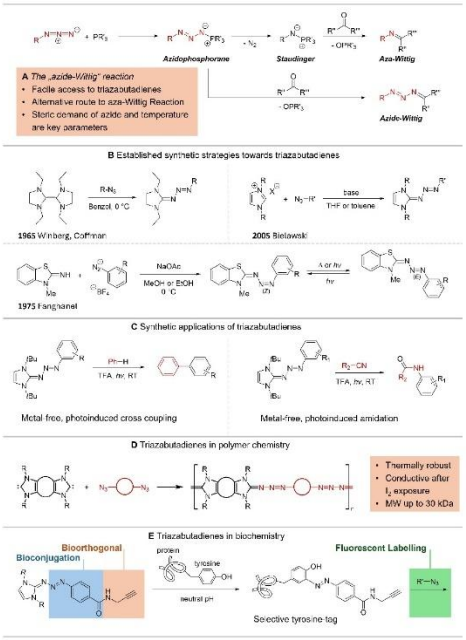

Figure 1. (**A**) Relation of aza-Wittig, Staudinger and "Azide-Wittig" reactions. (**B**) Strategies towards triazabutadienes. (**C**) Selected examples of TBD reactivity. (**D**) TBD-derived conjugated polymers. (**E**) TBDs in biochemistry.

[*] Kushik, Dr. A. Petrov, Prof. Dr. T. Beweries, Dr. C. Hering-Junghans
Leibniz Institute for Catalysis (LIKAT)
Albert-Einstein-Str. 29a
18059 Rostock (Germany)
E-mail: Torsten.beweries@catalysis.de
Christian.hering-junghans@catalysis.de
Dr. D. Ranieri, Dr. C. Hering-Junghans
Institut für Chemie, Otto-von-Guericke-Universität Magdeburg
Universitätsplatz
39106 Magdeburg (Germany)
L. Edelmann
Institut für Chemie, Universität Rostock
Albert-Einstein-Straße 3a
18059 Rostock (Germany)

PhC(H)NPh and Ph_3PO.[11] Generally, iminophosphoranes $R_3P{=}NR'$ form imines when reacted with ketones or aldehydes, in an aza-Wittig reaction (Figure 1A), which is also used to construct highly functionalized heterocycles.[12] Detailed mechanistic studies have revealed formation of azidophosphoranes $RN_3PR'_3$ as the primary intermediate, which then eliminates N_2 via a 4-membered transition state to form the respective iminophosphorane. However, when electron-rich or bulky phosphines are utilized, stable azidophosphoranes (or phosphazides) of the type $RN_3PR'_3$ can be formed.[13]

A class of substances related to azidophosphoranes, the key intermediate in the Staudinger reaction, are triazabutadienes (TBDs, or conjugated triazenes) with three nitrogen atoms in a conjugated diene.[14] Triazabutadienes were first introduced in 1965 by Winberg and Coffman.[15] Treatment of a bis(imidazolidine) with tosyl- or *p*-nitrophenyl azide at 0 °C afforded the corresponding TBDs (Figure 1B). Fanghänel and co-workers popularized benzothiazole-based systems, obtained in the base-assisted coupling of 3-methyl-2-iminobenzthiazoline with diazonium salts (Figure 1B).[16] In 2005, a general synthetic method towards TBDs utilizing in situ generated *N*-heterocyclic carbenes (NHCs) in the reaction with a variety of azides was reported (Figure 1B).[17] TBDs find applications in the synthesis of guanidines,[18] as diazotization or azidation reagents,[19] as ligands in rare-earth metal complexes,[20] in metal-free cross-coupling and amidation protocols (Figure 1,C),[21] as building blocks for polytriazenes (Figure 1D),[22] and as fluorescence sensors for the detection of Fe^{III} ions.[23] Lately, the potential of NHC-based triazabutadienes for biorthogonal protein functionalization was realized,[24] and applied for example in the selective protein modification under basic conditions in the midgut of mosquitos (Figure 1E).[24–25]

Despite the abundant use of NHC-derived TBDs, the synthetic availability of the $R_2C{=}N{-}N{=}N{-}R'$ unit is limited and synthetic alternatives to the two routes described above are missing. From a retrosynthetic point of view, azidophosphoranes with a nucleophilic N_γ atom should react with aldehydes or ketones in a Wittig-type reaction to give triazabutadienes. To the best of our knowledge there is a single report on such reactivity by Somsák and Leonidas. When treating a D-galactose-derived azide with nBu$_3$P in the presence of PhCHO, the formation of a thermally rather stable TBD was observed.[26] Moreover, the nucleophilicity of the N_γ atom in azidophosphoranes has been harnessed in the preparation of *H*-1,2,3-triazol-4-ols from α-azido esters,[27] or in the deimidogenation to give diazomethanes.[28] To achieve such azide-Wittig reactivity it is necessary to find the delicate balance between sterics of the group attached to the azide as well as to use sufficiently electron-rich phosphines. In here we describe the first systematic study of the "azide-Wittig" reaction based on a serendipitous finding, as a versatile synthetic avenue to TBDs.

In our quest to prepare P,N,P-type bisphosphaalkenes, 2,2′-iminobisbenzaldehyde was treated with two equivalents of Mes*P(PMe$_3$) (Mes* = 2,4,6-*t*Bu$_3$C$_6$H$_2$) (Figure 2). Surprisingly, only one phosphaalkene unit was selectively

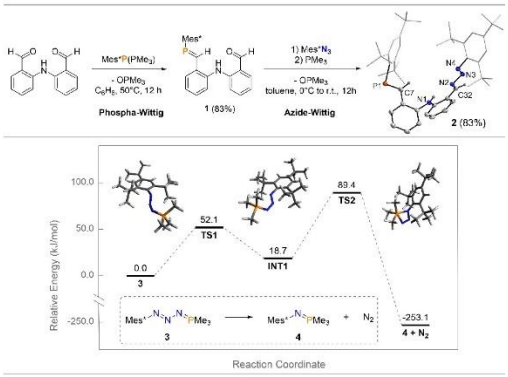

Figure 2. Top: Synthetic pathway to TBD **2**. Bottom: Computed thermal reaction pathway (DNLPO-CCSD(T)/def2TZVP(smd = benzene)// PBE0-D3/def2SVP, c° = 1 mol/L) for the formation of **4** from azidophosphorane **3**.

formed, giving **1** with an unreacted aldehyde group (Figure S1). Therefore, **1** was combined with Mes*N$_3$ and PMe$_3$ in a 1:1:1 ratio in toluene and the mixture was heated to 80 °C overnight. After work-up and recrystallization from *n*-hexane at −30 °C, crystals for single crystal X-Ray diffraction (SC-XRD) were obtained.[29] Structure elucidation revealed Mes*N$_3$-transfer in a Wittig-type reaction and formation of compound **2** incorporating an *E*-configured triazabutadiene arm with conjugated C=N (d(C32–N2) = 1.295(2) Å) and N=N (d(N3–N4) = 1.243(2) Å) double bonds (Figure 2). In solutions of **2** a characteristic ^{1}H NMR signal for the imine proton at 9.17 ppm (δ_{CN}(^{13}C) = 174.4 ppm) is detected, while a ^{31}P NMR signal at 271.3 ppm indicates the phosphaalkene unit. Under optimized conditions **2** can be obtained in 83 % yield at room temperature. To the best of our knowledge, this is the first instance of transferring an azide to a carbonyl group in a Wittig-type reaction, which we term "azide-Wittig" reaction hereafter.

This let us to study whether the azide-Wittig reaction is a general pathway for the construction of TBDs. The Staudinger reaction of a 1:1 mixture of Mes*N$_3$ and PMe$_3$ in toluene-d_8 was monitored by ^{31}P{^{1}H} NMR spectroscopy, showing two species at 29.3 and −22.1 ppm in a 97:3 ratio after 15 min. Based on DFT studies (Table S7) these were assigned to azidophosphorane Mes*N$_3$(PMe$_3$) (**3**; δ_{calc}(^{31}P) = 32.2 ppm) and iminophosphorane Mes*N(PMe$_3$) (**4**; δ_{calc}-(^{31}P) = −27.1 ppm), respectively. Within 9.5 h (Figure S169) **3** slowly converts to **4** upon extrusion of N_2. Computational investigations (DNLPO-CCSD(T)/def2TZVP(smd = benzene)//PBE0-D3/def2SVP) revealed a *trans*/*cis*-isomerization in **3** as the first reaction step (Figure 2, cf. p. S156 ff.). Through an energetically low-lying transition state (TS1), an intermediate (INT1) in which N_α and PMe$_3$ are *cis*-oriented is formed. From INT1, strongly exergonic N_2-elimination and formation of **4** proceeds via four-membered transition state TS2 (89.2 kJ/mol). TS2 is the rate-determining step and consequently, the observed azide-Wittig reaction is generally

faster than N_2 elimination in a kinetically controlled reaction.

Next a 1:1 mixture of Mes*N_3 and benzaldehyde in toluene was treated with PMe_3 (1 M in toluene) at 0 °C (Figure 3). After stirring overnight at ambient temperature *E*-triazabutadiene Mes*N_3C(H)Ph (**5a**) was quantitatively formed, with a characteristic C*H*N ^{1}H NMR signal at 8.98 ppm in C_6D6 (cf. Mes*NC(*H*)Ph 8.26 ppm).[30] After work-up (in air) and precipitation from MeCN at −30 °C, **5a** was afforded as an orange crystalline powder in 75 % isolated yield. SC-XRD experiments (Figure 3), showed that the PhCHN_3 moiety and central Mes* aryl ring in **5a** are nearly perpendicular to each other (Figure S3). We next tested different benzaldehydes, (Figure 3) and quantitative conversions were observed for benzaldehydes with electron withdrawing *para*-substituents affording TBDs (**5b**, **5c**, **5g**) in good yields after work-up. A *p*-NMe_2 group (**5h**) with a negative Hammett parameter resulted in incomplete conversion and only moderate isolated yield. Although less selective, a synthetically useful 4-NO_2 substituent was tolerated, albeit in lower yields due to unidentified side-products (**5i**, 47 %). With 3-Br benzaldehyde **5l** was obtained in 49 % yield. 2-OMe and 2-Me benzaldehyde were fully converted and TBDs **5j** and **5k** obtained in good yields. Ferrocenyl- (**5f**), 1-anthracenyl (**5m**) and 2-naphtylaldehyde (**5n**) were likewise tolerated. A 2,6-bis-triazabutadiene substituted pyridine (**5p**) was obtained in the reaction with 2,6-pyridinedicarbaldehyde (Figure S5), showing that heterocyclic aldehydes are likewise tolerated. Naturally occurring *E*-cinnamylaldehyde afforded after work-up the corresponding triazahexatriene with all three conjugated double bonds being *E*-configured (**5o**). With the terpenoid (*R*)-(+)-citronellal formation of the corresponding TBD **5q** as a yellow oil was achieved. In general, most of the reactions are quantitative based on ^{1}H NMR studies, and lower than expected yields are due to work-up. Although the aldehyde scope proved to be broad, ketones did not react.

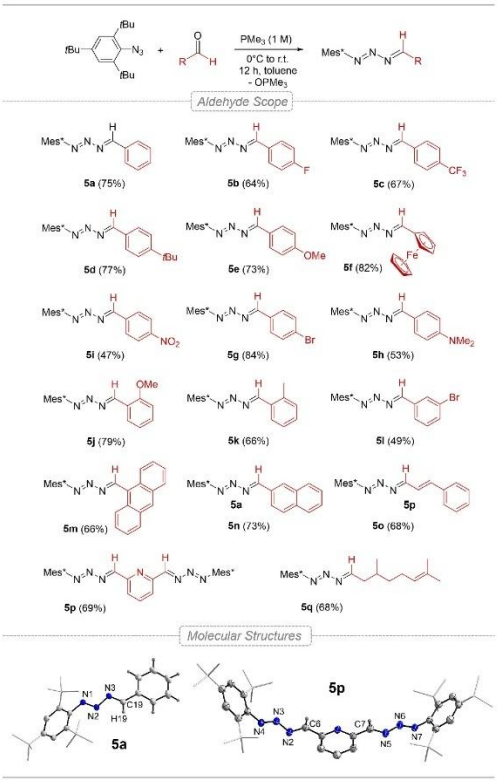

Figure 3. Aldehyde scope using PMe_3. Yields given correspond to isolated yields. Bottom: Molecular structures of **5a** and **5p**.

The thermally stable azidophosphorane AdN_3(P-$(NMe_2)_3$) (**6**) (Ad = 1-adamantyl; Figure S6, $\delta(^{31}P) = 42$ ppm) [31] was combined with benzaldehyde in C_6D_6 and after heating the mixture to 50 °C for one hour, a downfield resonance was observed in the ^{1}H NMR spectrum at 8.94 ppm (Figure S94), in line with the formation of TBD AdN_3C(H)Ph (**7a**) (cf. PhC(H)NAd 8.29 ppm).[32] Considering $OP(NMe_2)_3$ as an undesired byproduct, the thermal N_2-release from different azidophosphoranes with different steric profiles was investigated in silico.

The overall barrier for N_2-elimination in DippN_3P*n*Bu_3 (Dipp = 2,6-*i*$Pr_2C_6H_3$) was calculated at 74.0 kJ/mol, with a lower barrier for DippN_3PMe_3 (44.0 kJ/mol). Surprisingly, in the gas phase AdN_3PMe_3 is rather stable (77.5 kJ/mol), with a similar barrier found for the N_2 release in MesN_3P*n*Bu_3 (Mes = 2,4,6-$Me_3C_6H_2$) (Figure S194–198). Consequently, azide-Wittig reactivity should still be feasible if the reactions were carried out at lower temperatures using either P*n*Bu_3 or PMe_3. Variable temperature (VT) ^{31}P NMR spectroscopic studies on a 1:1 mixture of AdN_3 and PMe_3 in toluene-d_8 confirmed the relative stability of *trans*-AdN_3PMe_3 ($\delta(^{31}P) =$ 29.9 ppm; $\delta_{calc}(^{31}P) = 28.6$ ppm) which forms at −20 °C and converts to the *cis*-form (INT1, $\delta(^{31}P) = 10.4$ ppm; $\delta_{calc}(^{31}P) =$ 1.1 ppm) above −10 °C with N_2 elimination starting at 0 °C (Figure S171). Full conversion to iminophosphorane AdNPMe_3 ($\delta(^{31}P) = -14.7$ ppm) is detected at 24 °C, in line with the theoretically predicted low lying first transition state for the *cis*/*trans*-isomerization (32 kJ/mol), with the *cis*-isomer being favored by −1.2 kJ/mol.[33]

Consequently, AdN_3, benzaldehyde and PMe_3 were mixed in a 1:1:1 ratio in toluene at −78 °C (Figure 4). Warming to ambient temperature over a period of 3 h gave a yellow solution and after re-crystallization from *n*-hexane, AdN_3C(H)Ph (**7a**) was isolated as yellow crystalline solid (78 %). Using 4-OMe- or 4-*t*Bu-benzaldehyde under the same conditions, TBDs **7b** (Figure 4) and **7c** were afforded in 54 % or 77 % yield, respectively. When using FcCHO, in conjunction with P*n*Bu_3, TBD **7d** was isolated as a red solid in 63 % yield after recrystallization. Next, VT NMR experiments on a 1:1 mixture of DippN_3 and P*n*Bu_3 revealed that DippN_3P*n*Bu_3 is stable up to −20 °C (Figure S170), leading us to study the azide-Wittig reactivity below −30 °C. When a

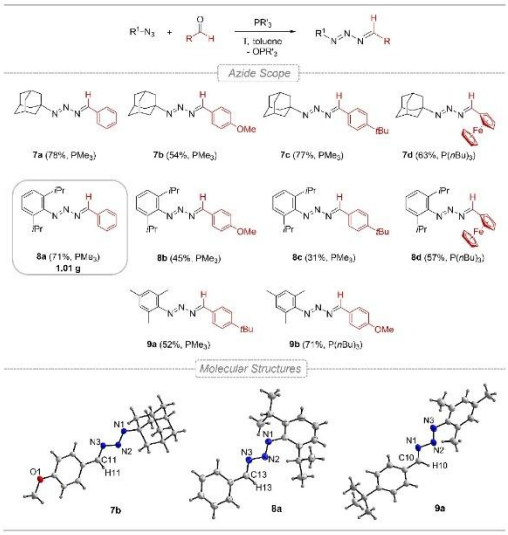

Figure 4. Azide scope of the Azide-Wittig reaction. The phosphine used is denoted, while exact reaction temperatures and further details are given in the ESI.

toluene solution of P*n*Bu$_3$, DippN$_3$ and benzaldehyde was warmed from −35 °C to ambient temperature a red solution was obtained. The removal of OP(*n*Bu)$_3$ proved difficult, nevertheless, crystallization from *n*-hexane, afforded DippN$_3$C(H)Ph (**8a**) as an orange crystalline solid. SC-XRD experiments showed that the planes of the Dipp and the PhC(H)N$_3$ units in **8a** are rotated against each other by ca. 45° (Figure 4), contrasting **5a** with perpendicular planes. On a larger scale **8a** (1 g DippN$_3$) was prepared using a 1 M PMe$_3$ solution at low temperature, giving **8a** on a gram-scale in 71 % yield. Likewise, 4-OMe- or 4-*t*Bu-benzaldehyde, were converted to TBDs **8b** and **8c** in moderate yields. The FcCHO-derived Dipp-substituted TBD **8d** is insoluble in *n*-hexane, thus P*n*Bu$_3$ was selected as phosphine in this case, giving **8d** in 57 % yield. DippN$_3$ reacted unselectively with 4-NO$_2$ and 4-CF$_3$-benzaldehydes (Figure S190).

As a last entry MesN$_3$ was tested: Although MesN$_3$C(H)Ph formed in the reaction with benzaldehyde using P*n*Bu$_3$ at −30 °C, it was found to be thermally labile towards N$_2$ elimination and formation of MesNC(H)Ph. Using 4-*t*Bu-benzaldehyde, MesN$_3$, and PMe$_3$ in toluene at −30 °C, facile synthesis of TBD **9a** as a thermally stable (Figure 4, T_{dec} = 109 °C) orange solid was achieved. When 4-OMe-benzaldehyde was used instead, TBD **9b** was found to crystallize readily from *n*-pentane and thus, P*n*Bu$_3$ was used in this case, giving **9b** in 71 % yield.

All reactions are initiated under an Ar atmosphere, however, work-up is carried out in air, foreshadowing that this protocol can be readily adapted. The Mes*N$_3$-derived TBDs **5a**–**p** are thermally robust and can be stored in moist air at ambient temperature. 4-*t*Bu-substituted variant **5d** is thermally stable in benzene at 80 °C for at least 12 h, while Mes-derivative **9a** cleanly formed the corresponding imine under the same conditions. Ad-substituted TBD **7c** mainly converted to 4-*t*Bu-benzonitrile when heated to 80 °C in benzene (Figure S175). This decomposition pathway is reminiscent of a recent report on the Cu-catalyzed benzonitrile formation from ketones.[34] Compound **9b** is stable in MeOD at 50 °C for 2 h, while after eight days in MeOD at ambient temperature the corresponding imine forms quantitatively (Figure S179). Surprisingly, **8a** and **9b** cleanly decomposed in the solid state when left in moist air at ambient temperature, giving the corresponding imines. No decomposition occurred at −30 °C. Such decomposition was not observed for the Ad-derivatives and combined TGA-DSC-MS studies on **7b** are in line with thermal decomposition at 111 °C through N$_2$-extrusion (Figure S182). Moreover, DSC studies on Mes*-derivatives **5a**–**5e** and **5i** showed thermal stability in the solid state. While **5a**, **5b** and **5d** decompose above 120 °C, TBD **5i** shows a sharp endothermic melting event (129 °C) followed directly by the onset of exothermic decomposition. UV/Vis experiments revealed strong absorptions in the UV-region at ca. 300 nm associated with π→π* transitions within the ArC(H)N$_3$ unit. In case of the Mes*-, Dipp- and Mes-derivatives low intensity absorbances at ca. 450 nm correspond to symmetry forbidden π→π* (HOMO-LUMO) transitions based on TD-DFT studies (Tables S8–13). The HOMO in aryl-substituted TBDs is best described as linear combination of an aryl π-orbital with admixing of the nitrogen lone pairs, while the LUMO is of π* character and fully delocalized over the ArC(H)N$_3$ unit. With increasing co-planarity of the ArC(H)N$_3$- and aryl azide group in the Dipp- and Mes-derivatives, the HOMO-LUMO transitions become more pronounced. NBO analyses clearly show the iminic carbon atom to be the nucleophilic site of the TBDs presented, while the N atoms all carry a negative partial charge, which is most pronounced for the N$_\gamma$-atom (Figure S197). In NHC-derived TBDs the N$_\alpha$ has been shown to be the preferred site for electrophilic functionalization.[25] Surprisingly, when TBDs **5d** and **5e** were treated with MeOTf no reaction was observed. Ferrocenyl derivative **5f** instead gave the corresponding dimethyliminium triflate **10** along with other unidentified products, clearly showing that the N$_\gamma$ atom is indeed the main nucleophilic site, a finding that should prove important for future applications of the unique TBDs presented in here.

This study demonstrates a general azide-Wittig reaction, which has been overlooked since the Staudinger's seminal report more than a century ago. Organic azides, aldehydes and phosphines are combined under thermal control, furnishing TBDs with unprecedented substitution patterns. Computational studies aided the reaction design, allowing the synthesis of a broad range of differently functionalized systems which should allow widespread applications of TBDs. Future studies will focus on rendering this transformation catalytic.

Supporting Information

Experimental procedures, complete characterization data, copies of NMR spectra, additional spectroscopic data and computational details (PDF). Calculated geometries (xyz). The authors have cited additional references within the Supporting Information.[35–66]

Caution! Covalent azides are potentially hazardous and can decompose explosively under various conditions! Appropriate safety precautions should be taken.

Acknowledgements

We gratefully acknowledge Dr. Anke Spannenberg (LIKAT) for the acquisition of X-ray data sets. We thank Dr. Marcus Klahn (LIKAT) for assistance with MS measurements, Andreas Koch (LIKAT) for carrying out VT NMR experiments and Dr. Christoph Kubis (LIKAT) for help with TG-DSC-MS experiments. We wish to thank the ITMZ at the University of Rostock for access to the cluster computer, and especially Malte Willert for his assistance with the queuing system and software installations. Dr. Jonas Bresien (University of Rostock) is acknowledged for providing the SLURM interface for Gaussian. Leon Ohms and Prof. Axel Schulz are acknowledged for help with DSC-measurements. The Deutsche Forschungsgemeinschaft (HE 7348/3-1) and Studienstiftung des deutschen Volkes (U12AB123456) are gratefully acknowledged for financial support. Open Access funding enabled and organized by Projekt DEAL.

Conflict of Interest

The authors declare no conflict of interest.

Data Availability Statement

The data that support the findings of this study are available in the supplementary material of this article.

Keywords: Azides · Triazabutadienes · Organic Synthesis · Phosphaalkenes · Wittig Reaction

[1] G. Wittig, G. Geissler, *Liebigs Ann. Chem.* **1953**, *580*, 44–57.
[2] G. Wittig, U. Schöllkopf, *Chem. Ber.* **1954**, *87*, 1318–1330.
[3] L. Longwitz, T. Werner, *Pure Appl. Chem.* **2019**, *91*, 95–102.
[4] Y. Yamamoto, S.-i. Kawaguchi, M. Nishimura, Y. Sato, Y. Shimada, A. Tabuchi, A. Nomoto, A. Ogawa, *J. Org. Chem.* **2020**, *85*, 14684–14696.
[5] a) M. W. Rathke, R. Kow, *J. Am. Chem. Soc.* **1972**, *94*, 6854–6856; b) T. Wang, S. Kohrt, C. G. Daniliuc, G. Kehr, G. Erker, *Org. Biomol. Chem.* **2017**, *15*, 6223–6232; c) T. Heitkemper, L. Naß, C. P. Sindlinger, *Angew. Chem. Int. Ed.* **2021**, *60*, 20055–20060.
[6] S. Shah, J. D. Protasiewicz, *Chem. Commun.* **1998**, 1585–1586.
[7] A. M. Borys, E. F. Rice, G. S. Nichol, M. J. Cowley, *J. Am. Chem. Soc.* **2021**, *143*, 14065–14070.
[8] a) P. Gupta, T. Taeufer, J.-E. Siewert, F. Reiß, H.-J. Drexler, J. Pospech, T. Beweries, C. Hering-Junghans, *Inorg. Chem.* **2022**, *61*, 11639–11650; b) P. Gupta, H.-J. Drexler, R. Wingad, D. Wass, E. Baráth, T. Beweries, C. Hering-Junghans, *Inorg. Chem. Front.* **2023**, *10*, 2285–2293.
[9] J. D. Protasiewicz, *Eur. J. Inorg. Chem.* **2012**, *2012*, 4539–4549.
[10] a) M. Fischer, S. Nees, T. Kupfer, J. T. Goettel, H. Braunschweig, C. Hering-Junghans, *J. Am. Chem. Soc.* **2021**, *143*, 4106–4111; b) P. Gupta, J.-E. Siewert, T. Wellnitz, M. Fischer, W. Baumann, T. Beweries, C. Hering-Junghans, *Dalton Trans.* **2021**, *50*, 1838–1844; c) T. Taeufer, F. Dankert, D. Michalik, J. Pospech, J. Bresien, C. Hering-Junghans, *Chem. Sci.* **2023**, *14*, 3018–3023.
[11] H. Staudinger, E. Hauser, *Helv. Chim. Acta* **1921**, *4*, 861–886.
[12] a) D. Moser, K. Jana, C. Sparr, *Angew. Chem. Int. Ed.* **2023**, *62*, e202309053; b) Z. Lao, P. H. Toy, *Beilstein J. Org. Chem.* **2016**, *12*, 2577–2587; c) L. Cai, K. Zhang, S. Chen, R. J. Lepage, K. N. Houk, E. H. Krenske, O. Kwon, *J. Am. Chem. Soc.* **2019**, *141*, 9537–9542; d) P. H. Lambert, M. Vaultier, R. Carrie, *J. Org. Chem.* **1985**, *50*, 5352–5356.
[13] M. W. P. Bebbington, D. Bourissou, *Coord. Chem. Rev.* **2009**, *253*, 1248–1261.
[14] a) K. Vaughan, M. F. G. Stevens, *Chem. Soc. Rev.* **1978**, *7*, 377–397; b) S. Patil, A. Bugarin, *Eur. J. Org. Chem.* **2016**, *2016*, 860–870; c) A. A. Suleymanov, K. Severin, *Angew. Chem. Int. Ed.* **2021**, *60*, 6879–6889.
[15] H. E. Winberg, D. D. Coffman, *J. Am. Chem. Soc.* **1965**, *87*, 2776–2777.
[16] E. Fanghänel, R. Hänsel, W. Ortmann, J. Hohlfeld, *J. Prakt. Chem.* **1975**, *317*, 631–640.
[17] D. M. Khramov, C. W. Bielawski, *Chem. Commun.* **2005**, 4958–4960.
[18] S. Lysenko, C. G. Daniliuc, P. G. Jones, M. Tamm, *J. Organomet. Chem.* **2013**, *744*, 7–14.
[19] M. Kitamura, M. Yano, N. Tashiro, S. Miyagawa, M. Sando, T. Okauchi, *Eur. J. Org. Chem.* **2011**, *2011*, 458–462.
[20] Z. R. Turner, R. Bellabarba, R. P. Tooze, P. L. Arnold, *J. Am. Chem. Soc.* **2010**, *132*, 4050–4051.
[21] a) E. Barragan, A. Noonikara Poyil, C.-H. Yang, H. Wang, A. Bugarin, *Org. Chem. Front.* **2019**, *6*, 152–161; b) E. Barragan, A. Noonikara-Poyil, A. Bugarin, *Asian J. Org. Chem.* **2020**, *9*, 593–599.
[22] D. J. Coady, D. M. Khramov, B. C. Norris, A. G. Tennyson, C. W. Bielawski, *Angew. Chem. Int. Ed.* **2009**, *48*, 5187–5190.
[23] D. Yi, Y. Wu, C. Chen, L. Wang, Q. Wang, L. Pu, S. Wei, *Chin. Chem. Lett.* **2019**, *30*, 1059–1062.
[24] A. N. Wijetunge, G. J. Davis, M. Shadmehr, J. A. Townsend, M. T. Marty, J. C. Jewett, *Bioconjugate Chem.* **2021**, *32*, 254–258.
[25] L. E. Guzmán, A. N. Wijetunge, B. F. Riske, B. B. Massani, M. A. Riehle, J. C. Jewett, *J. Am. Chem. Soc.* **2024**, *146*, 8480–8485.
[26] K. E. Szabó, E. Kyriakis, A.-M. G. Psarra, A. G. Karra, Á. Sipos, T. Docsa, G. A. Stravodimos, E. Katsidou, V. T. Skamnaki, P. G. V. Liggri, S. E. Zographos, A. Mándi, S. B. Király, T. Kurtán, D. D. Leonidas, L. Somsák, *J. Med. Chem.* **2019**, *62*, 6116–6136.
[27] S. D. Taylor, C. R. Lohani, *Org. Lett.* **2016**, *18*, 4412–4415.
[28] E. L. Myers, R. T. Raines, *Angew. Chem. Int. Ed.* **2009**, *48*, 2359–2363.
[29] Deposition Numbers 2361934 (for **1**), 2361935 (for **2**), 2361936 (for **5a**), 2361937 (for **5d**), 2361938 (for **5p**), 2361939 (for **6**), 2361940 (for **7b**), 2361941 (for **8a**), 2361942 (for **9a**) and2361943 (for **10**) contain the supplementary crystallographic data for this paper. These data are provided free of

charge by the joint Cambridge Crystallographic Data Centre and Fachinformationszentrum Karlsruhe Access Structures service.

[30] S. Vollbrecht, U. Klingebiel, D. Schmidt-Bäse, *Z. Naturforsch. B.* **1991**, *46*, 709–713.

[31] J. R. Goerlich, M. Farkens, A. Fischer, P. G. Jones, R. Schmutzler, *Z. Anorg. Allg. Chem.* **1994**, *620*, 707–715.

[32] M. A. Ashley, T. Rovis, *J. Am. Chem. Soc.* **2020**, *142*, 18310–18316.

[33] C. Widauer, H. Grützmacher, I. Shevchenko, V. Gramlich, *Eur. J. Inorg. Chem.* **1999**, *1999*, 1659–1664.

[34] B. Xu, Q. Jiang, A. Zhao, J. Jia, Q. Liu, W. Luo, C. Guo, *Chem. Commun.* **2015**, *51*, 11264–11267.

[35] J. Bresien, A. Hinz, A. Schulz, T. Suhrbier, M. Thomas, A. Villinger, *Chem. Eur. J.* **2017**, *23*, 14738–14742.

[36] H. Y. V. Ching, X. Wang, M. He, N. Perujo Holland, R. Guillot, C. Slim, S. Griveau, H. C. Bertrand, C. Policar, F. Bedioui, M. Fontecave, *Inorg. Chem.* **2017**, *56*, 2966–2976.

[37] K. Barral, A. D. Moorhouse, J. E. Moses, *Org. Lett.* **2007**, *9*, 1809–1811.

[38] T. Sasaki, A. Nakanishi, M. Ohno, *J. Org. Chem.* **1981**, *46*, 5445–5447.

[39] J. B. Bialecki, J. Ruzicka, A. B. Attygalle, *J. Labelled Compd. Radiopharm.* **2007**, *50*, 711–715.

[40] G. Du, Y. Wei, W. Zhang, Y. Dong, Z. Lin, H. He, S. Zhang, X. Li, *Dalton Trans.* **2013**, *42*, 1278–1286.

[41] W. Kandioller, J. Theiner, B. K. Kepplera, C. R. Kowol, *Inorg. Chem. Front.* **2022**, *9*, 412–416.

[42] G. M. Sheldrick, *Acta Crystallogr. Sect. A* **2015**, *71*, 3–8.

[43] G. M. Sheldrick, *Acta Crystallogr. Sect. C* **2015**, *71*, 3–8.

[44] L. J. Farrugia, *J. Appl. Crystallogr.* **2012**, *45*, 849.

[45] SADABS within APEX2; Bruker AXS Inc.: Madison, WI, (2014).

[46] a) F. Neese, *Wiley Interdiscip. Rev.: Comput. Mol. Sci.* **2012**, *2*, 73–78; b) F. Neese, *Wiley Interdiscip. Rev.: Comput. Mol. Sci.* **2018**, *8*, e1327; c) F. Neese, *Wiley Interdiscip. Rev.: Comput. Mol. Sci.* **2022**, *2*, e1606; d) F. Neese, F. Wennmohs, U. Becker, C. Riplinger, *J. Chem. Phys.* **2020**, *152*, 224108.

[47] M. J. Frisch, G. W. Trucks, H. B. Schlegel, G. E. Scuseria, M. A. Robb, J. R. Cheeseman, G. Scalmani, V. Barone, G. A. Petersson, H. Nakatsuji, X. Li, M. Caricato, A. V. Marenich, J. Bloino, B. G. Janesko, R. Gomperts, B. Mennucci, H. P. Hratchian, J. V. Ortiz, A. F. Izmaylov, J. L. Sonnenberg, D. Williams-Young, F. Ding, F. Lipparini, F. Egidi, J. Goings, B. Peng, A. Petrone, T. Henderson, D. Ranasinghe, V. G. Zakrzewski, J. Gao, N. Rega, G. Zheng, W. Liang, M. Hada, M. Ehara, K. Toyota, R. Fukuda, J. Hasegawa, M. Ishida, T. Nakajima, Y. Honda, O. Kitao, H. Nakai, T. Vreven, K. Throssell, J. A. Montgomery, Jr., J. E. Peralta, F. Ogliaro, M. J. Bearpark, J. J. Heyd, E. N. Brothers, K. N. Kudin, V. N. Staroverov, T. A. Keith, R. Kobayashi, J. Normand, K. Raghavachari, A. P. Rendell, J. C. Burant, S. S. Iyengar, J. Tomasi, M. Cossi, J. M. Millam, M. Klene, C. Adamo, R. Cammi, J. W. Ochterski, R. L. Martin, K. Morokuma, O. Farkas, J. B. Foresman, D. J. Fox. Gaussian 16, Revision C.01. Gaussian, Inc., Wallingford CT, **2016**; https://gaussian.com/gaussian16.

[48] C. Bannwarth, E. Caldeweyher, S. Ehlert, A. Hansen, P. Pracht, J. Seibert, S. Spicher, S. Grimme, *Comput. Mol. Sci.* **2020**, *11*, e01493.

[49] a) F. Weinhold, J. E. Carpenter, *The Natural Bond Orbital Lewis Structure Concept for Molecules, Radicals, and Radical Ions, in The Structure of Small Molecules and Ions*, R. Naaman, Z. Vager, Eds., Springer: Boston, MA, **1988**, pp. 227–236; b) F. Weinhold, C. R. Landis, *Discovering Chemistry with Natural Bond Orbitals*, John Wiley & Sons, Inc.: Hoboken, NJ, USA, **2012**; c) E. D. Glendening, J. K. Badenhoop, A. E. Reed, J. E. Carpenter, J. A. Bohmann, C. M. Morales, C. R. Landis, F. Weinhold. NBO 6.0. Theoretical Chemistry Institute, University of Wisconsin, Madison, WI (2013); https://nbo.chem.wisc.edu; d) F. Weinhold, C. R. Landis, E. D. Glendening, *Int. Rev. Phys. Chem.* **2016**, *35*, 399–440.

[50] a) S. H. Vosko, L. Wilk, M. Nusair, *Can. J. Phys.* **1980**, *58*, 1200–1211; b) C. Lee, W. Yang, R. G. Parr, *Phys. Rev. B* **1988**, *37*, 785–789; c) A. D. Becke, *Phys. Rev. A* **1988**, *38*, 3098–3100; d) B. Miehlich, *Chem. Phys. Lett.* **1989**, *157*, 200–206; e) A. D. Becke, *J. Chem. Phys.* **1993**, *98*, 5648–5652; f) P. J. Stephens, F. J. Devlin, C. F. Chabalowski, M. J. Frisch, *J. Phys. Chem.* **1994**, *98*, 11623–11627.

[51] a) S. Grimme, J. Antony, S. Ehrlich, H. A. Krieg, *J. Chem. Phys.* **2010**, *132*, 154104; b) S. Grimme, S. Ehrlich, L. Goerigk, *J. Comput. Chem.* **2011**, *32*, 1456–1465.

[52] F. Weigend, R. Ahlrichs, *Phys. Chem. Chem. Phys.* **2005**, *7*, 3297–3305.

[53] I. M. Alecu, J. Zheng, Y. Zhao, D. G. Truhlar, *J. Chem. Theory Comput.* **2010**, *6*, 2872–2887.

[54] a) R. Bauernschmitt, R. Ahlrichs, *Chem. Phys. Lett.* **1996**, *256*, 454–464; b) R. E. Stratmann, G. E. Scuseria, M. J. Frisch, *J. Chem. Phys.* **1998**, *109*, 8218–8224; c) M. E. Casida, C. Jamorski, K. C. Casida, D. R. Salahub, *J. Chem. Phys.* **1998**, *108*, 4439–4449.

[55] a) T. H. Jr. Dunning, *J. Chem. Phys.* **1989**, *90*, 1007–1023; b) R. A. Kendall, T. H. Jr. Dunning, R. J. Harrison, *J. Chem. Phys.* **1992**, *96*, 6796–6806; c) D. E. Woon, T. H. Jr. Dunning, *J. Chem. Phys.* **1993**, *98*, 1358–1371; d) K. A. Peterson, D. E. Woon, T. H. Jr. Dunning, *J. Chem. Phys.* **1994**, *100*, 7410–7415; e) T. Hashimoto, K. Hirao, H. Tatewaki, *Chem. Phys. Lett.* **1995**, *243*, 190–192; f) A. K. Wilson, T. van Mourik, T. H. Jr. Dunning, *J. Mol. Struct.* **1996**, *388*, 339–349.

[56] a) F. London, *J. Phys. Radium* **1937**, *8*, 397–409; b) R. McWeeny, *Phys. Rev.* **1962**, *26*, 1028–1034; c) R. Ditchfield, *Mol. Phys.* **1974**, *27*, 789–807; d) K. Wolinski, F. Hinton, P. Pulay, *J. Am. Chem. Soc.* **1990**, *112*, 8251–8260; e) J. R. Cheeseman, G. W. Trucks, T. A. Keith, M. J. Frisch, *J. Chem. Phys.* **1996**, *04*, 5497–5509.

[57] a) J. P. Perdew, K. Burke, M. Ernzerhof, *Phys. Rev. Lett.* **1996**, *77*, 3865–3868; b) J. P. Perdew, K. Burke, M. Ernzerhof, *Phys. Rev. Lett.* **1996**, *77*, 3865–3868; c) J. P. Perdew, K. Burke, M. Ernzerhof, *Phys. Rev. Lett.* **1997**, *78*, 1396–1396; d) C. Adamo, V. Barone, *J. Chem. Phys.* **1999**, *110*, 6158–6170.

[58] C. J. Jameson, A. De Dios, A. Keith Jameson, *Chem. Phys. Lett.* **1990**, *167*, 575–582.

[59] C. van Wüllen, *Phys. Chem. Chem. Phys.* **2000**, *2*, 2137–2144.

[60] a) G. Mills, H. Jónsson, G. K. Schenter, *Surf. Sci.* **1995**, *324*, 305–337; b) H. Jónsson, G. Mills, K. W. Jacobsen, *Nudged Elastic Band Method for Finding Minimum Energy Paths of Transitions, in Classical and Quantum Dynamics in Condensed Phase Simulations*, World Scientific, **1998**, pp. 385–404; c) G. Henkelman, H. Jónsson, *J. Chem. Phys.* **2000**, *113*, 9978–9985; d) G. Henkelman, B. P. Uberuaga, H. Jónsson, *J. Chem. Phys.* **2000**, *113*, 9901–9904; E; e) Maras, O. Trushin, A. Stukowski, T. Ala-Nissila, H. Jónsson, *Comput. Phys. Commun.* **2016**, *205*, 13–21; f) V. Ásgeirsson, B. O. Birgisson, R. Bjornsson, U. Becker, F. Neese, C. Riplinger, H. Jónsson, *J. Chem. Theory Comput.* **2021**, *17*, 4929–4945.

[61] a) J. Baker, *J. Comput. Chem.* **1986**, *7*, 385–395; b) H. B. Schlegel, *Optimization of Equilibrium Geometries and Transition Structures, in Advances in Chemical Physics: Ab Initio Methods in Quantum Chemistry Part I*, K. P. Lawley, Ed., John Wiley & Sons, **1987**, pp. 249–286; c) H. B. Schlegel, *Geometry Optimization on Potential Energy Surfaces, in Modern Electronic Structure Theory*, D. R. Yarkony, Ed., World Scientific, **1995**, pp. 459–500; d) F. Eckert, P. Pulay, H.-J. Werner, *J. Comput. Chem.* **1997**, *18*, 1473–1483.

[62] S. Grimme, *J. Chem. Theory Comput.* **2019**, *155*, 2847–2862.
[63] C. Bannwarth, S. Ehlert, S. Grimme, *J. Chem. Theory Comput.* **2019**, *15*, 1652–1671.
[64] a) C. Riplinger, F. Neese, *J. Chem. Phys.* **2013**, *138*, 034106; b) D. G. Liakos, M. Sparta, M. K. Kesharwani, J. M. L. Martin, F. Neese, *J. Chem. Theory Comput.* **2015**, *11*, 1525–1539; c) C. Riplinger, P. Pinski, U. Becker, E. F. Valeev, F. Neese, *J. Chem. Phys.* **2016**, *144*, 024109.
[65] C. J. Cramer, *Essentials of Computational Chemistry: Theories and Models*, John Wiley & Sons, Ltd, Chichester, UK, **2004**.
[66] A. V. Marenich, C. J. Cramer, D. G. Truhlar, *J. Phys. Chem. B* **2009**, *113*, 6378–6396.

Manuscript received: July 10, 2024
Accepted manuscript online: September 25, 2024
Version of record online: November 9, 2024

4.3 Coordination and C-H Activation of an Amidobis(phosphaalkene) at Rhodium(I)

Kushik, Mirko Rippke, Hans-Joachim Drexler, Fabian Dankert, Christian Hering-Junghans and Torsten Beweries

manuscript submitted

Contribution to this paper is 50%

ChemComm

COMMUNICATION

Coordination and C-H Activation of an Amidobis(phosphaalkene) at Rhodium(I)

Received 00th January 20xx,
Accepted 00th January 20xx

DOI: 10.1039/x0xx00000x

Kushik,[a] Mirko Rippke,[a] Hans-Joachim Drexler,[a] Fabian Dankert,[b] Christian Hering-Junghans[a]* and Torsten Beweries[a]*

Reactions of a highly basic monoanionic PNP type bis-phosphaalkene ligand with $[Rh(cod)(Cl)]_2$ furnish two dinuclear Rh(I) complexes which show C-H activation of the Mes* groups of the ligand and the presence of three different phosphaalkene coordination modes, respectively. Computational analyses suggests the presence of a unique Rh–Rh donor-acceptor interaction in the C-H activated complex.

Phosphaalkenes (PAs), $RP{=}CR_2$, are organophosphorus compounds characterised by a P=C double bond that are related to alkenes and their lighter group 15 homologues imines,[1] showing great potential for various applications in modern organophosphorus chemistry.[2] The coordination chemistry of PAs to transition metals is characterised by their unique ligand properties (HOMO P=C π-bond, s character of the lone pair at P, inverse polarity of the $P^{(\delta+)}$–$C^{(\delta-)}$ bond), making these compounds weaker σ donors than imines, but considerable π acceptors due to the low-lying P–C π* orbital (LUMO). Coordination of neutral PA ligands to late transition metals has been reported on several occasions,[3] and some of such complexes have also found applications in stoichiometric and catalytic transformations such as N-H activation,[4] aza-Claisen rearrangements,[5] or upgrading of alcohols.[6]

Although tri-[7] and tetradentate[8] PNP- (Figure 1, top left) and PPPP-type PAs have been reported, to the best our knowledge mono-anionic PNP pincer-type PA architectures have not been reported to date. This structural motif is well-studied for amido-bis(phosphines) and its structural variety and versatility for synthesis and catalysis has been highlighted on several occasions.[9] Recent examples include work by Ozerov and co-workers on group 9 PNP systems bearing diphenylamine based amido-bis(phosphine) ligands (Figure 1, top right) for alkyne dimerisation and C-H activation,[10] as well as studies by Gade and co-workers on the stabilisation of unusual T-shaped 14-electron Rh(I) using amido-bis(phosphine) PNP ligands based on a carbazole backbone.[11]

An extension of the concept of PA ligands to tridentate, monoanionic representatives is desirable, since the resulting pincer ligands would create a well-defined reactive site due to their meridional coordination to the metal in combination with the sterically demanding flanking substituents (Figure 1, bottom). The resulting system should possess the typical electronic properties of PAs and at the same time be able to stabilise highly reactive low-valent transition metals. In this contribution we present the synthesis and characterisation of the first monoanionic bis-PA ligands along with their coordination chemistry to Rh(I), resulting in the formation of two dinuclear Rh complexes that possess intact, as well as C-H activated PA donor sites, as well as a rare Rh(I)–Rh(I) donor-acceptor interaction in one case.

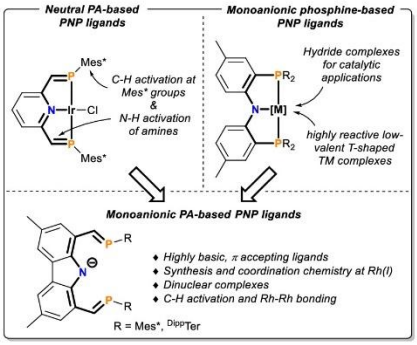

Figure 1. Contextualisation of this work. Mes* = 2,4,6-tBu_3-C_6H_2, ^{Dipp}Ter = 2,6-(2,6-$iPr_2C_6H_3$)-C_6H_3.

[a] *Leibniz-Institut für Katalyse e.V. (LIKAT Rostock), Albert-Einstein-Str. 29a, 18059 Rostock, Germany. Email: Christian.hering-junghans@catalysis.de, Torsten.beweries@catalysis.de*
[b] *University of Kassel, Heinrich-Plett Str. 40, 34132 Kassel, Germany.*
Supplementary Information available: Synthesis and characterization of compounds, NMR spectra, crystallographic, and computational details. CCDC 2451040-2451044. See DOI: 10.1039/x0xx00000x

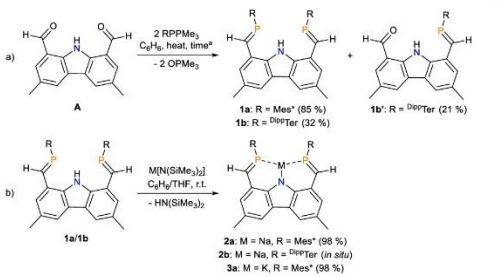

Scheme 1. a) Synthesis of novel ^{R2}PNP PA ligands **1a** and **1b**.[a] Conditions for **1a**: C_6H_6, 50 °C, 24 h; for **1b**: C_6H_6, 80 °C, 14 d. b) Synthesis of M[^{Mes*2}PNP] (M = Na (**2a**), K (**3a**)).

Novel PNP-based bis-PA pincer ligands were synthesised by treating 3,6-dimethyl-9H-carbazole-1,8-dicarbaldehyde (**A**) with two equivalents of the phospha-Wittig reagent Mes*PPMe$_3$ (Mes*= 2,4,6-*t*Bu$_3$-C$_6$H$_2$)[12] in benzene at 50 °C for 24 hours under the exclusion of light, giving the desired bis-PA ^{Mes*2}PNP (**1a**, Scheme 1) in good yield. ^{31}P{^{1}H} NMR analysis shows the PA units at 249.9 ppm, at the lower end of literature reported Mes*-substituted PA ligands ($\delta(^{31}P)$ 250 to 291 ppm),[Error! Bookmark not defined.] presumably due to delocalisation of electron density from the carbazole unit to the P–C π* orbitals. When heating a mixture of ^{Dipp}TerPPMe$_3$ and **A** in benzene in a 2:1 ratio to 80 °C for 14 days the analogous PNP ligand ^{DippTer2}PNP with ^{Dipp}Ter groups on the P atoms (**1b**) was prepared (Scheme 1, see ESI for details). The ^{31}P{^{1}H} NMR spectrum of the reaction mixture showed the characteristic resonance for bis-PA PNP ligand **1b** at 239.5 ppm. Beside mono-PA PNO species **1b'**, with only one PA arm and an intact aldehyde group,[13] is formed as indicated by a resonance at 244.6 ppm. In the ^{1}H NMR spectrum of **1b'** three deshielded resonances for the NH (10.80 ppm), C(O)H (9.73 ppm) and P=CH (9.23 ppm) protons, with the NH only showing a doublet signature, underline the presence of a single PA arm. By contrast bis-PA PNP ligands **1a** and **1b** show a triplet resonance (11.29 ppm, C_6D_6, J_{PH} = 11.6 Hz) for the NH proton due to coupling with two P atoms. The formation of **1b'** can be suppressed when using a slight molar excess of ^{Dipp}TerPPMe$_3$.

Crystals of **1a** suitable for single-crystal X-ray diffraction (SC-XRD) analysis were obtained from a saturated *n*-hexane solution at −30 °C overnight. SC-XRD analysis of **1a** (Figure 2) revealed the expected structure of the ^{Mes*2}PNP ligand with moderate hydrogen bonding interactions between the N-H proton and both phosphorus atoms of the PA unit, resulting in *E*-configured PA units (P1–C15 1.679(2), P2–C34 1.686(2) Å), with both Mes* substituents pointing away from the binding pocket. In **1b** both PA units are likewise *E*-configured (Figure S2), while one of the P atoms points away from the carbazole N atom to account for the increased steric strain from the ^{Dipp}Ter substituents. In both **1a** and **1b** the P=C bonds are nearly co-planar with the carbazole backbone.

To facilitate transmetalation, ligand **1a** was deprotonated using the non-nucleophilic bases M[N(SiMe$_3$)$_2$] (M = Na, K), in either benzene or THF at room temperature, yielding the alkali metal complexes [Na(^{Mes*2}PNP)] (**2a**) and [K(^{Mes*2}PNP)] (**3a**) in quantitative yields as red or violet solids, respectively. According to TD-DFT calculations the red colour of **2a** is associated with a π-π* transition, with the Na$^+$ resulting in a smaller HOMO-LUMO gap compared to **1a** and thus a red-shift in the longest wavelength absorption ($\lambda_{max,calc}$(**2a**) = 546.3 nm). Both salts are highly moisture sensitive, necessitating careful handling under strictly anhydrous conditions. The deprotonation of **1a** was confirmed by ^{1}H NMR spectroscopy, revealing the absence of the deshielded N-H signal. Moreover, IR spectroscopy showed the absence of the N–H stretching mode in the spectra of **2a** and **3a** (**1a**: $\tilde{\nu}$(N–H) = 3300 cm^{-1}). The ^{31}P{^{1}H} NMR spectra of the salts show considerably shielded signals for Na salt **2a** ($\delta(^{31}P)$ = 228.4 ppm) and K salt **3a** ($\delta(^{31}P)$ = 236.8 ppm) compared to the free ligand **1a**, reflecting the subtle electronic differences induced by the counterions. SC-XRD quality red crystals of **2a** were afforded by slow diffusion of Et$_2$O into a saturated *n*-hexane solution of **2a** at room temperature. The molecular structure of **2a** shows the Na ion in a distorted seesaw coordination environment (τ_4 = 0.32)[14] with the fourth coordination site occupied by Et$_2$O (note that Et$_2$O is only present in the solid state), resulting in Na located above the PNP mean plane. The Na contacts to the PNP ligand are in the expected range for elongated Na–N (Na1–N1 2.324(3) Å; Σr_{cov}(Na–N) = 2.26)[15] and Na–P single bonds (Na1–P1 2.735(2), Na1–P2 2.732(2) Å; Σr_{cov}(Na–P) = 2.66).[16] The PA units coordinate to Na in κ^P-fashion through the s-type lone pair on P, as indicated by short P–C distances (P1–C1 1.674(4), P2–C14 1.673(4) Å).

Next, **2a** was reacted with [Rh(cod)(Cl)]$_2$ in THF in a 2:1 molar ratio (Scheme 2), accompanied by a colour change from red to dark brown. The ^{31}P{^{1}H} NMR spectrum of the reaction mixture revealed two species, free ligand **1a** ($\delta(^{31}P)$ = 249.9 ppm) and a second species giving a doublet at 46.7 ppm ($^1J_{P-Rh}$ = 132 Hz), indicative of a Rh(I) complex (Scheme 2). The significant shielding of the ^{31}P NMR signal compared to ligand **1a** and two sets of doublets with a large $^2J_{H-H}$ coupling of 14 Hz for four diastereotopic benzylic protons in the ^{1}H NMR spectrum, indicated that the Mes*P=CH unit underwent intramolecular C–H addition/cyclisation to form a phospholanylmethyl (phosphaindane) moeity.[16] Such cyclisation reactions have been reported for PN-type PAs (e.g., [Rh(quin-P,N)$_2$]OTf, $\delta(^{31}P)$ = 55.1 ppm)[4a,4b] and BPEP-based systems [RhCl(Mes*$_2$-BPEP), $\delta(^{31}P)$ = 28.9 ppm).[17]

Surprisingly, SC-XRD analysis of green crystals obtained from a

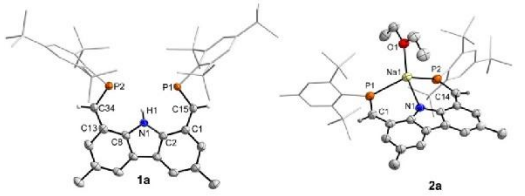

Figure 2. Molecular structures of **1a** (left) and **2a** (right). ORTEPs drawn at 50% probability. H atoms (except N*H* and RP=C*H*R) omitted and Mes* groups rendered as wireframe for clarity.

Please do not adjust margins

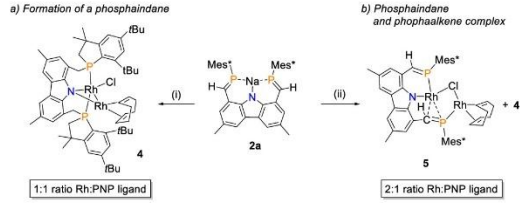

Scheme 2. Reactions of **2a** with varying amounts of $[Rh(cod)(Cl)]_2$. Conditions: (i) 0.5 $[Rh(cod)(Cl)]_2$, THF, 1 h, r.t.; (ii) $[Rh(cod)(Cl)]_2$, THF, 1 h, r.t.

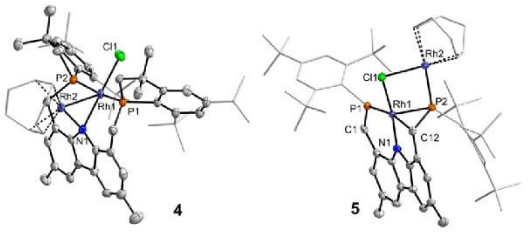

Figure 3. Molecular structures of complexes **4** and **5**. ORTEPs drawn at 50% probability. For clarity, hydrogen atoms are omitted and Mes* groups and cod ligands rendered as wireframe for clarity.

concentrated THF solution layered with *n*-pentane and stored at ambient temperature revealed the formation of the dinuclear Rh(I) phosphaindane complex **4** (Figure 3). When not considering the Rh–Rh interaction (Rh1–Rh2 2.6334(9), cf. Σr_{cov}(Rh–Rh) = 2.50 Å), Rh2 resides in a trigonal pyramidal coordination sphere, coordinated by cod and the carbazole N atom. This rather unusual coordination sphere for a 16-valence electron complex renders the metal centre Lewis-acidic.[18,19] By contrast, Rh1 is best described as a 16-valence electron square-planar Rh(I) centre (not considering the Rh–Rh interaction), rendering the metal centre Lewis-basic. Rh1 is coordinated by both phosphaindane arms in a *trans*-arrangement (Rh1–P1 2.311(2), Rh1–P2 2.317(2) Å), in addition to Cl^- and the carbazole N atom. Both metal centres are bridged by the carbazole N atom, with inequivalent Rh2–N1 (2.094(6) Å) and Rh1–N1 (2.149(7) Å) distances.

To elucidate the Rh–Rh bonding in complex **4**, DFT studies at the PBE0-D3/def2-SVP level of theory were carried out (see ESI for details). The HOMO is best described as non-bonding with significant d-orbital contribution at both Rh centres with a higher coefficient at the square planar Rh1 centre. The Rh1–Rh2 interaction is represented in HOMO-1 (Figure 4, top left), and shows donation from a dz^2 on Rh1 into a d-orbital at Rh2, while the Rh–N bonding is represented in HOMO-2 and HOMO-5. The LUMO is metal centred and thus the longest wavelength absorption ($\lambda_{max,exp.}$ = 652 nm, $\lambda_{max,calc.}$ = 609 nm) can be best described as a metal-to-metal charge transfer (HOMO-LUMO transition). An NBO analysis also shows a dz^2 orbital on Rh1 (Figure 4, top right), which is delocalised into a d-type lone valence at Rh2. In the NBO picture the sp^2-type lone pair on the carbazole N atom is delocalised into d-type lone valencies at each Rh centre. Complementary IBOs also illustrate the donor-acceptor character of the Rh–Rh bond (Figure 4, bottom left), while the electron localisation function (ELF) shows considerable localised electron density between the Rh atoms (Figure 4, bottom right). In line with this AIM analyses show a bond critical point.

Next the reaction of **2a** and $[Rh(cod)(Cl)]_2$ in a 1:1 molar ratio was studied to explore whether full ligand consumption could be achieved. The reaction mixture in THF at room temperature revealed the formation of **4** according to $^{31}P\{^1H\}$ NMR spectroscopy, along with a new set of signals; a doublet at 169.2 ppm ($^1J_{P-Rh}$ = 152 Hz) and a doublet of doublets at 125 ppm ($^1J_{P-Rh}$= 157 Hz, $^1J_{P-Rh}$ = 70 Hz). These lower field signals suggest the presence of intact P=C units and of another dinuclear Rh(I) species. SC-XRD analysis of dark red crystals revealed the first example of a dinuclear Rh(I) complex featuring three different coordination modes of its PA units (Figure 3, right). Both Rh atoms are μ-bridged by a chloride and one of the PA units (P2–C12 1.765(3) Å) shows both a side-on η^2-coordination to Rh1 and end-on η^1-κ^P coordination to Rh2. The P2–C12 distance is in line with a previously reported η^2-PA Ni complex (e.g., 1.773(8) Å).[20] Even though such coordination mode has been theoretically considered,[1] this is the first synthetic realisation of PA η^1,η^2-coordination. Interestingly, the P2–C12 PA is *Z*-configured, resulting in π-π interactions of the Mes* group at P2 with the phenyl ring of the carbazole moiety (distance between centroids of both rings = 3.686 Å)). The other PA unit shows a considerably shorter P1–C1 bond (1.694(2) Å), in line with P1 coordinating to Rh1 in η^1-fashion. The coordination sphere at Rh1 is completed by the carbazole N atom (Rh1–N1 1.975(2) Å) in *trans*-position to the μ-bridging Cl^-. The discovery of complex **5** adds a novel dimension to the coordination chemistry of PAs, expanding the known modes of interaction with transition metals.

According to TD-DFT studies the longest wavelength absorption ($\lambda_{max,exp.}$ = 796 nm, $\lambda_{max,calc.}$ = 735 nm) in the UV-Vis spectrum is associated with a HOMO-LUMO transition that can be best described as charge redistribution within the PNP framework with little contributions from the Rh centres. The second absorption at 564 nm is associated with an MLCT process (HOMO-1 to LUMO). The side-on coordination of the P2-C12 arm is best visualised in HOMO-1 and HOMO-5, while in the NBO picture this interaction is reflected in a Rh–P bonding orbital which is best described as an interaction of a Rh-centred d-orbital with the P–C π* orbital.

To determine whether the observed reactivity is exclusive to $[Rh(cod)(Cl)]_2$, further investigations were carried out using related group 9 metal precursors. $^{31}P\{^1H\}$ NMR monitoring of reactions of **2a** and 1 or 0.5 equivalents of $[Ir(cod)(Cl)]_2$ in THF indicated the formation of the protonated ligand **1a** (δ 250.0 ppm) as the major species along with several unidentified products that show resonances between 20-25 ppm and 150-250 ppm (see ESI for details), suggesting unselective formation of PA and phosphaindane complexes. Formation of the protonated form of the ligand, likely through proton abstraction from the solvent, supports the strong basicity of **2a**. While $^{31}P\{^1H\}$ NMR spectra of the reaction of **2a** with 1 equiv. of

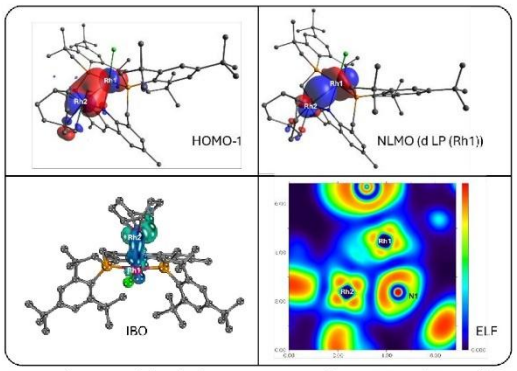

Figure 4. Illustration of the Rh–Rh interaction in complex **4**. HOMO-1 (PBE0-D3/def2-SVP), NLMO of a dz^2 type lone pair (LP) on Rh1, IBO of Rh–Rh interaction (r2SCAN-3c//PBE0-D3/def2-SVP), electron localisation function (ELF, PBE0-D3/def2-SVP).

$[Rh(coe)_2Cl]_2$ (coe = cyclooctene) show mainly phosphaindane type signals at ca. 50 ppm, using 0.5 equiv. of $[Rh(coe)_2Cl]_2$ mainly ligand **1a** was obtained. Similarly, reactions of **2a** with $[Rh(nbd)Cl]_2$ (nbd = 2,5-norbornadiene) produce mixtures of several species. However, in this case the reaction with 1 equiv. of $[Rh(nbd)Cl]_2$ shows minor signals at δ 172.8 and 137.3 ppm that could correspond to a species similar to **5**. These results suggest that the reactivity leading to **4** and **5** is unique for $[Rh(cod)Cl]_2$ and warrants further exploration to fully understand the underlying mechanisms.

The first anionic PNP-type bis-PA ligands **1a** and **1b** based on a carbazole backbone have been prepared and facile deprotonation yields their corresponding Na and K salts. With $[Rh(cod)(Cl)]_2$ a unique dinuclear Rh complex with a Rh–Rh donor-acceptor interaction is obtained, while with an excess of the Rh precursor a bis-PA complex with three different PA-coordination modes was accessed. Future studies will focus on expanding these concepts to main group elements and to utilise the Rh complexes in catalysis.

We thank the ITMZ at the University of Rostock for access to the cluster computer, and especially Malte Willert for his assistance with the queuing system and software installations. Dr. Jonas Bresien (University of Rostock) is acknowledged for providing the SLURM interface for Gaussian. The DFG (HE 7348/3-1) and Studienstiftung des Deutschen Volkes (U12AB123456) are gratefully acknowledged for financial support.

K.K.: Investigation, data curation, formal analysis, funding acquisition, writing – original draft. M.R.: Investigation and formal analysis. H.-J. D.: Investigation, formal analysis. F.D.: DFT calculations. C.H.-J. Conceptualisation, resources, DFT calculations, supervision, writing – review and editing. T.B.: Conceptualisation, funding acquisition, resources, supervision, writing – review and editing.

Conflicts of interest

There are no conflicts to declare.

Data availability

The data supporting this article have been included as part of the Supplementary Information. Crystallographic data has been deposited at the CCDC under identification numbers 2451040 (**1a**) 2451041 (**1b**), 2451042 (**2a**), 2451043 (**4**), and 2451044 (**5**), respectively. Further details can be obtained from the authors.

Notes and references

1 P. Le Floch, Coord. Chem. Rev., 2006, 250, 627-681.
2 A. Ziółkowska, J. Doroszuk, Ł. Ponikiewski, *Organometallics*, 2023, **42**, 505–537.
3 Selected examples: a) P. Gupta, T. Taeufer, J.-E. Siewert, F. Reiß, H.-J. Drexler, J. Pospech, T. Beweries and C. Hering-Junghans, *Inorg. Chem.*, 2022, **61**, 11639-11650; b) M. L. Nakashige, J. I. P. Loristo, L. S. Wong, J. R. Gurr, T. J. O'Donnell, W. Y. Yoshida, A. L. Rheingold, R. P. Hughes and M. F. Cain, *Organometallics*, 2019, **38**, 3338-3348; c) K. W. Magnuson, S. M. Oshiro, J. R. Gurr, W. Y. Yoshida, M. Gembicky, A. L. Rheingold, R. P. Hughes and M. F. Cain, *Organometallics*, 2016, **35**, 855-859; d) Y. Nakajima, Y. Nakao, S. Sakaki, Y. Tamada, T. Ono and F. Ozawa, J. Am. Chem. Soc., 2010, 132, 9934-9936.
4 Y.-H. Chang, Y. Nakajima, H. Tanaka, K. Yoshizawa and F. Ozawa, *J. Am. Chem. Soc.*, 2013, **135**, 11791-11794.
5 J. Dugal-Tessier, G. R. Dake and D. P. Gates, *Organometallics*, 2007, **26**, 6481-6486.
6 P. Gupta, H. J. Drexler, R. Wingad, D. Wass, E. Barath, T. Beweries and C. Hering-Junghans, *Inorg. Chem. Front.*, 2023, **10**, 2285-2293.
7 A. Jouaiti, M. Geoffroy and G. Bernardinelli, *Tetrahedron Lett.*, 1992, **33**, 5071-5074.
8 P. M. Miura-Akagi, M. L. Nakashige, C. K. Maile, S. M. Oshiro, J. R. Gurr, W. Y. Yoshida, A. T. Royappa, C. E. Krause, A. L. Rheingold, R. P. Hughes and M. F. Cain, *Organometallics*, 2016, **35**, 2224-2231.
9 J. C. Ott, D. Bürgy, H. Guan and L. H. Gade, *Acc. Chem. Res.*, 2022, **55**, 857-868.
10 W. Weng, C. Guo, R. Çelenligil-Çetin, B. M. Foxman and O. V. Ozerov, *Chem. Commun.*, 2006, 197-199.
11 L. K. Paschai Darian, J. Ballmann and L. H. Gade, *Angew. Chem. Int. Ed.*, 2024, **63**, e202416814.
12 P. Gupta, J.-E. Siewert, T. Wellnitz, M. Fischer, W. Baumann, T. Beweries and C. Hering-Junghans, *Dalton Trans.*, 2021, **50**, 1838-1844.
13 Kushik, A. Petrov, D. Ranieri, L. Edelmann, T. Beweries and C. Hering-Junghans, *Angew. Chem. Int. Ed.*, 2024, **63**, e202412982.
14 L. Yang, D. R. Powell, R. P. Houser, *Dalton Trans.*, 2007, 955-964.
15 P. Pyykkö and M. Atsumi, *Chem. Eur. J.*, 2009, **15**, 12770-12779.
16 F. Ozawa, and Y. Nakajima, *Chem. Rec.*, 2016, **16**, 2314-2323.
17 H.-o. Taguchi, Y.-H. Chang, K. Takeuchi and F. Ozawa, *Organometallics*, 2015, **34**, 1589-1596.
18 D. Ostendorf, C. Landis, and H. Grützmacher, *Angew. Chem. Int. Ed.*, 2006, **45**, 5169.
19 C. Schweinzer, P. Coburger and H. Grützmacher, *Adv. Sci.*, 2024, **11**, 2400072.
20 A. H. Cowley, R. A. Jones, C. A. Stewart, A. L. Stuart, J. L. Atwood, W. E. Hunter and H. M. Zhang, *J. Am. Chem. Soc.*, 1983, **105**, 3737-3738.

References

[1] K. B. Dillon, F. Mathey, J. F. Nixon, *Phosphorus : the carbon copy : from organophosphorus to phospha-organic chemistry*, J. Wiley, **1998**.
[2] F. Mathey, *Phosphorus-Carbon Heterocycl. Chem.*, Elsevier, **2001**.
[3] T. Gier, *J. Am. Chem. Soc.* **1961**, *83*, 1769-1770.
[4] K. Dimroth, P. Hoffmann, *Chem. Ber.* **1966**, *99*, 1325-1331.
[5] G. Märkl, *Angew. Chem.* **1966**, *78*, 907-908.
[6] A. J. Ashe III, *J. Am. Chem. Soc.* **1971**, *93*, 3293-3295.
[7] G. Becker, **1976**.
[8] T. C. Klebach, R. Lourens, F. Bickelhaupt, *J. Am. Chem. Soc.* **1978**, *100*, 4886-4888.
[9] J. I. Bates, J. Dugal-Tessier, D. P. Gates, *Dalton Trans.* **2010**, *39*, 3151-3159.
[10] F. Ozawa, M. Yoshifuji, *Dalton Trans.* **2006**, 4987-4995.
[11] P. L. Floch, *Coord. Chem. Rev.* **2006**, *250*, 627-681.
[12] D. P. Gates, *New Asp. Phosphorus Chem. V* **2005**, 107-126.
[13] L. Weber, *Coord. Chem. Rev.* **2005**, *249*, 741-763.
[14] F. Mathey, *Angew. Chem. Int. Ed.* **2003**, *42*, 1578-1604.
[15] S. Shah, J. D. Protasiewicz, *Coord. Chem. Rev.* **2000**, *210*, 181-201.
[16] M. Regitz, O. J. Scherer, R. Appel, *Multiple bonds and low coordination in phosphorus chemistry*, Thieme Medical Publishers, **1990**.
[17] M. W. Schmidt, P. N. Truong, M. S. Gordon, *J. Am. Chem. Soc.* **1987**, *109*, 5217-5227.
[18] P. v. R. Schleyer, D. Kost, *J. Am. Chem. Soc.* **1988**, *110*, 2105-2109.
[19] B. H. Gillon, D. P. Gates, M. A. Henderson, E. Janusson, J. S. McIndoe, *Can. J. Chem.* **2017**, *95*, 239-242.
[20] V. A. Wright, B. O. Patrick, C. Schneider, D. P. Gates, *J. Am. Chem. Soc.* **2006**, *128*, 8836-8844.
[21] S. C. Serin, G. R. Dake, D. P. Gates, *Macromolecules* **2016**, *49*, 4067-4075.
[22] M. Doux, A. Moores, N. Mézailles, L. Ricard, Y. Jean, P. L. Floch, *J. Organomet. Chem.* **2005**, *690*, 2407-2415.
[23] G. Recker, *Z. Anorg. Allg. Chem.* **1976**, *423*, 242-254.
[24] R. Appel, C. Casser, M. Immenkeppel, F. Knoch, *Angew. Chem. Int. Ed.* **1984**, *23*, 895-896.
[25] A. Jouaiti, M. Geoffroy, G. Bernardinelli, *Tetrahedron Lett.* **1992**, *33*, 5071-5074.
[26] H. Kawanami, K. Toyota, M. Yoshifuji, *Chem. Lett.* **1996**, *25*, 533-534.
[27] M. Yam, J. H. Chong, C.-W. Tsang, B. O. Patrick, A. E. Lam, D. P. Gates, *Inorg. Chem.* **2006**, *45*, 5225-5234.
[28] H.-o. Taguchi, D. Sasaki, K. Takeuchi, S. Tsujimoto, T. Matsuo, H. Tanaka, K. Yoshizawa, F. Ozawa, *Organometallics* **2016**, *35*, 1526-1533.
[29] J. D. Protasiewicz, *Eur. J. Inorg. Chem.* **2012**, *2012*, 4539-4549.
[30] S. Shah, J. D. Protasiewicz, *Chem. Commun.* **1998**, 1585-1586.
[31] Y. Nakajima, Y. Okamoto, Y.-H. Chang, F. Ozawa, *Organometallics* **2013**, *32*, 2918-2925.
[32] K. W. Magnuson, S. M. Oshiro, J. R. Gurr, W. Y. Yoshida, M. Gembicky, A. L. Rheingold, R. P. Hughes, M. F. Cain, *Organometallics* **2016**, *35*, 855-859.

[33] P. M. Miura-Akagi, M. L. Nakashige, C. K. Maile, S. M. Oshiro, J. R. Gurr, W. Y. Yoshida, A. T. Royappa, C. E. Krause, A. L. Rheingold, R. P. Hughes, *Organometallics* **2016**, *35*, 2224-2231.
[34] M. L. Nakashige, J. I. Loristo, L. S. Wong, J. R. Gurr, T. J. O'Donnell, W. Y. Yoshida, A. L. Rheingold, R. P. Hughes, M. F. Cain, *Organometallics* **2019**, *38*, 3338-3348.
[35] P. Gupta, T. Taeufer, J.-E. Siewert, F. Reiß, H.-J. Drexler, J. Pospech, T. Beweries, C. Hering-Junghans, *Inorg. Chem.* **2022**, *61*, 11639-11650.
[36] S. Holand, C. Charrier, F. Mathey, J. Fischer, A. Mitschler, *J. Am. Chem. Soc.* **1984**, *106*, 826-828.
[37] T. A. Van der Knaap, F. Bickelhaupt, J. G. Kraaykamp, G. Van Koten, J. P. Bernards, H. T. Edzes, W. S. Veeman, E. De Boer, E. J. Baerends, *Organometallics* **1984**, *3*, 1804-1811.
[38] R. Apfel, C. Casser, F. Knoch, *J. Organomet. Chem.* **1985**, *293*, 213-217.
[39] I.-P. Lorenz, W. Pohl, H. Nöth, M. Schmidt, *J. Organomet. Chem.* **1994**, *475*, 211-221.
[40] K. Knoll, G. Huttner, M. Wasiucionek, L. Zsolnai, *Angew. Chem. Int. Ed.* **1984**, *23*, 739-740.
[41] H. Eshtiagh-Hosseini, H. W. Kroto, J. F. Nixon, M. J. Maah, M. J. Taylor, *J. Chem. Soc., Chem. Commun.* **1981**, 199-200.
[42] T. C. Klebach, R. Lourens, F. Bickelhaupt, C. H. Stam, A. Van Herk, *J. Organomet. Chem.* **1981**, *210*, 211-221.
[43] H. W. Kroto, J. F. Nixon, M. J. Taylor, A. A. Frew, K. W. Muir, *Polyhedron* **1982**, *1*, 89-95.
[44] M. R. Kushik, Hans-Joachim Drexler, Fabian Dankert, Christian Hering-Junghans, Torsten Beweries *manuscript submitted* **2025**.
[45] K. Hayashi, M. Nakatani, A. Hayashi, M. Takano, M. Okazaki, K. Toyota, M. Yoshifuji, F. Ozawa, *Organometallics* **2008**, *27*, 1970-1972.
[46] Y. Nakajima, M. Nakatani, K. Hayashi, Y. Shiraishi, R. Takita, M. Okazaki, F. Ozawa, *New J. Chem.* **2010**, *34*, 1713-1722.
[47] Y. Nakajima, Y. Nakao, S. Sakaki, Y. Tamada, T. Ono, F. Ozawa, *J. Am. Chem. Soc.* **2010**, *132*, 9934-9936.
[48] Y. Nakajima, Y. Shiraishi, T. Tsuchimoto, F. Ozawa, *Chem. Commun.* **2011**, *47*, 6332-6334.
[49] Y. Nakajima, T. Tsuchimoto, Y.-H. Chang, K. Takeuchi, F. Ozawa, *Dalton Trans.* **2016**, *45*, 2079-2084.
[50] Y.-H. Chang, Y. Nakajima, F. Ozawa, *Organometallics* **2013**, *32*, 2210-2215.
[51] Y.-H. Chang, Y. Nakajima, H. Tanaka, K. Yoshizawa, F. Ozawa, *J. Am. Chem. Soc.* **2013**, *135*, 11791-11794.
[52] P. Gupta, H.-J. Drexler, R. Wingad, D. Wass, E. Baráth, T. Beweries, C. Hering-Junghans, *Inorg. Chem. Front.* **2023**, *10*, 2285-2293.
[53] F. Dankert, C. Hering-Junghans, *Chem. Commun.* **2022**, *58*, 1242-1262.
[54] J. Li, Z. Lu, L. L. Liu, *J. Am. Chem. Soc.* **2022**, *144*, 23691-23697.
[55] E. Rivard, W. A. Merrill, J. C. Fettinger, P. P. Power, *Chem. Commun.* **2006**, 3800-3802.
[56] A. N. Price, M. J. Cowley, *Chem. Eur. J.* **2016**, *22*, 6248-6252.
[57] A. N. Price, G. S. Nichol, M. J. Cowley, *Angew. Chem.* **2017**, *129*, 10085-10089.
[58] A. Koner, B. Morgenstern, D. M. Andrada, *Angew. Chem. Int. Ed.* **2022**, *61*, e202203345.

[59] A. M. Borys, E. F. Rice, G. S. Nichol, M. J. Cowley, *J. Am. Chem. Soc.* **2021**, *143*, 14065-14070.

[60] M. Fischer, C. Hering-Junghans, *Chem. Sci.* **2021**, *12*, 10279-10289.

[61] P. Gupta, J.-E. Siewert, T. Wellnitz, M. Fischer, W. Baumann, T. Beweries, C. Hering-Junghans, *Dalton Trans.* **2021**, *50*, 1838-1844.

[62] S. Nees, T. Wellnitz, F. Dankert, M. Härterich, S. Dotzauer, M. Feldt, H. Braunschweig, C. Hering-Junghans, *Angew. Chem. Int. Ed.* **2023**, *62*, e202215838.

[63] M. Fischer, S. Nees, T. Kupfer, J. T. Goettel, H. Braunschweig, C. Hering-Junghans, *J. Am. Chem. Soc.* **2021**, *143*, 4106-4111.

[64] S. Nees, F. Fantuzzi, T. Wellnitz, M. Fischer, J. E. Siewert, J. T. Goettel, A. Hofmann, M. Härterich, H. Braunschweig, C. Hering-Junghans, *Angew. Chem. Int. Ed.* **2021**, *60*, 24318-24325.

[65] S. Nees, F. Fantuzzi, T. Wellnitz, M. Fischer, J. E. Siewert, J. T. Goettel, A. Hofmann, M. Härterich, H. Braunschweig, C. Hering-Junghans, *Angew. Chem.* **2021**, *133*, 24520-24528.

[66] S. Nees, H. Beer, P. Just, L. M. Teichmeier, L. E. Christoffer, A. Guljam, Kushik, H. Braunschweig, C. Hering-Junghans, *ChemPlusChem* **2023**, *88*, e202300078.

[67] G. Wittig, G. Geissler, *Liebigs Ann. Chem.* **1953**, *580*, 44-57.

[68] M. W. Rathke, R. Kow, *J. Am. Chem. Soc.* **1972**, *94*, 6854-6856.

[69] T. Tomioka, R. Sankranti, T. G. Vaughan, T. Maejima, T. Yanase, *J. Org. Chem.* **2011**, *76*, 8053-8058.

[70] T. Tomioka, Y. Takahashi, T. G. Vaughan, T. Yanase, *Org. Lett.* **2010**, *12*, 2171-2173.

[71] C. Sun, B. Potter, J. P. Morken, *J. Am. Chem. Soc.* **2014**, *136*, 6534-6537.

[72] K. Hong, X. Liu, J. P. Morken, *J. Am. Chem. Soc.* **2014**, *136*, 10581-10584.

[73] J. R. Coombs, L. Zhang, J. P. Morken, *Org. Lett.* **2015**, *17*, 1708-1711.

[74] A. Pelter, B. Singaram, J. W. Wilson, *Tetrahedron Lett.* **1983**, *24*, 635-636.

[75] A. Pelter, D. Buss, A. Pitchford, *Tetrahedron Lett.* **1985**, *26*, 5093-5096.

[76] A. Pelter, K. Smith, S. Elgendy, M. Rowlands, *Tetrahedron Lett.* **1989**, *30*, 5643-5646.

[77] A. Pelter, K. Smith, S. Elgendy, M. Rowlands, *Tetrahedron Lett.* **1989**, *30*, 5647-5650.

[78] D. S. Matteson, R. A. Davis, L. A. Hagelee, *J. Organomet. Chem.* **1974**, *69*, 45-51.

[79] D. S. Matteson, R. J. Moody, P. K. Jesthi, *J. Am. Chem. Soc.* **1975**, *97*, 5608-5609.

[80] C. L. Johlman, C. F. Ijames, C. L. Wilkins, T. H. Morton, *J. Org. Chem.* **1983**, *48*, 2628-2629.

[81] M. P. Cooke, Jr., *J. Org. Chem.* **1994**, *59*, 2930-2931.

[82] H. Staudinger, J. Meyer, *Helv. Chim. Acta* **1919**, *2*, 635-646.

[83] M. W. P. Bebbington, D. Bourissou, *Coord. Chem. Rev.* **2009**, *253*, 1248-1261.

[84] P. ONYS'KO, N. Proklina, V. Prokopenko, Y. G. Gololobov, *Chem. Inf. Dienst* **1984**, *15*, no-no.

[85] M. P. Ponomarchuk, L. F. Kasukhin, M. V. Shevchenko, L. S. Sologub, V. P. Kukhar, *Zh. Obshch. Khim.* **1984**, *54*, 2468-2473.

[86] J. Tang, J. Dopke, J. G. Verkade, *J. Am. Chem. Soc.* **1993**, *115*, 5015-5020.

[87] J. Tejeda, R. Reau, F. Dahan, G. Bertrand, *J. Am. Chem. Soc.* **1993**, *115*, 7880-7881.

[88] K. Bieger, J. Tejeda, R. Reau, F. Dahan, G. Bertrand, *J. Am. Chem. Soc.* **1994**, *116*, 8087-8094.

[89] M. Alajarín, P. Molina, A. López-Lázaro, C. Foces-Foces, *Angew. Chem. Int. Ed.* **1997**, *36*, 67-70.
[90] A. M. Claudio Bianchini, M. Peruzzini, F. Vizza, F. Zanobini, *Coord. Chem. Rev.* **1992**, *120*, 193-208.
[91] M. Alajarín, A. Vidal, C. López-Leonardo, J. Berná, M. C. R. de Arellano, *Tetrahedron Lett.* **1998**, *39*, 7807-7810.
[92] M. Alajarín, C. López-Leonardo, J. Berná, J. W. Steed, *Tetrahedron* **2007**, *63*, 2078-2083.
[93] M. Alajarín, J. Berná, C. López-Leonardo, J. W. Steed, *Chem. Commun.* **2008**, 2337-2339.
[94] M. Alajarín, A. López-Lázaro, A. Vidal, J. Berná, *Chem. Eur. J.* **1998**, *4*, 2558-2570.
[95] M. Alajarín, C. López-Leonardo, A. Vidal, J. Berná, J. W. Steed, *Angew. Chem.* **2002**, *114*, 1253-1256.
[96] M. Alajarín, C. López-Leonardo, J. Berná, *Tetrahedron* **2006**, *62*, 6190-6202.
[97] M. Alajarín, C. López-Leonardo, J. Berná, *Org. Lett.* **2007**, *9*, 4631-4634.
[98] S. Bontemps, H. Gornitzka, G. Bouhadir, K. Miqueu, D. Bourissou, *Angew. Chem. Int. Ed.* **2006**, *45*, 1611-1614.
[99] S. Bontemps, G. Bouhadir, K. Miqueu, D. Bourissou, *J. Am. Chem. Soc.* **2006**, *128*, 12056-12057.
[100] M. Sircoglou, S. Bontemps, M. Mercy, N. Saffon, M. Takahashi, G. Bouhadir, L. Maron, D. Bourissou, *Angew. Chem. Int. Ed.* **2007**, *46*, 8583.
[101] S. Bontemps, M. Sircoglou, G. Bouhadir, H. Puschmann, J. A. Howard, P. W. Dyer, K. Miqueu, D. Bourissou, *Chem. Eur. J.* **2008**, *14*, 731-740.
[102] S. Bontemps, G. Bouhadir, W. Gu, M. Mercy, C. H. Chen, B. M. Foxman, L. Maron, O. V. Ozerov, D. Bourissou, *Angew. Chem.* **2008**, *120*, 1503-1506.
[103] A. Fischbach, P. R. Bazinet, R. Waterman, T. D. Tilley, *Organometallics* **2008**, *27*, 1135-1139.
[104] J. Vergnaud, M. Grellier, G. Bouhadir, L. Vendier, S. Sabo-Etienne, D. Bourissou, *Organometallics* **2008**, *27*, 1140-1146.
[105] M. W. Bebbington, S. Bontemps, G. Bouhadir, D. Bourissou, *Angew. Chem. Int. Ed.* **2007**, *46*, 3333-3336.
[106] S. Moebs-Sanchez, G. Bouhadir, N. Saffon, L. Maron, D. Bourissou, *Chem. Commun.* **2008**, 3435-3437.
[107] G. L. Hillhouse, G. V. Goeden, B. L. Haymore, *Inorg. Chem.* **1982**, *21*, 2064-2071.
[108] A. Danopoulos, R. Hay-Motherwell, S. Cafferkey, T. N. Sweet, M. Hursthouse, *J. Chem. Soc., Dalton Trans.* **1997**, 3177-3184.
[109] V. Cadierno, M. Zablocka, B. Donnadieu, A. Igau, J. P. Majoral, A. Skowronska, *Chem. Eur. J.* **2000**, *6*, 345-352.
[110] K. Vaughan, M. F. G. Stevens, *Chem. Soc. Rev.* **1978**, *7*, 377-397.
[111] S. Patil, A. Bugarin, *Eur. J. Org. Chem.* **2016**, *2016*, 860-870.
[112] A. A. Suleymanov, K. Severin, *Angew. Chem.* **2021**, *133*, 6955-6965.
[113] H. E. Winberg, D. D. Coffman, *J. Am. Chem. Soc.* **1965**, *87*, 2776-2777.
[114] E. Fanghänel, R. Hänsel, W. Ortmann, J. Hohlfeld, *J. Prakt. Chem.* **1975**, *317*, 631-640.
[115] D. M. Khramov, C. W. Bielawski, *Chem. Commun.* **2005**, 4958-4960.

[116] F. W. Kimani, J. C. Jewett, *Angew. Chem.* **2015**, *127*, 4123-4126.
[117] J. He, F. W. Kimani, J. C. Jewett, *J. Am. Chem. Soc.* **2015**, *137*, 9764-9767.
[118] S. Patil, K. White, A. Bugarin, *Tetrahedron Lett.* **2014**, *55*, 4826-4829.
[119] S. Patil, A. Bugarin, *Acta Crystallogr. Sect. E Struct. Rep. Online* **2014**, *70*, 224-227.
[120] D. Jishkariani, C. D. Hall, A. Demircan, B. J. Tomlin, P. J. Steel, A. R. Katritzky, *J. Org. Chem.* **2013**, *78*, 3349-3354.
[121] Kushik, A. Petrov, D. Ranieri, L. Edelmann, T. Beweries, C. Hering-Junghans, *Angew. Chem. Int. Ed.* **2024**, *63*, e202412982.
[122] R. A. Kunetskiy, I. Císařová, D. Šaman, I. M. Lyapkalo, *Chem. Eur. J.* **2009**, *15*, 9477-9485.
[123] S. Lysenko, C. G. Daniliuc, P. G. Jones, M. Tamm, *J. Organomet. Chem.* **2013**, *744*, 7-14.
[124] M. Kitamura, N. Tashiro, T. Okauchi, *Synlett* **2009**, *2009*, 2943-2944.
[125] M. Kitamura, M. Yano, N. Tashiro, S. Miyagawa, M. Sando, T. Okauchi, Wiley Online Library, **2011**.
[126] D. J. Coady, C. W. Bielawski, *Macromolecules* **2006**, *39*, 8895-8897.
[127] D. J. Coady, D. M. Khramov, B. C. Norris, A. G. Tennyson, C. W. Bielawski, *Angew. Chem.* **2009**, *121*, 5289-5292.
[128] C. Wang, H. Chen, Z. Wang, J. Chen, Y. Huang, *Angew. Chem. Int. Ed.* **2012**, *51*, 7242.
[129] C. Wang, H. Chen, Z. Wang, J. Chen, Y. Huang, *Angew. Chem.* **2012**, *124*, 7448-7448.
[130] A. Hafner, S. Bräse, *Angew. Chem. Int. Ed.* **2012**, *51*, 3713-3715.
[131] A. Hafner, S. Bräse, *Angew. Chem.* **2012**, *124*, 3773-3775.
[132] A. Mohammadi, *J. Mol. Liq.* **2014**, *193*, 69-73.
[133] E. V. Sadtchikova, V. S. Mokrushin, *Mendeleev Commun.* **2002**, *12*, 70-72.
[134] D. M. Khramov, C. W. Bielawski, *J. Org. Chem.* **2007**, *72*, 9407-9417.
[135] A. H. Cowley, F. Gabbai, R. Schluter, D. Atwood, *J. Am. Chem. Soc.* **1992**, *114*, 3142-3144.
[136] X. Li, D. Lei, M. Y. Chiang, P. P. Gaspar, *J. Am. Chem. Soc.* **1992**, *114*, 8526-8531.
[137] S. Shah, M. C. Simpson, R. C. Smith, J. D. Protasiewicz, *J. Am. Chem. Soc.* **2001**, *123*, 6925-6926.
[138] A. Hofmann, T. Tröster, T. Kupfer, H. Braunschweig, *Chem. Sci.* **2019**, *10*, 3421-3428.
[139] G. J. P. Britovsek, V. C. Gibson, O. D. Hoarau, S. K. Spitzmesser, A. J. P. White, D. J. Williams, *Inorg. Chem.* **2003**, *42*, 3454-3465.
[140] B. Xu, Q. Jiang, A. Zhao, J. Jia, Q. Liu, W. Luo, C. Guo, *Chem. Commun.* **2015**, *51*, 11264-11267.
[141] P. Pyykkö, M. Atsumi, *Chem. Eur. J.* **2009**, *15*, 12770-12779.
[142] L. K. Paschai Darian, J. Ballmann, L. H. Gade, *Angew. Chem. Int. Ed.* **2024**, *63*, e202416814.